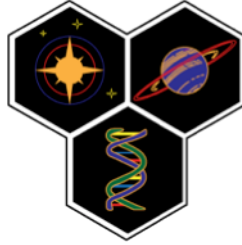


NASA Space Science and Astrobiology

Fourth Annual Jamboree
March 8, 2016





Welcome to the Fourth Annual Ames Space Sciences and Astrobiology Jamboree!

The Space Science and Astrobiology Division at NASA Ames Research Center consists of over 50 civil servants and more than 110 contractors, co-ops, post-docs and associates. Researchers in the division are pursuing investigations in a variety of fields including exoplanets, planetary science, astrobiology and astrophysics. In addition, division personnel support a wide variety of NASA missions including (but not limited to) Kepler, SOFIA, LADEE, JWST, and New Horizons. With such a wide variety of interesting research going on, distributed among three branches in at least 5 different buildings, it can be difficult to stay abreast of what one's fellow researchers are doing. Our goal in organizing this symposium is to facilitate communication and collaboration among the scientists within the division, and to give center management and other ARC researchers and engineers an opportunity to see what scientific research and science mission work is being done in the division.

We are also continuing the tradition within the Space Science and Astrobiology Division to honor one senior and one early career scientist with the Pollack Lecture and the Early Career Lecture, respectively. With the Pollack Lecture, our intent is to select a senior researcher who has made significant contributions to any area of research within the space sciences, and we are pleased to honor Dr. David DesMarais this year. With the Early Career Lecture, our intent is to select a young researcher within the division who, by their published scientific papers, shows great promise for the future in any area of space science research, and we are pleased to honor Dr. Christiaan Boersma this year.

We hope you can take advantage of the day to learn something new and meet some new faces!

Sincerely,

Science Organizing Committee

Tim Lee
Mark Fonda
Jessie Dotson
Jeff Hollingsworth
Linda Jahnke

Fourth Annual Space Sciences Jamboree
March 8, 2016

8:00 am	Registration & Poster Setup
8:30 am	Michael Bicay: Welcome & Announcements
8:45 am	<i>Outstanding Early Career Space Scientist Lecture:</i> Christiaan Boersma: A 21 st Century Approach to Astronomical PAH Spectroscopy: Mining the Treasure Trove
9:45 am	Xinchuan Huang: Computational IR Line Lists for IR Astronomy and Exoplanets
10:05 am	Tom Greene: Characterizing Transiting Exoplanet Atmospheres with the James Webb Space Telescope
10:25 am	Poster Session (odd number posters) & Coffee Break
11:10 am	Knicole Colón: The NASA K2 Mission Exploring Planets, Stars and Beyond
11:30 am	Dale Cruikshank: Pluto and Charon seen with New Horizons -- Surface Compositions
11:50 am	Eric Becklin: Pluto Occultation with SOFIA on 29 June 2015 in Support of New Horizons Flyby: Occultation Evidence for Haze
12:10 pm	Poster Session / Lunch
1:15 pm	Tori Hoehler: Power and Biological Potential
1:35 pm	Niki Parenteau: Global Surface Photosynthetic Biosignatures Prior to the Rise of Oxygen
1:55 pm	Luis Teodoro: Ionizing Radiation of the Surface of Europa: Implications for the Search of Evidence of Life
2:15 pm	Thomas Murphy: A radiative transfer model for packed beds -- sediments, biofilms, and microbial mats
2:35 pm	Darlene Lim: BASALT -- Biologic Analog Science Associated with Lava Terrains
2:55 pm	Poster Session (even number posters) & Coffee Break
3:15 pm	Amanda Cook: Multicolor Imagery and Spectroscopy Instrumentation for Planetary Surface Prospecting of Volatiles
4:00 pm	Rick Elphic: Using Neutron Spectroscopy to Constrain the Composition and Provenance of Phobos and Deimos
4:20 pm	<i>Pollack Lecture:</i> David DesMarais: Early Biospheres in the Context of the Biogeochemical Carbon Cycles
5:20 pm	Remove Posters

ID	Title	Corresponding Author
Astrobiology Posters		
AB.1	Pure and N-substituted Small Cyclic Hydrocarbon Synthesis in the Gas Phase: Path to PAHs and PANHs	Partha Bera
AB.2	The Formation of Nucleobases from the Irradiation of Purine in Astrophysical Ices	Scott Sandford
AB.3	Sugars and Sugar Derivatives in Residues Produced from the UV Irradiation of Astrophysical Ice Analogs	Michel Nuevo
AB.4	Molecular Crowding and Evolution of Ligase Ribozymes	Milena Popovic
AB.5	The Affect of the Space Environment on the Survival of <i>Halorubrum chaoviator</i> and <i>Synechococcus</i> (Nägeli): Data from the Space Experiment OSMO on EXPOSE-R	Rocco Mancinelli
AB.6	Ecological Genomics of the Newly Discovered Filamentous Diazotrophic Cyanobacterium, ESFC-1	Richard Craig Everroad
AB.7	Transformations and Fates of Lipid Biomarkers in Microbial Mat Ecosystems	Linda Jahnke
AB.8	Nitrogen Cycle in Microbial Mats: Completely Unknown?	Oksana Coban
AB.9	Nearing the Cold-Arid Limits of Microbial Life in Permafrost of an Upper Dry Valley, Antarctica	Chris McKay
AB.10	Xeropreservation of Million-Year-Old Functionalized Lipid Biomarkers in Hyperarid Soils in the Atacama Desert, Chile	Mary Beth Wilhelm
AB.11	Seeking Signs of Life in Nili Patera with Icelandic Sinter Field Exploration	J.R. Skok
AB.12	The CROMO Drilling Project	Michael Kubo
AB.13	The LASSEN Astrobiology Intern Program	David DesMarais
AB.14	The Last Possible Outposts for Life on Mars	Alfonso Davila
AB.15	Morphologic and Morphometric Indications of Meltwater-Driven Gully Formation on Mars	Natalie Glines
AB.16	Hollow Nodules Gas Escape Sedimentary Structures in Lacustrine Deposits on Earth and Gale Crater (Mars).	Rosalba Bonaccorsi
AB.17	Perchlorate Reducing Bacteria: Evaluating the Potential for Growth Utilizing Nutrient Sources Identified on Mars	Kathryn Bywaters
AB.18	Search for Upper Limit on Chlorobenzene in the Original GCMS data set	Melissa Guzman
AB.19	Hypersaline Environments as Analogs for Habitats on Past Mars	Angela Detweiler
AB.20	Changes in the Salt Crust Microbial Community After Exposure to Martian Conditions.	Heather Smith
AB.21	Building a Biosignature Rock Sample Library and Developing Automated Classifiers	Virginia Gulick
AB.22	Elucidating the Abiotic Origins of Citric Acid Cycle Compounds Detected in Carbonaceous Meteorites.	Andro Cooper Rios
AB.23	Rare and Common Sugar Derivatives in Carbonaceous Meteorites: Anomalous Enantiomer Excesses and Racemic Mixtures	George Cooper
AB.24	Upper Atmosphere Detection of Meteoritic Organics by a Mid-	David Summers

	Infrared Small Satellite Spectrometer (MIRSSS)	
AB.25	Wildlife Photography in Extreme Environment at the Microbial Scale	Chris McKay
AB.26	Microbial Ecology and Space Life Science: Applications for Human Space Exploration	Skylar Laham
AB.27	Isolation and Characterization of Perchlorate Resistant Halophiles from Big Soda Lake	Toshitaka Matsubara
AB.28	Biomining Materials from E-Waste	Jesica Urbina-Navarrete
AB.29	“POWERCELL” on EuCROPIS: The Interface Between Mars Resources and Human Exploration	Lynn Rothschild
Astrophysics Posters		
AP.1	Computing Anharmonic Vibrational Spectra for Polycyclic Aromatic Hydrocarbons: Naphthalene, Anthracene, and Tetracene	Tim Lee
AP.2	PAH-Mineral Interactions. A Laboratory Approach to Astrophysical Catalysis	Gustavo Cruz-Diaz
AP.3	Recent Progresses in Laboratory Astrophysics with Ames’ COSMIC Facility: Interstellar and Planetary Applications	Farid Salama
AP.4	Laser Induced Emission Spectroscopy of Cold and Isolated Neutral PAHs and PANHs: Implications for the Red Rectangle Emission	Selma Bejaoui
AP.5	Calibrating the Charge State of Polycyclic Aromatic Hydrocarbons Across Reflection Nebulae	Christiaan Boersma
AP.6	Determining the Gas Mass of Protoplanetary Disks	Uma Gorti
AP.7	Testing Tidal Synchronization with Heartbeat Stars	Susan Thompson
AP.8	Observing Y-Dwarfs with JWST	Thomas Roellig
AP.9	How Does the Cosmic Web Influence Galaxy Evolution?	Mehmet Alpaslan
AP.10	An HI Survey of Extremely Isolated Early-type Galaxies	Pamela Marcum
AP.11	Resolved Dust Emission Analysis in IC1459 and NGC2768	Alexandre Amblard
Exoplanet Posters		
EP.1	Estimation of Chromatic Errors from Broadband Images For High Contrast Imaging	Dan Sirbu
EP.2	Why Alpha Centauri is a Particularly Good Target for Direct Imaging of Exoplanets	Ruslan Belikov
EP.3	Long-Term Stability of Planets in the Alpha Centauri System	Jack Lissauer
EP.4	The Frequency of Giant Impacts on Earth-Like Worlds	Elisa Quintana
EP.5	Small Stars with Small Planets from K2: The K2 M Dwarf Program	Joshua Schlieder
EP.6	DAVE: Detection and Vetting of Exoplanets (in K2)	Fergal Mullally
EP.7	How We Roll – The NASA K2 Mission Science Products and Their Performance Metrics	Jeffrey Van Cleve
EP.8	Photochemical Hazes in Exoplanetary Atmospheres	Hiroshi Imanaka
EP.9	Titan-Like Exoplanets: Variations in Geometric Albedo and Limb Transit Height with Haze Production Rate	Chris McKay

Planetary Atmosphere and Climate		
PA.1	K2 Observations of a Variable Planet: Neptune as Model of Brown Dwarf Variability	Mark Marley
PA.2	Earth 2.7 Billion Years Ago Had Half the Air Pressure of Today	SanJoy Som
PA.3	Non-Thermal Escape of Molecules from Planetary Atmospheres	Marko Gacesa
PA.4	What Have We Learned from the LADEE Mission?	Richard Elphic
PA.5	Rainfall Estimates To Sustain an Unfrozen Lake in Gale Crater Mars 3.5 Gy Ago	Robert Haberle
PA.6	Salts as Water Ice Cloud Nuclei on Mars	Delia Santiago-Materese
PA.7	Constraining Early Martian PCO ₂ from In Situ Mineralogical Analysis at Gale crater	Thomas Bristow
PA.8	Production and Analyses of Titan Laboratory Aerosols Analogs at Low Temperature with the NASA Ames Titan Haze Simulation (THS) experiment	Ella Sciamma-O' Brien
PA.9	Large-Scale Weather Disturbances in Mars' Southern Extratropics	Jeffery Hollingsworth
Planetary Surfaces & Interiors		
PS.1	Oxygen released during analysis of Mars surface materials: A comparison of Viking and Curiosity Mission Results.	Kathryn Bywaters
PS.2	The Lost River of Mars: Losing and Gaining Paleostreams in the Navua Valles, NE Hellas	Henrik Hargitai
PS.3	Geomorphological Mapping of the Encounter Hemisphere on Pluto	Oliver White
PS.4	The Geophysical Significance of Sesquinary Ejecta: Phobos and Luna Case Studies	Michael Nayak
PS.5	The H-G Relation and its Effect on Diameter and Albedo (pv) and Taxonomy: A Case Study of Near-Earth Asteroid (NEA) 3691 Bede	Diane Wooden
PS.6	Meteorite Fractures and Scaling for Atmospheric Entry	Katie Bryson
PS.7	Physical Properties of Ordinary Chondrites	Daniel Ostrowski
PS.8	Magnetite Laboratory Reflectance Spectra Modeled using Hapke Theory and Existing Optical Constants	Ted Roush
PS.9	A New Method -- Potentially Suitable for Spacecraft Instrumentation -- for Dating Recent Volcanism on Planetary Surfaces	Derek Sears
PS.10	A Sample Delivery System for Planetary Surface Missions	David Willson
PS.11	Sample Delivery Challenges For an Auger-Based Mission: Contamination Paths, Mixing, And Dilution of Results	Arwen Dave
PS.12	Overview of NASA FINESSE (Field Investigations to Enable Solar System Science and Exploration) Science and Exploration Project	Jennifer Heldmann
PS.13	Near Earth Asteroid Characteristics for Asteroid Threat Assessment	Jessie Dotson

Title: A 21st Century Approach to Astronomical PAH Spectroscopy: Mining the Treasure Trove

Authors : Dr. Christiaan Boersma

Science Topic : 2016 Outstanding Early Career Space Scientist Lecture

Polycyclic aromatic hydrocarbons (PAHs) are an important constituent of interstellar dust. Intermediate in size between molecules and classical dust particles, PAHs possess characteristics of both. This unique property, coupled with their spectroscopic response to changing conditions and the ability to convert ultraviolet to infrared (IR) radiation, makes them powerful probes of astronomical objects at all stages of the stellar life cycle. PAH emission can dominate as much as 20% of the total IR luminosity in the many Galactic and extragalactic objects where they are seen and they are thought to hold up to 10-15% of all cosmic carbon. Due to their omnipresence and stability, PAHs play important roles in many astronomical environments and a defining role in the star- and planet formation process; and perhaps even in the origin of life.

This lecture gives a historical overview of the development of the PAH hypothesis and the connection it has with NASA Ames Research Center. It will dive into the richness of the PAH spectrum and how it can be used to determine the state of the PAH population in terms of charge, composition, structure, size, etc. Subsequently, the changing state of the PAH population within and between astronomical objects provides insight into the associated changing local astrophysical environment. In turn, this provides clues on the formation and evolution of stars and planets.



Fig. 1: Announcement poster for the NASA Ames PAH IR Spectroscopic Database as presented at the 213th AAS in Long Beach, CA.

Over the past two decades laboratory experiments and quantum chemical calculations have been carried out at NASA Ames Research Center to test and refine the PAH hypothesis. This work has resulted in an unrivaled collection of PAH spectra that has been assembled into a database. The NASA Ames PAH IR Spectroscopic Database (PAHdb) houses this collection and provides online access (www.astrochemistry.org/pahdb/) to the data and powerful on-line and downloadable IDL tools (*AmesPAHdbIDL Suite*) that interact with the data.

PAHdb is a paradigm shift in the way astronomical PAH spectra are analyzed and interpreted. A bottom-up approach, where astronomical PAH spectra are fitted and analyzed with the authentic PAH spectra in PAHdb, now allows for the first *quantitative* analysis of the astronomical PAH spectrum.

This 21st century approach toward PAH spectroscopy taps into the treasure trove of information hidden in the astronomical PAH spectrum and provides a new way to probe conditions in astrophysical environments.

Computational IR Line Lists for IR Astronomy and Exoplanets

Xinchuan Huang, David W. Schwenke, and Timothy J. Lee
NASA Ames Research Center, Moffett Field, CA 94035, USA
Email: Xinchuan.Huang-1@nasa.gov

Science Topic: 1. Astrophysics; 2. Exoplanet; 3. Planetary Atmosphere

Current high-resolution IR databases of astronomically interesting molecules are not capable of supporting complete and accurate spectral analysis, atmospheric modeling, and simulations for varied celestial objects and environments where gas phase molecules can exist, e.g. exoplanets, the ISM, Titan, Venus, etc. Most databases only contain transitions derived from reduced Hamiltonian models fit from a limited number of recorded lines. The largest problems associated with these databases are the lack of “prediction” capability and completeness. These limitations originate from the nature of the molecule, the experimental setup and sensitivity, the temperature, and the complexity of spectral congestion, etc. The only realistic path that can lead us to the required IR databases is to combine high level first-principles theoretical computations with high-resolution experimental studies. Through our approach of combining “Best Theory” and “High-resolution Experiment”, the IR line lists we computed have achieved the critical level of precision to be trusted by spectroscopists, i.e. a **Prediction Accuracy** of 0.01-0.03 cm^{-1} for rovibrational IR line positions, 10 MHz or better for Far IR line positions, 1-3% uncertainty for the intensity of the strongest IR bands, and 5-20% for much weaker bands. In this talk we will show examples of the following: a) how bad the IR database deficiencies are; b) what we have accomplished in the last 10 years for NH_3 , CO_2 and SO_2 ; c) how well the most recent experiments agree with our line list predictions; d) what impact and collaborations we have made; e) plus, why we are the only US group working in this field, and how our line list predictions compare to the “ExoMol” project group at UCL.

Characterizing transiting exoplanet atmospheres with the James Webb Space Telescope

Tom Greene¹, Mike Line^{1,2,3,4}, Jonathan Fortney⁴

¹ NASA Ames Research Center, Moffett Field, CA 94035, USA

² Hubble Postdoctoral Fellow

³ School of Earth and Space Exploration, Arizona State University, Tempe, AZ 85287, USA

⁴ Department of Astronomy and Astrophysics, University of California, Santa Cruz, CA 95064, USA

Science Topic: Exoplanets, Observatories and Instrumentation

We explore how well James Webb Space Telescope (*JWST*) spectra will likely constrain bulk atmospheric properties of transiting exoplanets. We start by modeling the atmospheres of archetypal hot Jupiter, warm Neptune, warm sub-Neptune, and cool super-Earth planets with clear, cloudy, or high mean molecular weight atmospheres. Next we simulate the $\lambda = 1 - 11 \mu\text{m}$ transmission and emission spectra of these systems for several *JWST* instrument modes for single transit and eclipse events. We then perform retrievals to determine how well temperatures and molecular mixing ratios (CH_4 , CO , CO_2 , H_2O , NH_3) can be constrained. We find that $\lambda = 1 - 2.5 \mu\text{m}$ transmission spectra will often constrain the major molecular constituents of clear solar composition atmospheres well. Cloudy or high mean molecular weight atmospheres will often require full $1 - 11 \mu\text{m}$ spectra for good constraints, and emission data may be more useful in cases of sufficiently high F_p and high F_p/F_* . Strong temperature inversions in the solar composition hot Jupiter atmosphere should be detectable with $1 - 2.5 \mu\text{m}$ emission spectra, and $1 - 5 + \mu\text{m}$ emission spectra will constrain the temperature-pressure profiles of warm planets. Transmission spectra over $1 - 5 + \mu\text{m}$ will constrain $[\text{Fe}/\text{H}]$ values to better than 0.5 dex for the clear atmospheres of the hot and warm planets studied. Carbon-to-oxygen ratios can be constrained to better than a factor of 2 in some systems. I will also present a brief summary of the *JWST* science timeline, including key dates for proposals, launch, and observations.

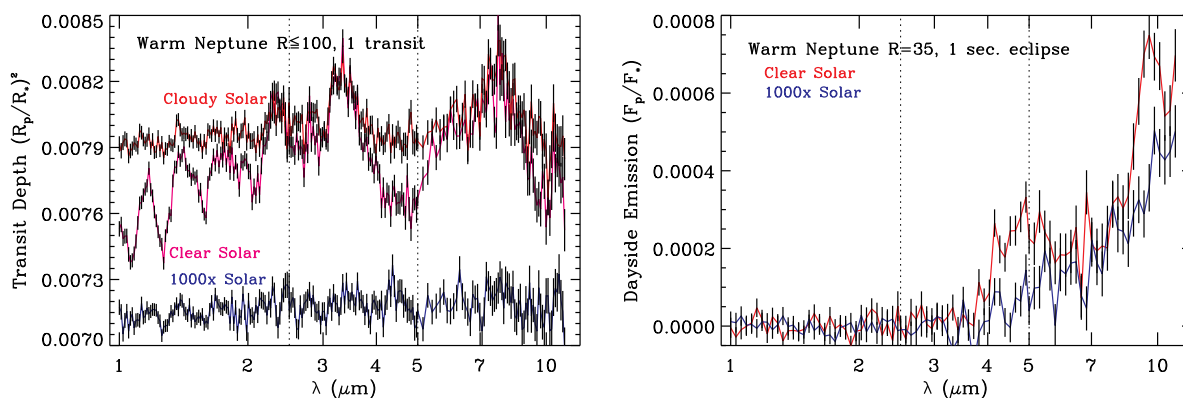


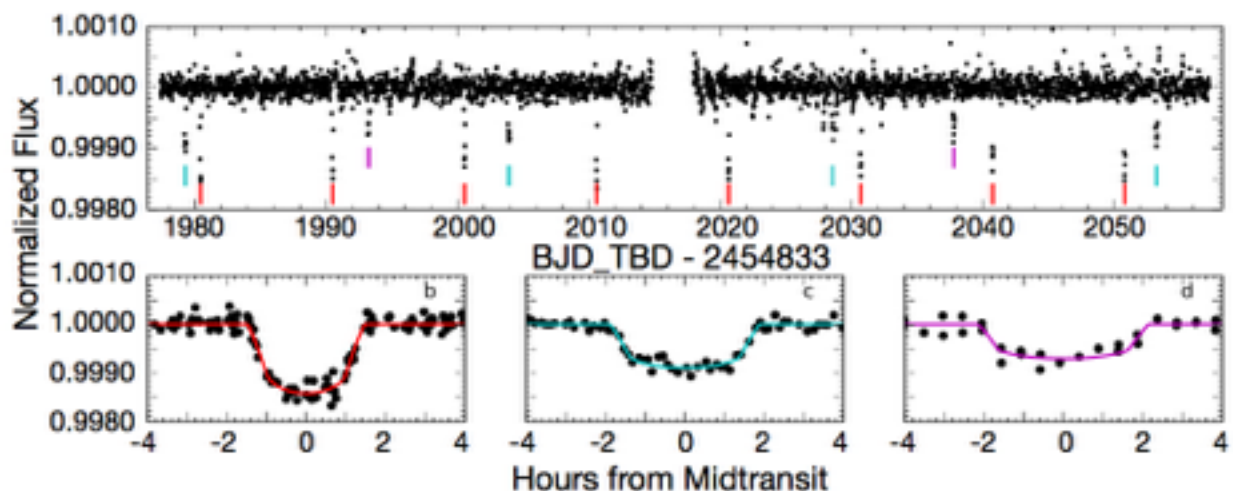
Figure 1: Simulated transmission (left) and emission (right) spectra of several atmospheres of a warm Neptune planet with system parameters of GJ 436b. The spectra are simulated for a single transit or secondary eclipse with equal time on the star alone for each instrument mode. The simulated spectra include a noise instance and are presented as colored curves. The black error bars denote 1σ of noise composed of random and systematic components. Dashed lines show the wavelength range boundaries of the chosen NIRISS SOSS ($1 - 2.5 \mu\text{m}$), NIRCcam grism ($2.5 - 5 \mu\text{m}$), and MIRI LRS ($5 - 11 \mu\text{m}$) instrument modes.

The NASA K2 Mission Exploring Planets, Stars, and Beyond

*Knicole Colón, Thomas Barclay, Geert Barentsen, Steve Howell
Kepler/K2 Guest Observer Office*

Science Topic: Astrophysics

The NASA Kepler mission launched in 2009 and observed a single region of the Galaxy for four years. During its lifetime, Kepler discovered thousands of transiting extrasolar planets and also revolutionized the field of stellar astrophysics thanks to its ability to produce extremely high precision measurements of the brightness of stars. After a second reaction wheel failed on the Kepler spacecraft in 2013, the NASA K2 mission was born. K2 has been observing a variety of astrophysical targets in different fields along the ecliptic in ~80 day campaigns since 2014. The science goals of the K2 mission involve time variable observations of Solar System objects, extrasolar planets, star clusters, supernovae, and more. With about two years of scientific observations completed, K2 has already extended the legacy of the Kepler mission by making a number of its own exciting discoveries. For example, in the field of exoplanets, K2 has discovered small super-Earth-size planets orbiting in the habitable zone of nearby cool M dwarf stars. K2 has also revealed different classes of variability in young stars as well as a surprising variety of pulsations in the Pleiades “Seven Sisters” stars. K2 is also providing insight into the progenitors of Type Ia supernovae. Closer to home, K2 is observing planets and asteroids in our own solar system, providing light curves that are unrivaled in their precision and time-baseline. Finally, K2 is about to begin a gravitational microlensing experiment by observing stars located in the Galactic bulge. With approximately two more years of observations expected from K2, many more exciting discoveries are anticipated. In this presentation, I will provide an overview of the K2 mission, present its current status, review major results from the mission in all areas of astrophysics, and discuss anticipated results from future K2 campaigns.



The above figure shows the K2 light curve of K2-3 (top), a nearby M dwarf star with three transiting super-Earth-size planets (Crossfield et al. 2015, ApJ, 804, 10). The bottom panels show the phase-folded photometry and best-fit transit models for each of the planets. Planet K2-3d is located in the habitable zone around its cool host star.

Pluto and Charon Seen With *New Horizons*--Surface Compositions

Dale P. Cruikshank (with contributions from the *New Horizons* Composition team)

NASA's *New Horizons* spacecraft flew past Pluto, Charon, and the four small satellites on July 14, 2016, returning a wealth of images, spectra, and information on the atmosphere and the charged particle and dust environment. Pluto exhibits a remarkable range of surface activity, on timescales ranging from seasonal to geological. Much of this activity is enabled by volatile ices like N₂ and CO that are easily mobilized even at the extremely low temperatures prevalent on Pluto's surface. What makes Pluto's surface especially interesting is the interaction between the volatile ices and inert materials such as H₂O ice that are sufficiently strong and durable to support rugged topography. Pluto's rigid H₂O ice is not mobile on its own, but it is sculpted in a great variety of ways by the action of volatile ices. CH₄ ice appears to play a distinct and unique role, enabled by its intermediate volatility. CH₄ ice condenses at high altitudes and on the winter hemisphere, contributing to the construction of some of Pluto's more unusual and distinctive landforms.

Extremely red and non-volatile tholins coat an ancient, heavily-cratered equatorial belt. A vast, glacially-flowing expanse of volatile ices including N₂ and CO modifies the surrounding H₂O bedrock. CH₄-ice condenses on crater rims and mountain ridges. Pluto's albedo contrasts are extreme, among the most striking seen in the Solar System. The H₂O-ice rich surface of Pluto's large moon Charon revealed surprises of its own. Charon's northern latitudes exhibit distinctly reddish tholin coloration. The latitudinal distribution of this coating suggests a thermally-controlled deposition process. Localized areas on Charon rich in NH₃ ice are unlike anything seen on other outer Solar System icy bodies.

In the Ames Astrochemistry Lab the surface chemistry of Pluto is synthesized by energy deposition in a layer of ice representing a mix of N₂, CH₄, and CO (100:1:1)--ices detected from ground-based spectroscopy and confirmed by *New Horizons*. UV irradiation and keV electron bombardment of this Pluto ice mix, in experiments done separately, both produce a refractory, brightly colored tholin that has been analyzed by various techniques. Analysis reveals ketones, carboxylic acids, alcohols, aldehydes, amides, nitriles, and urea. UV fluorescence shows a sizable aromatic component, and a study of the results of two-step laser desorption-mass spectroscopy is in progress. In terms of chemical content, the Pluto ice tholin shows some similarity to the soluble organic fraction of some of the carbonaceous meteorites, although without any evidence for amino acids in the tholin.

References:

Materese, C. K., Cruikshank, D., P., Sandford, S. A., Imanaka, H., Nuevo, M. 2015. Ice chemistry on outer solar system bodies: Electron radiolysis of N₂-, CH₄-, and CO-containing ices. *Astrophys. J.* 812:150 (9pp).

Stern, S. A. and the *New Horizons* team. 2015, The Pluto system: Initial results from its exploration by *New Horizons*. *Science* 350 (issue 6258) pp. 1815-1-8.

Pluto Occultation with SOFIA on 29 June 2015 in Support of the New Horizons Flyby: Occultation Evidence for Haze

Amanda S Bosh^{1,2}, Michael J Person³, Carlos Zuluaga³, Amanda A Sickafoose^{3,22}, Stephen E Levine², Jay M Pasachoff⁴, Bryce A Babcock⁴, Edward W. Dunham², Ian McLean⁵, Jürgen Wolf⁶, Fumio Abe⁷, Eric Becklin^{5,8}, Thomas A Bida², Len P. Bright², Tim Brothers³, Grant Christie⁹, Peter L. Collins², Rebecca F Durst⁴, Alan C. Gilmore¹⁰, Ryan Hamilton⁸, Hugh C. Harris¹¹, Chris Johnson⁵, Pamela M. Kilmartin¹⁰, Molly R Kosiarek³, Karina Leppik⁸, Sarah Logsdon⁵, Robert Lucas¹², Shevill Mathers¹³, C.J.K. Morley¹⁴, Tim Natusch⁹, Peter Nelson¹⁵, Haydn Ngan⁹, Enrico Pfüller⁶, Hans-Peter Röser⁶, Stephanie Sallum¹⁶, Maureen Savage⁸, Christina H Seeger⁴, Hosea Siu³, Chris Stockdale¹⁷, Daisuke Suzuki¹⁸, Thanawuth Thanathibodee³, Trudy Tilleman¹¹, Paul J. Tristram¹⁹, William Vacca⁸, Jeffrey Van Cleve⁸, Carolle Varughese²⁰, Luke W. Weisenbach³, Elizabeth Widen²¹ and Manuel Wiedemann⁶, (1)Massachusetts Institute of Technology, Earth, Atmospheric, and Planetary Sciences, Cambridge, MA, United States, (2)Lowell Observatory, Flagstaff, AZ, United States, (3)Massachusetts Institute of Technology, Cambridge, MA, United States, (4)Williams College, Williamstown, MA, United States, (5)University of California Los Angeles, Los Angeles, CA, United States, (6)Universität Stuttgart, Stuttgart, Germany, (7)Nagoya University, Nagoya, Japan, (8)Universities Space Research Association Moffett Field, Moffett Field, CA, United States, (9)Auckland Observatory, Auckland, Australia, (10)University of Canterbury, Christchurch, New Zealand, (11)U.S. Naval Observatory Flagstaff Station, Flagstaff, AZ, United States, (12)Sydney University, Sydney, Australia, (13)Southern Cross Observatory, Cambridge, Australia, (14)Sandy Ridge Observatory, Moe, Australia, (15)Ellinbank Observatory, Ellinbank, Australia, (16)Steward Observatory, Tucson, AZ, United States, (17)Hazelwood Observatory, Melbourne, Australia, (18)University of Notre Dame, Notre Dame, IN, United States, (19)Mt. John University Observatory, Lake Tekapo, New Zealand, (20)Earth & Sky Limited, Lake Tekapo, New Zealand, (21)United States Antarctic Program, McMurdo Station, Antarctica, (22)South African Astronomical Observatory

Abstract

We report on a very successful observation of the Pluto Occultation of a bright star (R~12mag) on 29 June 2015 with four instruments on SOFIA. The SOFIA Aircraft was deployed from Christchurch New Zealand. Observations were performed at four wavelengths from 0.4 to 1.8 microns. Pre-event astrometry allowed for an in-flight update to the SOFIA team with the result that SOFIA was deep within the central flash zone. Combined analysis of the data sets, including complementary ground based observations, leads to the result that Pluto's middle atmosphere is essentially unchanged from 2011 and 2013 (Person et al. 2013; Bosh et al. 2015); there has been no significant expansion or contraction of the atmosphere. Additionally, we find that a haze component in the atmosphere is required to reproduce the light curves obtained. This haze scenario has implications for understanding the photochemistry of Pluto's atmosphere.

TITLE: *Power and Biological Potential*

AUTHORS: Tori M. Hoehler, Sanjoy Som, Chris Kempes, and Bo Barker Jørgensen

SCIENCE TOPIC: Astrobiology

ABSTRACT: The potential present day habitability of solar system bodies beyond Earth is limited to subsurface environments, where the availability of energy in biologically useful form is a paramount consideration. Energy availability is commonly quantified in terms of molar Gibbs energy changes for metabolisms of interest, but this can provide an incomplete and even misleading picture. A second aspect of life's requirement for energy – the rate of delivery, or power – strongly influences habitability, biomass abundance, growth rates, and, ultimately, rates of evolution. We are developing an approach to quantify metabolic power, using a cell-scale reactive transport model in which physical and chemical environmental parameters are varied. Simultaneously, we evaluate cell-specific energy flux requirements and their dependence on environmental “extremes”. Comparison of metabolic power supply and demand provides a constraint on how biomass abundance varies across a range of environmental parameters, and thereby a prediction of the relative habitability of different environments. We are evaluating the predictive capability of this approach through comparison to observed distributions of microbial abundance in a range of subsurface (predominantly serpentinizing) systems.

Global surface photosynthetic biosignatures prior to the rise of oxygen

M.N. Parenteau^{1,2}, N.Y. Kiang³, R.E. Blankenship⁴, E. Sanromá^{5,6}, E. Pallé^{5,6}, T.M. Hoehler²,
B.K. Pierson⁷, V.S. Meadows⁸

¹SETI Institute, Mountain View, CA 94043, Mary.N.Parenteau@nasa.gov; ²NASA Ames Research Center, Moffett Field, CA 94035; ³NASA Goddard Institute for Space Studies, New York, NY 10025; ⁴Departments of Biology and Chemistry, Washington University in St. Louis, St. Louis, MO 63130; ⁵Instituto de Astrofísica de Canarias (IAC), Vía Láctea s/n 38200, La Laguna, Spain; ⁶Departamento de Astrofísica, Universidad de La Laguna, Spain; ⁷Biology Department, University of Puget Sound, Tacoma, WA, 98416; ⁸Astronomy Department, University of Washington, Seattle, WA 98195.

Science topic: Exoplanets

The study of potential exoplanet biosignatures -- the global impact of life on a planetary environment -- has been informed primarily by the modern Earth, with little yet explored beyond atmospheric O₂ from oxygenic photosynthesis out of chemical equilibrium, and its accompanying planetary surface reflectance feature, the vegetation “red edge” reflectance. However, these biosignatures have only been present for less than half the Earth’s history, and recent geochemical evidence suggests that atmospheric O₂ may have been at very low - likely undetectable - levels, until 0.8 Ga (Planavsky et al., 2014, Science 346:635-638). Given that our planet was inhabited for very long periods prior to the rise of oxygen, and that a similar period of anoxygenic life may occur on exoplanets, more studies are needed to characterize remotely detectable biosignatures associated with more evolutionarily ancient anoxygenic phototrophs.

Our measurements of the surface reflectance spectra of pure cultures of anoxygenic phototrophs revealed “NIR edge(s)” due to absorption of light by bacteriochlorophyll (Bchl) pigments. We used the pure culture spectra to deconvolve complex spectra of environmental samples of microbial mats. We observed multiple NIR edges associated with multiple pigments in the mats. We initially expected only to detect the absorption of light by the pigments in the surface layer of the mat. Surprisingly, we detected cyanobacterial Chl *a* in the surface layer, as well as Bchl *c* and Bchl *a* in the anoxygenic underlayers. This suggests that it does not matter “who’s on top,” as we were able to observe pigments through all mat layers due to their different absorption maxima. The presence of multiple pigments and thus multiple “NIR edges” could signify layered phototrophic communities and possibly strengthen support for the detection of a surface exoplanet biosignature. In general, the proposed work will inform the search for life on exoplanets at a similar stage of evolution or biogeochemical state as the pre-oxic Earth.

Ionizing Radiation on the Surface of Europa: Implications for the Search for Evidence of Life. L. F. A. Teodoro^{1,4}; A. F. Davila^{1,2}; C. P. McKay¹; L. R. Dartnell³, R. C. Elphic¹, ¹NASA ARC, ²SETI, ³Department of Physics and Astronomy, University of Leicester, UK, ⁴BAERI. (luis.f.teodoro@nasa.gov)

Introduction: Europa's subsurface ocean is a possible abode for life, but it is inaccessible with current technology. However, 'Chaos' regions on the surface might provide direct access to materials originated from shallow pockets of liquid water within the ice shell, or even the subsurface ocean itself [1–6]. These would be ideal locations to search for possible evidence of life, such as organic biomarkers. The best case environment for such evidence would be the orbital "upstream" hemisphere, shielded from much of Jupiter's radiation belt flux, but where galactic cosmic rays (GCRs) still interact with surface materials. GCRs that strike unimpeded Europa's surface produce ionizing radiation in the form of high-energy electrons, protons, gamma rays, neutrons and muons. The effects of ionizing radiation in matter always involve the destruction of chemical bonds and the creation of free radicals. Both can destroy organic biomarkers over time [7, 8].

Using ionizing radiation transport codes, we recreated the most-favorable radiation environment on the surface of Europa, and evaluated its possible effects on organic biomarkers within the shallow ice-shell.

Methods: We performed a full Monte-Carlo simulation of the nuclear reactions induced by the Galactic cosmic rays hitting Europa's surface using the Planet-cosmic code [9]. This code is based on the GEANT-4 toolkit for the transport of particles through matter. The computational domain was comprised of 20 m of water ice. To model the GCR primary spectra for $Z = 1-26$ (protons to iron nuclei) we assumed the CREAME96 model under solar minimum.

Results: Our preliminary results show that the flux of ionizing radiation as a function of depth in Europa's ice shell is similar in magnitude to that estimated for the surface on Mars for pure ice [10]. As expected, pure ice results in an extensive environment of energetic neutrons, protons, electrons, muons and gamma rays, whose flux is highest within the top few meters. The flux of ionizing radiation can be converted into dosage at the molecular level using a "biologically-weighted" scheme [10]. The derived radiation dose at 1 meter depth is 0.3 Gy/yr. We emphasize that these results likely represent a best-case scenario for Europa, an estimation of the radiation environment resulting from galactic cosmic rays alone. Further work will focus on also taking into account the Jovian radiation environment. However, previous work has shown that this radiation environment is less penetrative (decimeters) [4]. We also expect that the presence of Jupiter will create anisotropies in the distribution of the GCR radiation environment.

Discussion: Our results indicate that dormant micro-

organisms within the top 1 meter of regolith of the most favorable European hemisphere would likely be killed in less than 150 kyr due to cumulative radiation damage. This survival time applies to radiation-resistant organisms such as *Deinococcus radiodurans*. More importantly, organic biomarkers such as complex biomolecules (i.e. proteins) would be severely damaged by ionizing radiation (either directly or indirectly) within the top 1 meter in time scales of 1-2 million years. For example, the immunoresponse (an indicator of molecular integrity) of several biological polymers, including proteins and exopolysaccharides, diminishes by >90% after exposure to 500 kGy of electron radiation, equivalent to 1.6 Myr exposure at 1 meter depth in Europa's ice-shell. Even smaller doses are sufficient to break the backbone of proteins into smaller fragments. Smaller organic molecules of astrobiological interest, such as amino acids, would also be affected by ionizing radiation. The D_{10} value for the radiolytic decomposition of glycine and alanine is reached after exposure to 20-30 MGy [8], equivalent to 60-90 Myr exposure at 1 meter depth in Europa's ice shell.

Our preliminary results indicate that even the best-case European radiation environment, created by galactic cosmic rays alone, biomolecules would be heavily damaged quickly. Complex organic molecules, including biomarkers, could become heavily processed in the top 1 meter in time scales >1 million years, and smaller organic molecules such as amino acids could be severely damaged in time scales <100 million years. Model age estimates of Europa's surface range between 60 and 100 million years [11], which would place serious limits on the preservation of organic biomarkers near the surface. However, age estimates of Chaos regions are lacking, and might be critical to the success of life detection missions. Hence, a better constraint on the surface age of Chaos regions on Europa might be critical to the success of such missions. If surface ice deposits are fresh and young, biomarkers may be preserved. For this reason it is important to confirm the existence of putative plumes of icy particles at Europa, such as exist at Enceladus. Such fresh particles, very recently erupted from deep liquid reservoirs, might be relatively undamaged and more likely to bear intact biomarkers. On the other hand, such particles are exposed to the full brunt of the Jovian radiation environment.

References: [1] Carr, M. H. et al. *Nature* 1998, 391, 363–365. [2] Greenberg, R. et al. *Icarus* 1999, 141, 263–286. [3] Goodman, J. C. J. *Geophys. Res.* 2004, 109. [4] Pappalardo, R. T. et al. *Nature* 1998, 391, 365–368. [5] Head, J. W. et al. *J. Geophys. Res.* 1999, 104, 27143. [6] Pappalardo, R. T. et al. *Astrobiology* 2013, 13, 740–773. [7] Dartnell, L. R. *Astrobiology* 2011, 11, 551–582. [8] Kminek, G.; Bada, J. *Earth Planet. Sci. Lett.* 2006, 245, 1–5. [9] Desorgher, L. et al. *Inter. J. Modern Physics. A* 20, 2005, 6802-6804. [10] Dartnell, L. R.; Desorgher, L.; Ward, J. M.; Coates, A. J. *Geophys. Res. Lett.* 2007, 34, 4–9. [11] Zahnle, K.; Alvarellos, J. L.; Dobrovolskis, A.; Hamill, P. *Icarus* 2008, 194, 660–674

A radiative transfer model for packed beds – sediments, biofilms, and microbial mats

Thomas E. Murphy, Stuart Pilorz, and Leslie E. Prufert-Bebout

Science topic: Astrobiology

Much of early life on Earth existed as single-celled organisms growing within sediment beds such as siliciclastic and carbonate sands, soils, and precipitated salt crusts in hypersaline or desert environments. These environments interact with incident light in such a way that the light regime at depth within these mineral matrices can vary significantly from the incident regime in terms of both magnitude and spectral content. This is particularly important for photosynthetic microorganisms, which require certain fluxes of photosynthetically active radiation, but are sensitive to excessive fluxes of ultraviolet (UV) radiation. A thorough understanding of the interaction of light with potentially habitable sediment beds is critical for modeling primary productivity on the early Earth, as well as for remotely detecting extraterrestrial biosignatures.

Previous research has focused on quantifying light regimes within biologically inhabited and uninhabited sediments, predominantly through an experimental approach. These experimental studies have elucidated general trends of light attenuation within sediments, but were inherently constrained in terms of the spectrum, direction, and angular distribution of incident light, as well as sediment type and grain size. On the other hand, a modeling approach can aid researchers in quickly and inexpensively investigating photic zone depths within a wide variety of sediment beds under a variety of incident light regimes.

This talk will present a radiative transfer tool we have built for modeling interaction between light and large particles such as quartz sands, salt grains, and microorganisms. The model traces rays through beds of explicitly defined particles (defined mineral compositions), which are modeled as spheroids. By tracking the fate of hundreds of thousands of simulated rays, we can quantify biologically important quantities such as the wavelength-dependent scalar irradiance (or fluence rate) as a function of depth within the bed, for given mineral type, fluid type between grains, grain size, and incident irradiance. By comparing the attenuation rates of photosynthetically useful light and harmful ultraviolet light, we can hypothesize on the locations and thickness of habitable zones below the surface.

The model presented here can also be used to simulate radiative transfer in densely packed systems of photosynthetic microorganisms. For such systems, the model can simulate not only the depth dependence of photosynthetically useful irradiance, but also the spectral reflectance signature, which is critical for remote biosignature detection.

This talk will describe the radiative transfer model we have built, including validation cases in which model output is compared to previously published experimental data. Then, several examples will be presented demonstrating the utility of the model in simulating radiative transfer in inhabited and uninhabited sediments under natural sunlight.

BASALT

Biologic Analog Science Associated with Lava Terrains

Authors: Darlene S.S. Lim, Jen Heldmann, Richard Elphic, Anthony Colaprete, Chris McKay, Andrew Mattioda, Linda Kobayashi, M. Deans, D. Lees, T. Cohen, Grace Lee, Trey Smith, Jessica Marquez, Steve Hillenius, Jeremy Frank, Terry Fong and BASALT team

This presentation will provide an overview of the BASALT (Biologic Analog Science Associated with Lava Terrains) program. BASALT research addresses Science, Science Operations, and Technology. Specifically, BASALT is focused on the investigation of terrestrial volcanic terrains and their habitability as analog environments for early and present-day Mars. Our scientific fieldwork is conducted under simulated Mars mission constraints to evaluate strategically selected concepts of operations (ConOps) and capabilities with respect to their anticipated value for the joint human and robotic exploration of Mars.

a) Science: The BASALT science program is focused on understanding habitability conditions of early and present-day Mars in two relevant Mars-analog locations (the Southwest Rift Zone (SWRZ) and the East Rift Zone (ERZ) flows on the Big Island of Hawai'i and the eastern Snake River Plain (ESRP) in Idaho) to characterize and compare the physical and geochemical conditions of life in these environments and to learn how to seek, identify, and characterize life and life-related chemistry in basaltic environments representing these two epochs of martian history.

b) Science Operations: The BASALT team will conduct real (non-simulated) biological and geological science at two high-fidelity Mars analogs, all within simulated Mars mission conditions (including communication latencies and bandwidth constraints) that are based on current architectural assumptions for Mars exploration missions. We will identify which human-robotic ConOps and supporting capabilities enable science return and discovery.

c) Technology: BASALT will incorporate and evaluate technologies in to our field operations that are directly relevant to conducting the scientific investigations regarding life and life-related chemistry in Mars-analogous terrestrial environments. BASALT technologies include the use of mobile science platforms, extravehicular informatics, display technologies, communication & navigation packages, remote sensing, advanced science mission planning tools, and scientifically-relevant instrument packages to achieve the project goals.

MULTICOLOR IMAGERY AND SPECTROSCOPY INSTRUMENTATION FOR PLANETARY SURFACE PROSPECTING OF VOLATILES. A. M. Cook^{1,2}, A. Colaprete¹, T. L. Roush¹, S. J. Thompson³, J. E. Benton^{1,4}, J. B. Forcione¹, R. Bielawski¹, E. Fritzler^{1,2}, R. McMurray¹. ¹NASA Ames Research Center, M/S 245-6, Moffett Field, CA 94035, ²Millennium Engineering and Integration, M/S 213, Moffett Field, CA 94035, ³Intrinsyx Technologies Corporation, Moffett Field, CA 94035, ⁴Wyle Engineering, Moffett Field, CA 94035.

Introduction: We present a demonstration of an instrument system built at NASA Ames Research Center, for in situ near-infrared spectral observations and visible imagery of planetary surfaces. The Near-InfraRed Volatile Spectrometer System (NIRVSS) is comprised of two main structural components, pictured in Figure 1: the spectrometer box, which houses two NIR spectrometers, and the “bracket” which includes a camera, 8 LEDs, optical fiber mounts for the spectrometers, a near-infrared source lamp, and 4 radiometers for long-wave infrared calibration purposes. The primary science goal of NIRVSS is to detect and characterize the abundance of OH and other volatiles on planetary surfaces.

Resource Prospector Mission: The current instrument design is driven primarily by requirements of the Resource Prospector rover mission to the lunar poles in ~2020. For this mission, NIRVSS serves as a prospecting instrument, mounted to the underside of the rover, viewing the ground over which the rover traverses. The two spectrometers span adjacent wavelength ranges (1.59 - 2.39 and 2.31- 3.39 microns) that target the detection of OH bands indicative of water, and other volatiles on the lunar surface. The near-IR source on the bracket projects a beam onto the ground beneath the rover, which is scattered and reflected back up in to the optical inputs for the spectrometer fibers. The four radiometers (8, 10, 12.5, and 25 microns) are

calibration instruments for low temperature surfaces with blackbody peaks outside of the range of the spectrometers. Finally, the newly-updated Drill Observation Camera (DOC) is outfitted with 8 LED illumination sources at 410, 540, 640, 740, 905, 940, 1050 nm, and a white broadband LED.

All components of NIRVSS are meant for use during both rover prospecting operations, and drilling operations over specific targets of interest. The system would provide the mission’s first measurements of increased OH-signatures, as subsurface soils are delivered to the surface by the RP drill.

Other Missions and Field Applications: The NIRVSS instrument provides capabilities that are useful beyond the Resource Prospector mission. A version of the instrument was used for a science-driven field campaign in the Mojave desert in 2014, to search for signs of hydration at the base of a cinder cone near Zzyzx. NIRVSS is slated for use in 2016 field tests in Idaho and at Mauna Kea, Hawaii. Likewise, missions to other planetary bodies would benefit from the use of the NIRVSS instrument, to identify water and other volatile materials in planetary soils, whether through spectroscopy, imaging, or a combination of both.

Figure 2 shows an example of mineralogical features in rock samples from a recent field test; rock inclusions are distinguishable by the DOC imaging system using the bank of multiwavelength LEDs on the bracket. These images can be correlated with spectral data from the same scene to confirm the presence of certain minerals as seen in 1.5 to 3.4-micron absorption bands.

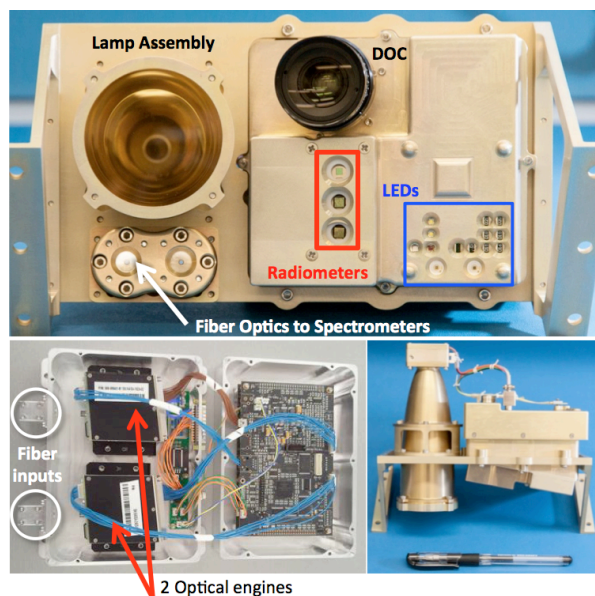


Figure 0. The NIRVSS Instrument

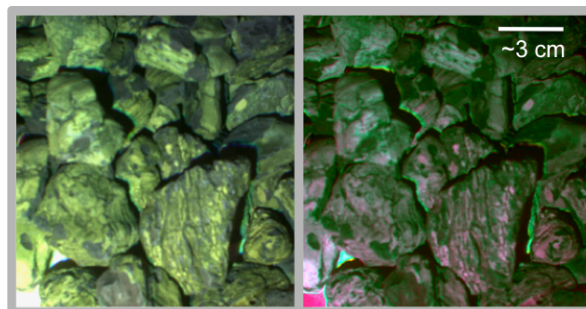


Figure 2. Example images from the Drill Observation Camera (DOC), demonstrating the ability of the NIRVSS system to distinguish small-scale mineralogical variation in sample rocks.

Using Neutron Spectroscopy to Constrain the Composition and Provenance of Phobos and Deimos

R. C. Elphic¹, P. Lee², M. E. Zolensky³, D. W. Mittlefehldt³, L. F. Lim⁴, A. Colaprete¹,
¹NASA Ames Research Center, Moffett Field, CA 94035 USA ²SETI Institute,
Mountain View, CA 94043 USA, ³NASA Johnson Space Center, Houston, TX 77058
USA, ⁴NASA Goddard Space Flight Center, Code 691, Greenbelt, MD 20771 USA

The origin of the martian moons Phobos and Deimos is obscure and enigmatic. Hypotheses include the capture of asteroids originally from the outer main belt or beyond, residual material left over from Mars' formation, and accreted ejecta from a large impact on Mars, among others. Measurements of reflectance spectra indicate a similarity to dark, red D-type asteroids, but could indicate a highly space-weathered veneer. Here we suggest a way of constraining the near-surface composition of the two moons, for comparison to known meteoritic compositions. Neutron spectroscopy, particularly the thermal and epithermal neutron flux, distinguishes clearly between various classes of meteorites and varying hydrogen (water) abundances. Perhaps most surprising of all, a rendezvous with Phobos or Deimos is not necessary to achieve this. A low-cost mission based on the LADEE spacecraft design in an eccentric orbit around Mars can encounter Phobos every 2 weeks. As few as five flyby encounters at speeds of 2.3 km/sec and closest-approach distance of 3 km provide sufficient data to distinguish between ordinary chondrite, water-bearing carbonaceous chondrite, ureilite, Mars surface, and aubrite compositions. A one-Earth year mission design includes many more flybys at lower speeds and closer approach distances, as well as similar multiple flybys at Deimos in the second mission phase, as described in the Phobos And Deimos Mars Environment (PADME) mission concept. This presentation will describe the expected thermal and epithermal neutron fluxes based on MCNP6 simulations of different meteorite compositions and their uncertainties.



"IT'S UNIFIED AND IT'S A THEORY, BUT IT'S NOT THE UNIFIED THEORY WE'VE ALL BEEN LOOKING FOR."

Pure and N-substituted Small Cyclic Hydrocarbon Synthesis in the Gas Phase: Path to PAHs and PANHs

Partha P. Bera^{1,2}, Timothy J. Lee², Roberto Peverati³, and Martin Head-Gordon³

1. Bay Area Environmental Research Institute
2. Space Science and Astrobiology Division, NASA Ames Research Center
3. University of California – Berkeley, Berkeley, CA

Science topic: Astrochemistry/Astrobiology

Molecules from simple to as complex as fullerenes have been identified in various astrophysical environments such as the interstellar media, dark clouds, hot cores, outflows of carbon stars, proto-planetary disks, and in the atmospheres of (exo)planets. How these large polyatomic molecules are synthesized in such exotic conditions is not well known, although various models exist. Molecular ions, including positive and negative ions have been identified in the atmospheres of other solar system bodies such as in the ionosphere of Titan. Barrier-less ion-molecule interactions may play a major role – ions provide electrostatic steering force – in guiding molecules towards each other and initiating reactions. We study these condensation pathways to determine whether they are a viable means of forming large pure and nitrogen-containing hydrocarbon chains, stacks, and even cyclic compounds. We employed accurate quantum chemical methods to investigate the processes of growth, structures, mechanisms, and spectroscopic properties, such as UV-Visible and vibrational IR spectra of the ensuing ionic products after pairing small carbon, hydrogen, and nitrogen-containing molecules with similar hydrocarbon ions. We found the molecular building blocks of polycyclic aromatic hydrocarbons such as phenyl cations can form very easily by the combination of smaller hydrocarbons followed by hydrogen loss. We have investigated how nitrogen atoms are incorporated into the carbon ring during growth. Specifically, we explored the mechanisms by which the synthesis of pyrimidine will be feasible in the atmosphere of Titan in conjunction with ion-mobility experiments. We used accurate *ab initio* coupled cluster theory, Møller-Plesset perturbation theory, density functional theory (DFT), and coupled cluster theory (CCSD(T)) quantum chemical methods together with large correlation consistent basis sets in these investigations. We found that a series of hydrocarbons with a specific stoichiometric composition prefers cyclic molecule formation rather than chains.

P. P. Bera, Martin Head-Gordon, and Timothy J. Lee *Astron & Astrophys.* 535, A74, (2011)

P. P. Bera, M. Head-Gordon, and T. J. Lee, 15, 2012-2023, *Phys. Chem. Chem. Phys.* (2013)

P. P. Bera, R. Peverati, M. Head-Gordon, and T. J. Lee, *J. Phys. Chem. A*, 118, 10109 (2014)

A. Hamid, P. P. Bera, T. J. Lee, S. Aziz, A. Al-Youbi, M. S. El-Shall, *J. Phys. Chem. Lett.* 5, 3392-3398 (2014)

P. P. Bera, Roberto Peverati, Martin Head-Gordon and Timothy J. Lee, *Phys. Chem. Chem. Phys.* 17, 1859 (2015)

R. Peverati, P. P. Bera, Martin Head-Gordon and Timothy J. Lee, Submitted to *ApJ*, (2015)

THE FORMATION OF NUCLEOBASES FROM THE IRRADIATION OF PURINE IN ASTROPHYSICAL ICES. S. A. Sandford¹, C. K. Materese^{1,2}, and M. Nuevo^{1,2}, ¹NASA Ames Research Center (Scott.A.Sandford@nasa.gov), ²Bay Area Environmental Research Institute.

Introduction: *N*-heterocycles have been identified in meteorites and their extraterrestrial origins have been suggested by isotopic ratio measurements [1]. Although small *N*-heterocycles have never been detected in the ISM, recent experiments in our lab have shown that the irradiation of the aromatic molecules benzene (C₆H₆) and naphthalene (C₁₀H₈) in mixed molecular ices leads to the formation of *O*- and *N*-heterocyclic molecules [2]. Among the class of *N*-heterocycles are the nucleobases, which are of astrobiological interest because they are the information bearing units of DNA and RNA. Nucleobases have been detected in meteorites [3–4], with isotopic signatures that are also consistent with an extraterrestrial origin [1]. Three of the biologically relevant nucleobases (uracil, cytosine, and guanine) have a pyrimidine core structure while the remaining two (adenine and guanine) possess a purine core. Previous experiments in our lab have demonstrated that all of the biological nucleobases (and numerous other molecules) with a pyrimidine core structure can be produced by irradiating pyrimidine in mixed molecular ices of several compositions [5–7].

In this work, we study the formation of purine-based molecules, including the nucleobases adenine, and guanine from the ultraviolet (UV) irradiation of purine in ices consisting of mixtures of H₂O and NH₃ at low temperature. The experiments are designed to simulate the astrophysical conditions under which these species may be formed in the interstellar medium, dense molecular clouds, or on the surfaces of icy bodies of the Solar System.

Experimental: Gas mixtures were prepared in bulbs attached to a glass line. The relative proportions of each component was established by partial pressure. An evacuated sample tube containing pure purine was prepared separately, attached to the vacuum chamber, and wrapped with heat tape and a thermocouple to monitor the temperature. The bulbs containing gas mixtures were deposited on an aluminum foil attached to a cold finger (< 20 K) along with purine from the heated sample tube. The combined ice formed from the gases and purine were simultaneously irradiated with an H₂-discharge lamp emitting UV photons (Lyman α at 121.6 nm and a continuum at ~160 nm). After irradiation, samples are warmed to room temperature, and refractory residues are recovered for derivatization and analysis using gas chromatography coupled with mass spectroscopy.

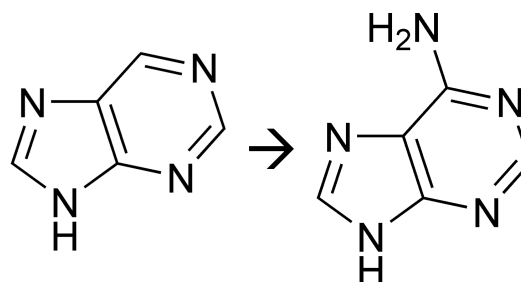


Fig. 1. The UV photoirradiation of purine (left) in H₂O and NH₃, containing ices leads to the production of functionalized purines including the nucleobase adenine (right).

Results: The UV irradiation of our experimental ice mixtures results in the formation of refractory residues containing functionalized purines. This included the nucleobases adenine (Figure 1) and possibly guanine, in addition to hypoxanthine, isoguanine, aminopurines, and 2,6-diaminopurine. Notably, while adenine is one of the most abundant photoproducts of these UV-irradiation experiments, guanine appears to be produced with very low to undetectable levels of abundance. One possible explanation of this is the propensity of guanine to form strong hydrogen bonds with itself and other molecules, greatly reducing its solubility in most solvents and thereby making it more difficult to derivatize and detect in the GC-MS. Another possible explanation for the low abundance may be that guanine production is far less favorable than some alternative structural isomers.

References: [1] Martins Z. et al. (2008) *Earth Planet. Sci. Lett.*, 270, 130. [2] Materese et al. 2015. *ApJ* 800, 116 [3] van der Velden W. and Schwartz A. (1977) *Geochim. Cosmochim. Acta*, 41, 961. [4] Stoks P. and Schwartz A. (1979) *Nature*, 282, 709. [5] Nuevo M. et al. 2009. *Astrobiology* 9:683–695. [6] Nuevo M. et al. 2012. *Astrobiology* 12:295–314. [7] Materese et al. 2013. *Astrobiology* 13:948–962.

Sugars and Sugar Derivatives in Residues Produced from the UV Irradiation of Astrophysical Ice Analogs

Michel Nuevo,^{1,2,*} Scott A. Sandford,¹ and George W. Cooper¹

¹NASA Ames; ²BAER Institute

*e-mail: michel.nuevo-1@nasa.gov

Topic: Astrobiology

A large variety and number of organic compounds of prebiotic interest are known to be present in carbonaceous chondrites. Among them, one sugar (dihydroxyacetone) as well as several sugar acids, sugar alcohols, and other sugar derivatives have been reported in the Murchison and Murray meteorites [1]. Their presence, along with amino acids, amphiphiles, and nucleobases [2-6] strongly suggests that molecules essential to life can form abiotically under astrophysical conditions. This hypothesis is supported by laboratory studies on the formation of complex organic molecules from the ultraviolet (UV) irradiation of simulated astrophysical ice mixtures consisting of H₂O, CO, CO₂, CH₃OH, CH₄, NH₃, etc., at low temperature. In the past 15 years, these studies have shown that the organic residues recovered at room temperature contain amino acids [7-9], amphiphiles [4], nucleobases [10-13], as well as other complex organics [14-16].

However, no systematic search for the presence of sugars and sugar derivatives in laboratory residues have been reported to date, despite the fact that those compounds are of primary prebiotic significance. Indeed, only small (up to 3 carbon atoms) sugar derivatives including glycerol and glyceric acid have been detected in residues so far [14-16]. In this work, we carried out a systematic search for sugars and sugar-related compounds in organic residues produced from the UV irradiation of simple CH₃OH and H₂O+CH₃OH ices, and show that they contain several sugar alcohols up to 5 carbon atoms long, as well as sugars and sugar acids up to 4 carbon atoms long [17]. Results are briefly compared with meteoritic data [1].

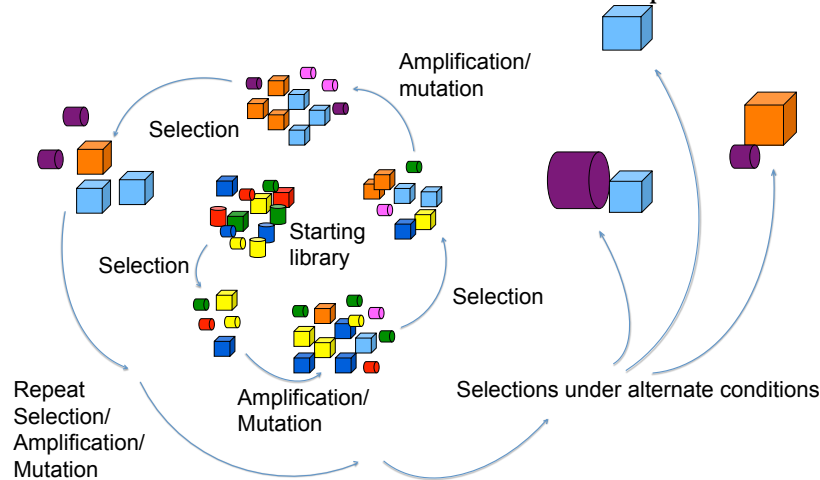
References:

[1] Cooper, G.W., et al., *Nature*, **414**, 879 (2001). [2] Kvenvolden, K., et al., *Nature*, **228**, 923 (1970). [3] Cronin, J.R. & Pizzarello, S., *Science*, **275**, 951 (1997). [4] Dworkin, J.P., et al., *PNAS*, **98**, 815 (2001). [5] Folsome, C.E., et al., *Nature*, **232**, 108 (1971). [6] Stoks, P.G. & Schwartz, A.W., *Nature*, **282**, 709 (1979). [7] Bernstein, M.P., et al., *Nature*, **416**, 401 (2002). [8] Muñoz Caro, G.M., et al., *Nature*, **416**, 403 (2002). [9] Nuevo, M., et al., *OLEB*, **38**, 37 (2008). [10] Nuevo, M., et al., *Astrobiol.*, **9**, 683 (2009). [11] Nuevo, M., et al., *Astrobiol.*, **12**, 295 (2012). [12] Materese, C.K., et al., *Astrobiol.*, **13**, 948 (2013). [13] Nuevo, M., et al., *ApJ*, **793**, 125 (2014). [14] Nuevo, M., et al., *Astrobiol.* **2010**, *10*, 245 (2010). [15] de Marcellus, P., et al., *Astrobiol.*, **11**, 847 (2011). [16] de Marcellus, P., et al., *PNAS*, **112**, 965 (2015). [17] Nuevo, M., et al., *In prep.*

Molecular crowding and evolution of ligase ribozymes
 Milena Popović and Mark A. Ditzler
 Astrobiology

Abstract

The cellular environments in which RNA functions in contemporary biology are characterized by extensive macromolecular crowding which is a feature likely shared by protocellular life and by the environments of prebiotic synthesis from which life emerged. Despite its importance, this environmental parameter has not been explored through *in vitro* evolution. To learn about the impact of molecular crowding on evolution of RNA ligases and, in general, RNA function, we have evolved ligase ribozymes in buffered solutions and under crowded conditions. Populations evolved under crowded conditions display similar levels of activity in both the buffered solutions and under crowded conditions. In contrast, populations evolved in buffered solutions show a marked decrease in activity when assayed under crowded conditions. These findings suggest that different environments result in evolution of different environmental specificities.



Poster

The affect of the space environment on the survival of *Halorubrum chaoviator* and *Synechococcus* (Nägeli): Data from the Space Experiment OSMO on EXPOSE-R

R. L. Mancinelli, Bay Area Environmental Research Institute, MS 239-4 NASA Ames Research Center, Moffett Field CA 94043, USA

Topic: Astrobiology

We have shown using ESA's Biopan facility flown in Earth orbit that when exposed to the space environment for two weeks the survival rate of *Synechococcus* (Nägeli), a halophilic cyanobacterium isolated from the evaporitic gypsum-halite crusts that form along the marine intertidal, and *Halorubrum chaoviator* a member of the Halobacteriaceae isolated from an evaporitic NaCl crystal obtained from a salt evaporation pond, were higher than all other test organisms except *Bacillus* spores. These results led to the EXPOSE-R mission to extend and refine these experiments as part of the experimental package for the external platform space exposure facility on the ISS. The experiment was flown in February 2009 and the organisms were exposed to low-Earth orbit for nearly 2 years. Samples were either exposed to solar UV-radiation ($\lambda > 110$ nm or $\lambda > 200$ nm, cosmic radiation [dosage range 225 to 320 mGy], or kept in darkness shielded from solar UV-radiation. Half of each of the UV radiation exposed samples and dark samples were exposed to space vacuum and half kept at 10^5 pascals in argon. Duplicate samples were kept in the laboratory to serve as unexposed controls. Ground simulation control experiments were also performed. After retrieval, organism viability was tested using Molecular Probes Live-Dead Bac-Lite stain and by their reproduction capability. Samples kept in the dark, but exposed to space vacuum had a $90 \pm 5\%$ survival rate compared to the ground controls. Samples exposed to full UV radiation for over a year were bleached and although results from Molecular Probes Live-Dead stain suggested $\sim 10\%$ survival, the data indicate that no survival was detected using cell growth and division using the most probable number (MPN) method. Those samples exposed to attenuated UV radiation exhibited limited survival. Results from of this study are relevant to understanding adaptation and evolution of life, the future of life beyond earth, the potential for interplanetary transfer of viable microbes via meteorites and dust particles as well as spacecraft, and the physiology of halophiles.

Ecological genomics of the newly discovered filamentous diazotrophic cyanobacterium, ESFC-1

R Craig Everroad, Angela M Detweiler, Leslie Prufert-Bebout, Brad M Bebout

Science topic: Astrobiology

Cyanobacteria played a key role in the evolution of the early Earth. The ecology of these photoautotrophs is important; they provide a model for exploring the relationships between ecology, evolution and biogeochemistry. The nonheterocystous filamentous cyanobacterium, strain ESFC-1, is a recently described member of the order *Oscillatoriales* within the *Cyanobacteria*. ESFC-1 has been shown to be a major diazotroph in the intertidal microbial mat system at Elkhorn Slough, CA, USA. Based on phylogenetic analyses of the 16S RNA gene, ESFC-1 appears to belong to a unique, genus-level divergence; the draft genome sequence of this strain has now been determined. Here we report features of this genome as they relate to the ecological functions and capabilities of strain ESFC-1. One striking feature of this cyanobacterium is the apparent lack of either the uptake or bi-directional hydrogenases typically expected to be found within a diazotroph. Culture-based experiments exploring the hydrogen-related metabolic processes of ESFC-1 also indicate these hydrogenases are absent. The combination of genomics with culture-based experimental research is a powerful tool for understanding microbial processes in complex ecosystems.

Transformations and Fates of Lipid Biomarkers in Microbial Mat Ecosystems

Linda Jahnke¹, Carina Lee², Mary Nichol Parenteau^{1,3}, Megan Carlson^{1,4}, Mike Kubo^{1,3}, Gorden Love², David Des Marais¹

¹NASA Ames Exobiology Branch, ²University of California Riverside, ³SETI Institute, ⁴Santa Clara University

Topic: Astrobiology

The study of well-preserved evaporitic microbial assemblages and silicified stromatolites have contributed substantially to Precambrian paleobiology. Over two decades of research at Guerrero Negro have created an extensive database on the biogeochemistry, diversity and organic biomarkers of these mats. Cyanobacterial mats differ from typical marine sediments in ways that can affect organic diagenesis. Mats typically have less available iron, higher rates of sulfur cycling and more abundant cyanobacterial sheaths and other EPS. Heterotrophs degrade biomolecules and provide smaller compounds to other biota, but functionalized biomarkers are also sequestered in macromolecules and thus protected from further diagenesis. The application of *hydropyrolysis* (HyPy) can identify biomarkers in these macromolecules and help characterize the processes involved in their preservation.

In this study we have attempted to characterize the solvent-extractable biomarkers in the mat and underlying sediments to link this work with previous studies of microbial diversity and by using HyPy to characterize lipid biomarkers bound to the insoluble biopolymer fractions.

Cyanobacterial mats are one of the most diverse ecosystems known, which is further reflected by their highly diverse lipid composition. Solvent extractables include intact polar lipids characteristic of the viable community. Changes in fatty acid community structure were apparent with depth. Abundant sterol ($C_{29}>C_{27}>C_{28}$) was present in the surface 2mm. With depth, sterol abundance and molecular variation increased, and formation of sterenes became prevalent. Only small amounts of hopanoids were recovered from the surface. Free hopanes and hopanic acid increased with depth but methylated compounds were rare. By contrast, HyPy released relatively high amounts of extended hopanes, including methyl forms, with roughly equivalent hopane to sterane ratios. These preliminary observations indicate that hopanoids are more readily sequestered during diagenesis as a potential consequence of early binding of their polyol side-chains.

Lipid Biomarker Abundance in Surface Guerrero Negro Mat and Lower Anaerobic Community

Right Panel: Pond 4 mat core (note mm scale) with sampled layers showing extractable lipids and cell numbers (based on total ester-linked fatty acid).

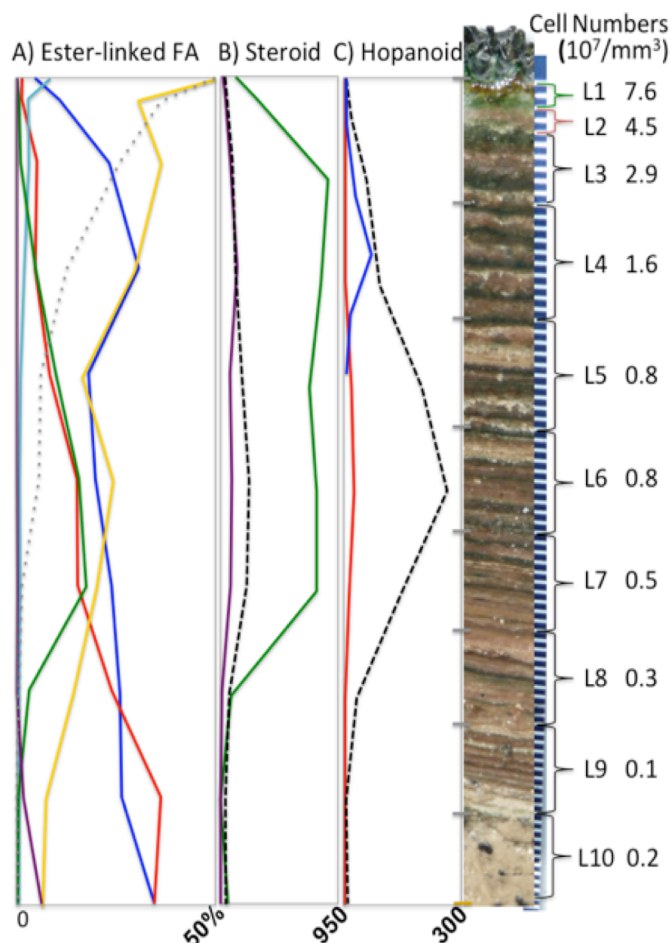
Panel A) Total intact polar lipid fatty acids (IPL-FA) ranging from 17,045 (L1) to 126 (L9), 209 (L10) $\mu\text{g/g}$ carbon (DOTS).

Individual IPL-fatty acids shown as % of total. **GOLD**, monounsaturated; **AQUA**, polyunsaturated; **BLUE**, total branched (iso-, anteiso-, 10Me16, 10Me18); **RED**, normal-long chain (C_{22} to C_{32}); **GREEN**, 2Me- and 2,X-diMe- C_{17} to C_{24} ; **PURPLE** vinyl ether dimethylacetals.

Panels B and C, $\mu\text{g/g}$ carbon:

B) Steroids: **GREEN**, sterols (below 50 mm sterols present only as unresolved complex mixture); **PURPLE**, tetrahymenol and Me-tetrahymenol; Dashed, diagenetic sterane/-ene and steric acid.

C) Hopanoids: **BLUE**, extractable bacteriohopanepolyol; **RED**, diploptene; Dashed, diagenetic hopanol, hopanate and hopane/-ene.



Nitrogen cycle in microbial mats: completely unknown?

Oksana Coban, Brad Bebout

Science topic: Astrobiology

Microbial mats are thought to have originated around 3.7 billion years ago, most likely in the areas around submarine hydrothermal vents, which supplied a source of energy in the form of reduced chemical species from the Earth's interior. Active hydrothermal vents are also believed to exist on Jupiter's moon Europa, Saturn's moon Enceladus, and on Mars, earlier in that planet's history. Microbial mats have been an important force in the maintenance of Earth's ecosystems and the first photosynthesis was also originated there.

Microbial mats are believed to exhibit most, if not all, biogeochemical processes that exist in aquatic ecosystems, due to the presence of different physiological groups of microorganisms therein. While most microbially mediated biogeochemical transformations have been shown to occur within microbial mats, the nitrogen cycle in the microbial mats has received very little study in spite of the fact that nitrogen usually limits growth in marine environments.

The aim of this research is a determination of a complete nitrogen budget for a photosynthetic microbial mat. For this, quantification of both in situ sources (N fixation, mineralization of organic nitrogen and uptake of both inorganic and organic nitrogen from the overlying water) and sinks (ammonium and nitrate assimilation, nitrification, denitrification, dissimilatory nitrate reduction, and anaerobic ammonium oxidation) of nitrogen in photosynthetic microbial mats will be performed. A detailed investigation of nitrogen transformations in microbial mats will be performed with a particular focus on recently described, but poorly understood, processes, e.g., anammox and dissimilatory nitrate reduction, and an emphasis on understanding the role that nitrogen cycling may play in generating biogenic nitrogen isotopic signatures and biomarker molecules.

The research will use a combination of measurements of stable isotopic signatures, stable isotope labeling, and molecular ecological techniques not previously deployed in microbial mats. Measurements of environmental controls on nitrogen cycling will offer insight into the nature of co-evolution of these microbial communities and their planets of origin. Identifying the spatial (microscale) as well as temporal (diel and seasonal) distribution of nitrogen transformations, e.g., rates of nitrification and denitrification, within mats, particularly with respect to the distribution of photosynthetically-produced oxygen, is anticipated.

The results of this work will help us to improve our understanding of the cycle of the element most responsible for limiting the production of biomass on Earth and improved an ability to use stable isotopes of nitrogen, and nitrogen containing compounds, in our search for life elsewhere.

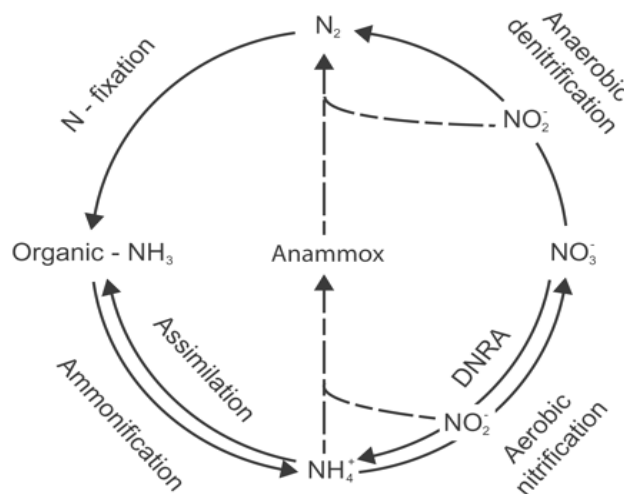


Figure 1 Microbial nitrogen cycle (from Trimmer et al. 2003)

Nearing the cold-arid limits of microbial life in permafrost of an upper dry valley, Antarctica

J. Goordial (McGill), A. Davila (NASA/SETI), D. Lacelle (U Ottawa), W. Pollard (McGill), M.M. Marinova (NASA/SpaceX), C.W. Greer (McGill), J. DiRuggiero (JHU), C.P. McKay (NASA) and L.G. Whyte (McGill)

Topic: Astrobiology

Characterized as among the most old, cold and arid environments on Earth, the Upper McMurdo Dry Valleys (UDV) in Antarctica, are one of the harshest environments on earth for life. Soils experience wide temperature fluctuations, cold temperatures, extreme aridity, oligotrophy, high incidence radiation and physical disturbance. This region is the only place on Earth where there is the presence of both permanently frozen ice-cemented ground (permafrost) overlain with a layer of dry, ice-free permafrost soil. University Valley is a high elevation (1800 m) UDV, which never experiences air temperatures above 0°C, and is one of the coldest and driest places on Earth. Erosion of the valley walls form the valley floor, and are lined with photosynthetic and heterotrophic cryptoendolithic communities which live in the protected and more clement conditions provided by the lithic habitat. In the present study we sought to (1) characterize the microbial biomass and community composition in dry and ice-cemented permafrost, (2) examine the molecular capacity for cold-adapted cryptoendolithic and permafrost communities through metagenomic data and (3) determine whether University Valley permafrost soils and cryptoendoliths support active microbial life at ambient conditions.

Bacterial and fungal isolates were cultured at cold and subzero temperatures. Only 6 microorganisms have been isolated from permafrost, two of which (a *Rhodococcus* sp., and *Rhodotorula* sp.) are capable of subzero growth down to -5°C and -10°C respectively. Microbial biomass measurements by direct cell counts found very low biomass (10^3 cells g⁻¹) in dry and ice cemented permafrost, orders of magnitude below permafrost from the Arctic or lower Dry Valley soils. No measureable CO₂ respiration was detectable in University Valley permafrost either *in situ* or by using radiolabelled respiration assays. The results of the permafrost respiration assays contrasted with those measured in the cryptoendolith samples, where microbial activity was detected at temperatures down to -20°C. 454 Pyrosequencing was carried out throughout two permafrost cores and two cryptoendoliths, and high diversity and heterogeneity was found in Bacterial communities, but low diversity in Archaeal and Fungal communities. Surprisingly, permafrost samples were found to share very few OTUs with cryptoendolith samples which are thought to seed the valley floor.

Metagenomic sequencing indicates that cryptoendolithic microorganisms are adapted to the harsh environment and capable of metabolic activity at *in situ* temperatures, possessing a suite of stress response and nutrient cycling genes to fix carbon under the fluctuating conditions that the sandstone rock would experience during the summer months. In contrast, permafrost soils have a lower richness of stress response genes, and instead are enriched in genes involved with dormancy and sporulation.

Our results underlie two different habitability conditions under extreme cold and dryness: the permafrost soils that select for traits which emphasize survival and dormancy rather than growth and activity by a functional cold adapted community; and the cryptoendolithic environment that selects for organisms capable of growth under extremely oligotrophic, arid, and cold conditions. Our results add to a growing body of evidence that life in such extreme environments is limited to specialized lithic habitats at very small scales.

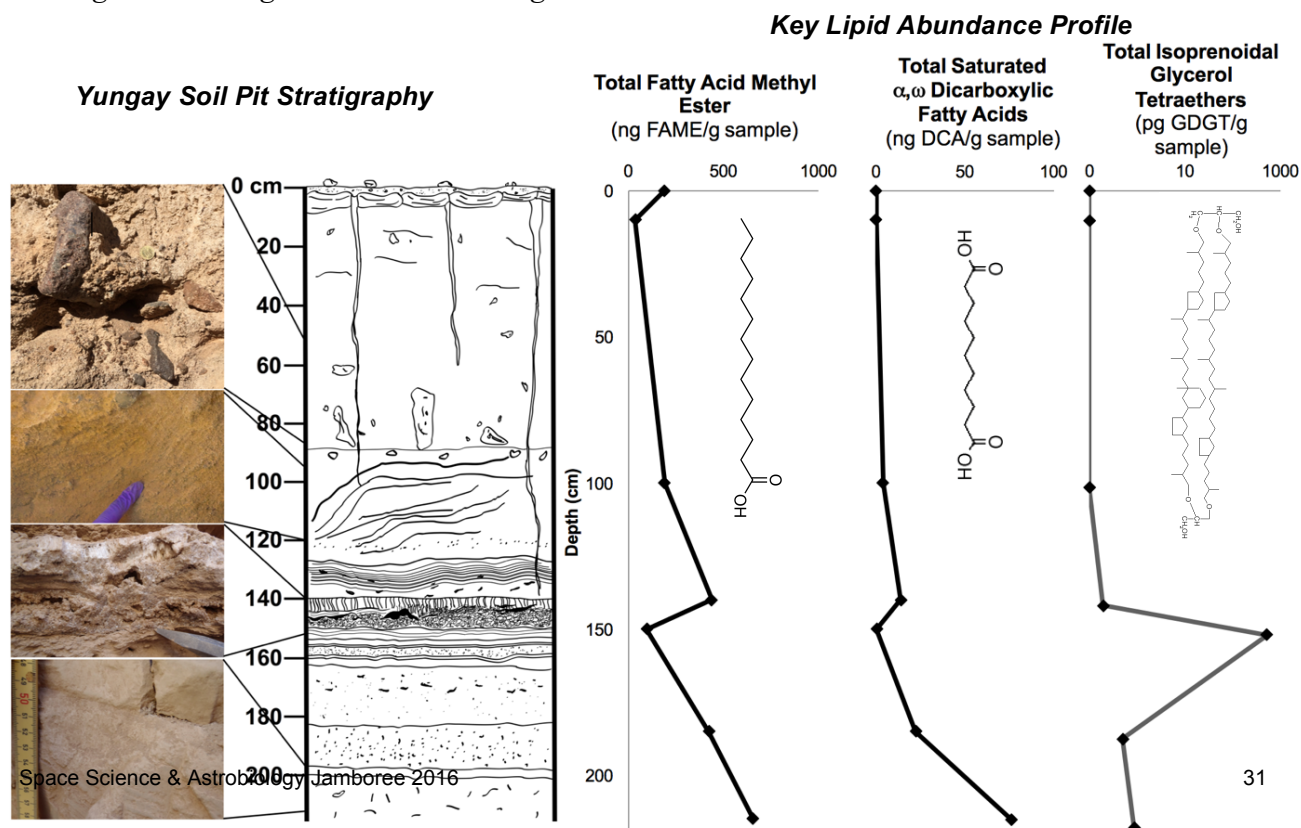
Publication: Goordial et al. (2016) The ISME Journal advance online publication, 19 January 2016; doi:10.1038/ismej.2015.239.

Xeropreservation of million-year-old functionalized lipid biomarkers in hyperarid soils in the Atacama Desert, Chile

Mary Beth Wilhelm (*Georgia Tech/NASA Ames SST & SSX*), Alfonso F. Davila (*SETI*), Mary N. Parenteau (*SETI, NASA Ames SSX*), Linda L. Jahnke (*NASA Ames SSX*), Jennifer L. Eigenbrode (*NASA Goddard*), Roger Summons (*MIT*), Xiaolei Liu (*MIT*), Brian N. Stamos (*UT Arlington*), James Wray (*GT*), Shane S. O'Reilly (*MIT*), Amy Williams (*Towson University, NASA Goddard*)

Topic: Astrobiology

Abstract: The accumulation and degree of preservation of lipid biomarkers was investigated in hyperarid soils in the Yungay region of the Atacama Desert. Lipids from seven soil horizons in a 2.5 m vertical soil profile were extracted and analyzed using GC-MS and LC-MS. Diagnostic modern, functionalized lipids and geolipids were detected, and increased in abundance and diversity with depth. The highest concentrations were found in a layered clay unit at the bottom of the profile. The remarkable degree of structural and chemical preservation of functional groups and unsaturated bonds indicate that minimal degradation has occurred since the time of deposition. Given that the clay horizon had been sealed off from exposure to rainwater and modern surficial processes for the last 2 My by an upper well-cemented halite unit, the dominant preservation process in this hyperarid setting is xeropreservation (preservation by drying). Characterization of such a process is key for understanding the potential preservation of organics in extremely hyperarid Martian sediments. In addition, the vertical succession of lipid biomarkers reflects major changes in microbial and eukaryotic groups possibly linked to changes in the hydrological regime, and can be used to reconstruct the process of environmental change in the region since the Neogene.



Seeking Signs of Life in Nili Patera with Icelandic Sinter Field Exploration.
John Roma (J.R.) Skok
Astrobiology

The past decade of Martian orbital and surface exploration has made it clear that the planet could have supported life as we know it in multiple times and locations. The next step in astrobiological exploration will be to find the evidence for and characterize any preserved Martian life. The jump from confirming habitability to finding life will be difficult and likely require a systemic surface exploration of multiple, specific sites. One site, the sinter mounds of the Nili Patera caldera, provides the ideal combination of hot, neutral to alkaline waters that can develop or support life and the sinter precipitation to preserve it. Nili Patera also provides deposits that are well mapped from orbit allowing a mission to pinpoint the target rocks.

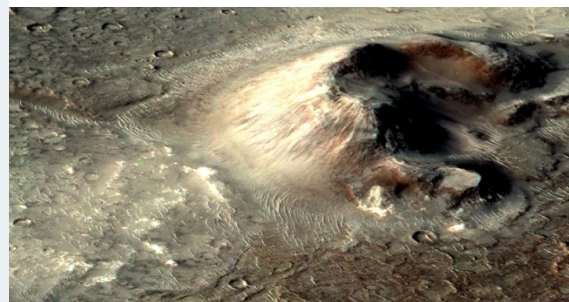
With this target known, we can develop the mission, the payload and the science to fit the goals. Several sinter field sites in Iceland were selected as an analog mission site. They were selected to provide diversity in scale, chemistry and complexity. At each site, we asked the same questions that would drive a mission to Mars. Was there life? What are its preserved properties? What are the environmental history of the sinters and the volcanic history of the local terrain? These questions were investigated with spectral, compositional and morphological analysis. By investigating these questions in Iceland, we will determine which observations, in terms of terrain access and instrument selection are required for mission success on Mars.

We report the results from the August 2015 expedition, the first of two planned field seasons. This summer was focused on finalizing the field locations, acquiring mapping data and an initial sampling campaign to determine expected composition and calibrate instruments for year two. With this information, we will determine an investigation plan consistent with a range of mission types from robotic lander to sample return to human exploration. We will also determine the instruments required by the site diversity. By the end of the project we should know what mission types can provide the required results. Which instruments are required for basic mission success and the cost benefit of additional analysis and what basic science questions must be investigated before sending a focused mission to determine the past existence of life in the Nili Patera sinter mounds.

Iceland Sinter



Martian Sinter



TITLE: *Science Outreach: The CROMO Drilling Project*

AUTHORS: Kubo, M. D. Y., Hoehler, T. M., Schrenk, M., McCollom, T., Cardace, D.

SCIENCE TOPIC: Astrobiology

ABSTRACT: Earth appears to be the only body in the solar system capable of supporting a surface biosphere in the present. To understand, better, the factors that would support the habitability of subsurface environments, we are investigating the microbial community associated with an actively serpentinizing system in northern California. Specifically, a dedicated drilling project with subsequent monitoring has enabled the development of a subsurface “microbial observatory” – the Coast Range Ophiolite Microbial Observatory (CROMO) – in which biological dynamics can be examined within a changing physicochemical context. The observatory is sited on the McLaughlin Natural Reserve, and was developed in close coordination with the UC Natural Reserve System.

In the fall of 2015, we were invited to develop an outreach exhibit for an event at the University of California System’s Office of the President, and subsequently at the UC Davis Natural Reserve System’s 50th Anniversary Fair at U.C. Davis. These exhibits created a unique opportunity to conduct outreach relating to CROMO, and to astrobiology in general, with an audience of prominent non-scientists, including policy makers within and outside the UC system. The poster developed for these events, and a discussion of the interactions had there, will be presented.

THE LASSEN ASTROBIOLOGY INTERN PROGRAM. David J. Des Marais¹, Sandra L. Dueck¹, Hilary B. Davis², Mary N. Parenteau³ and Michael D. Kubo^{1,3}, ¹Exobiology Branch, NASA Ames Research Center, Moffett Field, CA, ²Technology for Learning, North Kingston, RI, ³SETI Institute, Mountain View, CA (Mail Stop 239-4, NASA Ames Research Center, Moffett Field, CA 94035; david.j.desmarais@nasa.gov)

Science topic: Astrobiology

Since 2009 scientists on the Ames Team of the NASA Astrobiology Institute have collaborated with staff at Lassen Volcanic National park and Red Bluff High School, CA to offer this program to junior and senior students. The program provided an authentic place-based hand-on educational opportunity for students to interact directly with research scientists as they learned concepts in astrobiology, conducted field and laboratory research and prepared technical reports.

Concepts: Students learned about the following key concepts in astrobiology: 1) Geological processes interact with solar radiation to shape planetary climates. Such interactions can create and sustain habitable environments where diverse life forms can persist, forming a biosphere. 2) Our biosphere consisted solely of microbial life for more than 80% of its documented 3.7 billion year history. 3) Certain key resources and clement conditions must be available simultaneously to create habitable environments. These requirements can be met in diverse ways that, in turn, can sustain diverse life forms. 4) Volcanic hydrothermal processes create habitable environments. Hydrothermal activity has occurred on Mars. Thus Lassen Volcanic National Park (LVNP) enables research on environments that also occurred on other planets and are key targets to search for life.

Implementation: The curriculum followed the progression of a scientific investigation, starting with literature review and fieldwork and ending with written reports and oral presentations. Each part provided opportunities for students to acquire skills that they would need in a science or technology career.

Online lectures on astrobiology. Recorded online lectures provides the students with basic background about astrobiology (geology, microbiology, water chemistry, etc.). This allowed us to focus on hands-on activities and discussions when we met with the students weekly either in person or via videoconference.

Fieldwork. Three research teams, each consisting of juniors led by a senior, documented volcanic rocks, mineral deposits, hot spring waters and microbial life in Warner Valley, LVNP. They investigated and compared these features at three sites – a near-neutral pH stream and an alkaline and an acidic hot spring.

Laboratory exercises. Students conducted laboratory experiments to analyze minerals in rocks, investigate reactions between rock and simulated spring waters, and culture microorganisms collected in the field.

Examples of student findings. 1) Relative abundances of elements in spring water solutes correlated with the relative elemental abundances in the rocks hosting the springs. 2) Volcanic gases and their oxidation products can greatly enhance rates of rock weathering relative to rates that occur in surface waters. 3) The pH of spring waters reflected the effects of volcanic gases and their reactions with volcanic rocks. 4) Solutes in hot spring waters provided key nutrients for microbes. 5) The abundance and diversity of microbes decreased from neutral pH streams to alkaline hot spring waters to highly acidic hot spring waters. 6) The abundance and nature of microbes were affected by a combination of geological and hydrological processes. 7) Thoughtfully designed laboratory experiments can help to interpret field data but these experiments also have limitations in simulating natural processes.

Written and oral reports. Each student prepared a report to present data and discuss relationships between volcanic rocks and gases, spring waters and microbial communities. The students critiqued each other's draft reports during several states of their preparation during the program. The class presented its findings orally to the school, parents and public at their final evening "graduation" event.

Evaluation: Surveys were administered to students before and after their lectures, labs, fieldwork and discussions with scientists. Students' work was scored using rubrics (labs, progress reports, final report, oral presentation). Parents, teachers, rangers, Ames staff and students completed end-of-year surveys on program impact. Students had a unique and highly valued learning experience with NASA scientists. They understood what scientists do through authentic research and by observing what scientists are like as individuals. Students became familiar with astrobiology and how it can be pursued in the lab and in the field. Student interest increased markedly in astrobiology, interdisciplinary studies and science generally. Testimonials from several graduates revealed that their program participation influenced their decisions regarding college majors in science, technology and education.

Acknowledgements: The NASA Astrobiology Institute provided financial support. We thank Steve Zachary (National Park Service), Dave Michael and Fred Null (Red Bluff High School), and Kirsten Fristad (NASA Postdoctoral Program) for their substantial, invaluable contributions.

The last possible outposts for life on Mars

Alfonso F. Davila

Science Topic: Astrobiology

The evolution of habitable conditions on Mars is often tied to the existence of aquatic habitats and largely constrained to the first billion years of the planet. We propose an alternate, lasting evolutionary trajectory that assumes the colonization of land habitats before the end of the Hesperian period (c.a. 3 billion years ago) at a pace similar to life on Earth. Based on the ecological adaptations to increasing dryness observed in dryland ecosystems on Earth, we reconstruct the most likely sequence of events leading to a late extinction of land communities on Mars. We propose a trend of ecological change with increasing dryness from widespread edaphic communities to localized lithic communities and finally to communities exclusively found in hygroscopic substrates, reflecting the need for organisms to maximize access to atmospheric sources of water. If our thought process is correct, it implies the possibility of life on Mars until relatively recent times, perhaps even the present.

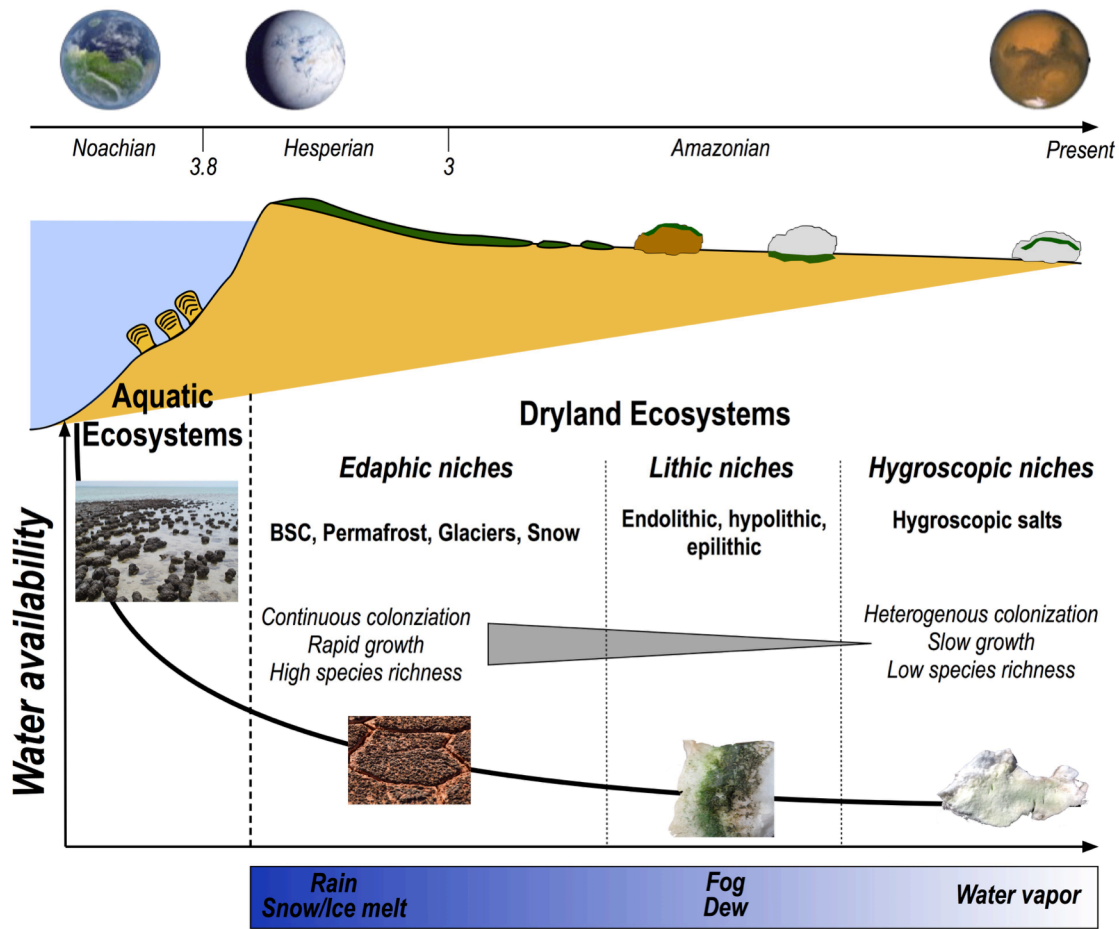


Figure 1. Proposed sequence of ecological transitions on Mars with increasing dryness, assuming an early colonization of land. After the disappearance of aquatic environments, land habitats (edaphic, lithic, and lastly hygroscopic) would still be available, based on different sources of atmospheric water.

Morphologic and Morphometric Indications of Meltwater-Driven Gully Formation on Mars

N. H. Glines^{1,2}, V. C. Gulick^{1,2}, P. Freeman^{1,2,3}, H. Hargitai¹. ¹NASA Ames Research Center, MS 239-20,

(natalie.glines@nasa.gov, virginia.c.gulick@nasa.gov), ²SETI Institute, ³U.C. Santa Cruz. Topic: Astrobiology

Introduction: Moni is a ~5km diameter crater in the southern mid-latitude highlands of Mars (47.01°S, 18.77°E). Despite relatively low regional gully density, Moni has a high concentration of gullies, and its floor exhibits arcuate ridges interpreted as remnant degraded glacial features, such as glacial moraines, located below gully debris aprons. The gullies of Moni Crater are interesting because they dissect into, and beyond, the crater rim. **Here we document morphologic and morphometric evidence in Moni Crater that water ice deposits associated with glacial and peri/paraglacial processes, have significantly altered gully headwalls. It is likely that meltwater was a key mechanism involved in the development of gullies, consistent with the shallow runoff-like drainage patterns observed in gully alcove heads.** Using TES and THEMIS data, we record that Moni surface pressures reach 5.26mbar, and temperatures approach 32°C during Ls 285°, near the peak of southern summer (Ls 270°). Temperatures may exceed 0°C between ~Ls 285° and 330°.

Morphologic Analysis: (1) *Arcuate Ridges* rise ~30m above surrounding floors. On the north ridge we find a bench or laterally continuous terrace between 1160 and 1170m elevation. (2) *Boulder* mapping, using shadows and contrast, reveals a clustering preference: over 80% of exposed boulders are located in the center of the crater or in the ridges, while the fewest boulders/m² are located between ridges and cratered walls. (3) *Moni Crater floor* in the southeast is characterized by raised patterned ground encircled by a partially hidden ridge. Light-toned dunes, superposed by gully aprons, cover the floor. Boulders appear perched atop these dunes, observed to be immobile, suggesting induration. Elevation profiles reveal significant symmetry, and slope aspects and height/width ratios similar to TARs on Mars. (4) *Gullies* (Fig.1) are preferentially pole-facing. North wall gullies have the greatest degree of incision and branching, and incise the fractured headwall up to 6m, forming shallow channels on the crater rim.

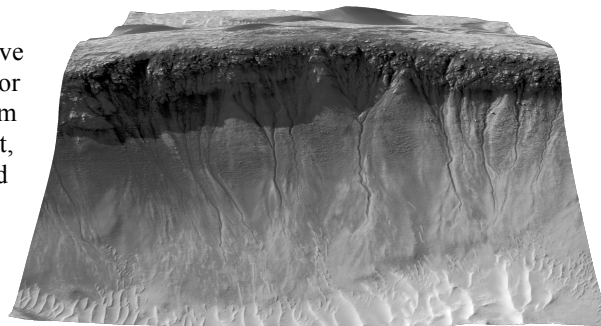


Figure 1: Moni Crater north wall gullies; 3D perspective view of HiRISE orthoimage over DTM DTEEC 007110 1325 006820 1325.

Interpretation & Morphometric Synthesis: Headwall incision morphologies suggest gully formation by liquid water flows. Larger degraded channels suggest greater discharge volumes in the past. If liquid water persisted in Moni for any significant time, it is likely to have ponded within the north arcuate ridge enclosure. The ridge curvature may be ablational, indicating an originally high level of ice slunk away from the wall. One ridge peak appears twisted in a sublimational contraction. Morphometry suggests volatile loss from Moni gullies: an average of 64% of the material eroded from 8 gully headwalls may be unaccounted for. After considering computational error, aeolian transport of finer-grained material, and long-term compaction, a volume discrepancy remains, likely the evaporation and sublimation of water and ice.

Proposed Timeline: 1) Cold conditions promote snow/ice accumulation as icy floor fill and an ice-rich subsurface. 2) Debris from the ice-fractured rim slides down a snow/ice bank, similar to a supraglacial flow till moraine or protalus rampart, and accumulates above ice at the foot of the wall. 3) Climate change excavates exposed surface ice between the debris and wall to form an ablation hollow. Floor ice ablates, and debris cover compaction prevents further ablation. 4) Gully channels develop from meltwater flows. Channel formation, meltwater ponding, and snow/ice accumulation are seasonal. 5) Deposition and larger gully flows taper off, and snow/ice, particularly in protected, shaded headwalls, melts seasonally to form smaller channels. Volatile loss from debris is likely due to either infiltration of meltwater back into the subsurface or the sublimation of ice and liquid water. 6) Floor sublimation till has fully depressed. Ice persists as an ice-cored ridge and debris-covered ice in the southeast floor.

Conclusions: The proposed timeline explains ridge formation, the gullies' deep headwall incision, older channel formation, the volume discrepancy, and curious boulder placements. Glacial and post-glacial mechanisms can independently explain the patterns and morphologies observed in Moni. Considering the great amount of ice we interpret has been removed from Moni Crater, and the temperature variance recorded today, it is likely that Moni has seen recurring periods of deposition, freezing, melting, and sublimation. These warmer periods likely release the melt water to form the gullies. More recent channel modifications could be from remnant ice melt and sublimation, and CO₂ frost actions. Volume discrepancies interpreted as resulting from volatile loss are consistent with gully deposits of lithic sediments and water-ice. Thus, the deposits comprise prime astrobiological and resource exploration targets.

Hollow Nodules gas escape sedimentary structures in Lacustrine Deposits on Earth and Gale Crater (Mars).

^(1,2) Bonaccorsi, R., ^(2,3) Willson, D., ⁽⁴⁾ Fairén, AG., ⁽⁵⁾ Baker, L., ⁽²⁾ McKay, CP., ⁽²⁾ Zent, AP., and ⁽⁶⁾ Mahaffy, P.

⁽¹⁾SETI Institute; ⁽²⁾NASA Ames Res. Center; ⁽³⁾KISS Institute; ⁽⁴⁾Cornell University; ⁽⁵⁾University of Idaho, Moscow; ⁽⁶⁾NASA GFSC.

One intriguing novel sedimentary feature imaged by Curiosity's Mastcam and MAHLI instruments in Gale Crater are mm-sized circular rimmed hollow nodules (HNs) (Figure 1A), pitting the Sheepbed mudstone of Yellowknife Bay Formation [1,2]. Several mechanisms for primary and secondary formation of HNs have been discussed, such as: (1) Diagenetic dissolution of soluble mineral phases; or, (2) Gas bubbles released shortly after sediment deposition due to abiotic and/or biotic reactions and rapid lithification [1-3 and refs. therein].

We found the first high-fidelity analog for the formation of HN in the Sheepbed mudstone. Our data and observations support the gas bubble hypothesis.

To date, no terrestrial analogue structures of hollow nodules with similar shape, distribution, and composition have been described in the literature in support of the gas bubble hypothesis [2].

In an ephemeral pond in Ubehebe Crater, Death Valley Natl. Park, CA., we observed the formation of hollow nodule sedimentary structures (Figure 1B) produced by gas bubbles (Figure 1C) that are strikingly similar to those imaged by the MSL rover (Figure 1A).

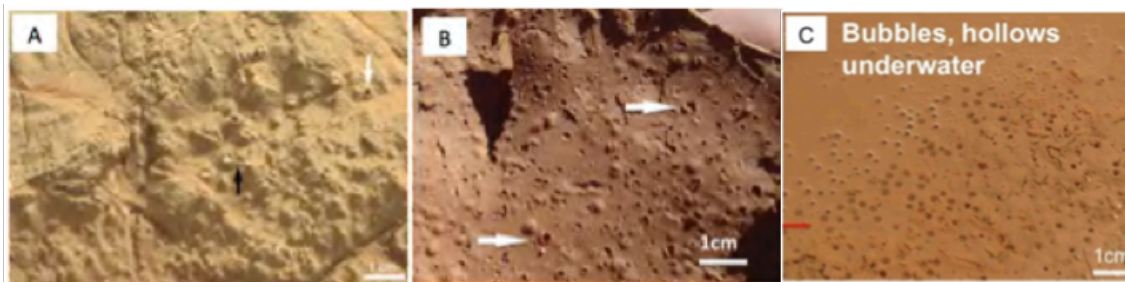


Figure 1. HNs (white arrows) imaged by Mastcam-100, sol 159, Yellowknife Bay Site (A). Mini hollows in the dry mud (B) formed by bubbles (C).

Ubehebe Crater (UC) surface sediment hollow nodules were sampled, imaged, and measured (N=637). Ubehebe's HNs show similar shape, distribution, and composition to those found in GC[6,7]. UC in-situ observations suggest the gas bubbles were generated within the slightly reducing ephemerally submerged mud; these intra-crater deposits remain otherwise extremely dry year around, i.e., Air_rH ~2-5%; ground H₂O wt%: 1-2%; air/ground T: 45-48°C/67-70°C [4-5].

In the terrestrial case HNs formed directly as gas escape structure without involving concretionary growth around primary void space caused by gas bubbles trapped in an increasingly cohesive clay-rich matrix.

If present, surface hollow nodules are easy to see in dry clay-rich mud in lacustrine sediments, so they could represent a new indicator of ephemeral but habitable/inhabited environments on both Earth and Mars.

References: [1] Grotzinger J.P. et al. (2014), *Science* 343, 124277. [2] Stack et al. (2014) *JGR, Planets* 119343, 1243480. [4] Bonaccorsi R. et al. (2012) *AGU Fall Meeting*, Abstract #P11B-1839. [5] Bonaccorsi, R. et al. (2014) *AGU Fall Meeting*, Paper #EP53A-3632. [6] McLennan, S.M. et al. (2014) *Science* 343, 1244734. [7] Ming D.W. et al. (2014) *Science*, 343, 1245267.

PERCHLORATE REDUCING BACTERIA: EVALUATING THE POTENTIAL FOR GROWTH UTILIZING NUTRIENT SOURCES IDENTIFIED ON MARS Kathryn F. Bywaters (SST/NPP), Chris McKay (SST) and Richard C. Quinn (SST/SETI Institute)

Introduction: Perchlorate reducing bacteria may serve as model organisms for potential life forms that could exist on Mars. Due to the high reduction potential of perchlorate it can be utilized in microbial metabolism as an electron acceptor [1]. Perchlorate was discovered to be present in martian surface materials (~0.5% wt.) using the Wet Chemistry Laboratory and the Thermal and Evolved Gas Analyzer on the Phoenix Lander [2]. An apparent widespread distribution of perchlorate on Mars was confirmed using the Sample Analysis at Mars (SAM) instrument suite on the Mars Curiosity Rover [3].

Nutrient sources that may support microbial metabolism on Mars potentially exist in the form of carbon as formate, nitrogen as nitrate, and phosphorus potentially as phosphate. Formic acid synthesis may occur on Mars due to UV irradiation of CO, CO₂ and small quantities of water vapor [4]. The SAM investigation has detected oxidized nitrogen-bearing compounds on Mars and these results support nitrate in concentrations ranging from 110-1100 ppm [5]. The analysis of elemental composition of the “Paso Robles” evaporitic deposits on Husband Hill, using the Athena Science instrument package on Spirit, indicates the presence of Ca-phosphate [6].

Previous findings have shown that *A. suillum* strain PS does not grow in media containing 10 mM formate and 5 mM ammonium, but that *A. suillum* strain MissR does [7]. Given the results of Stern et al. [5], nitrate may be a more viable nitrogen source on Mars compared to ammonium. Although Phoenix Wet Chemistry Laboratory data may show possible low levels of ammonium [8], it is unclear if these levels are significant relative to measurement error, sensor cross sensitivities, and potential contamination.

To evaluate the potential for microbial growth through the utilization nutrient sources identified on Mars, perchlorate-reducing bacteria were cultured in media containing phosphate and different combinations of nitrogen and carbon sources, including formate and nitrate.

Methods: *Azospira suillum* strain PS (formally *Dechlorosoma suillum* strain PS) was anaerobically grown in 4 different media treatments: 1) 5 mM ammonium chloride, 10 mM sodium acetate, 5 mM magnesium perchlorate, 5 mM monosodium phosphate, 7 mM disodium phosphate; 2) 8 mM sodium nitrate, 10 mM sodium acetate, 5 mM magnesium perchlorate, 5 mM monosodium phosphate, 7 mM disodium phosphate; 3) 10 mM sodium nitrate, 20 mM sodium formate, 5 mM monosodium phosphate, 7 mM disodium phosphate, 5 mM magnesium perchlorate; 4) 10 mM sodium nitrate, 10 mM sodium formate, 5 mM monosodium phosphate, 7 mM disodium phosphate, 5 mM magnesium perchlorate. Five replicates were done for all treatments.

Growth curves of *A. suillum* strain PS for each treatment were obtained by measuring optical density at 600 nm. To obtain growth curves, measurements were taken approximately every 24 hours over a 5-day period.

Results: Figure 1 shows the growth curves for the four different treatments. Growth rates during the exponential growth phase (between time steps 72 and 84 hours) for the treatments were: 1) ammonium and acetate 2.2 ± 0.3 doublings day⁻¹; 2) nitrate and acetate 2.3 ± 0.3 doublings day⁻¹; 3) nitrate and 20 mM formate 3.0 ± 0.1 doublings day⁻¹. Growth rates between treatment 1 and 2 showed no significant difference. The final measured biomass values for treatment 1 or 2 were 20% higher when compared with treatment 3.

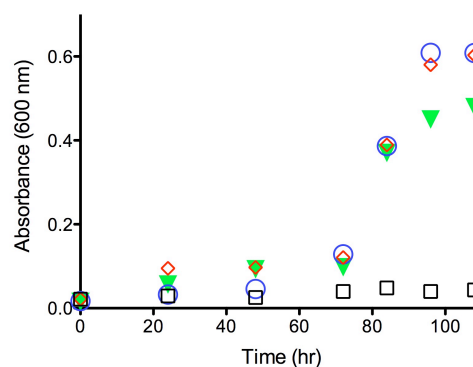


Figure 1. Growth curves for *A. suillum* strain PS cultured with media containing phosphate and different combinations of nitrogen and carbon sources. The four different media treatments were: 1) 5 mM ammonium chloride and 10 mM sodium acetate (blue), 2) 8 mM sodium nitrate and 10 mM sodium acetate (red), 3) 8 mM sodium nitrate and 20 mM sodium formate (green) and 4) 8 mM sodium nitrate and 10 mM sodium formate (black). Data points represent an average of n = 5 replicate experiments.

Summary: Our experiments show that that *A. suillum* strain PS can utilize formate in combination with nitrate. Although *A. suillum* strain PS, does not grow in treatment 4 media, it does grow in treatment 3 media, which contains 20 mM formate and 10 mM nitrate. The final measured biomass values for all treatments in our experiments indicate that, although sodium acetate may be more efficiently utilized, sodium formate is a viable electron donor. These results will be discussed in the context of on going growth experiments, which examine water availability of hydrated perchlorate salts and brines.

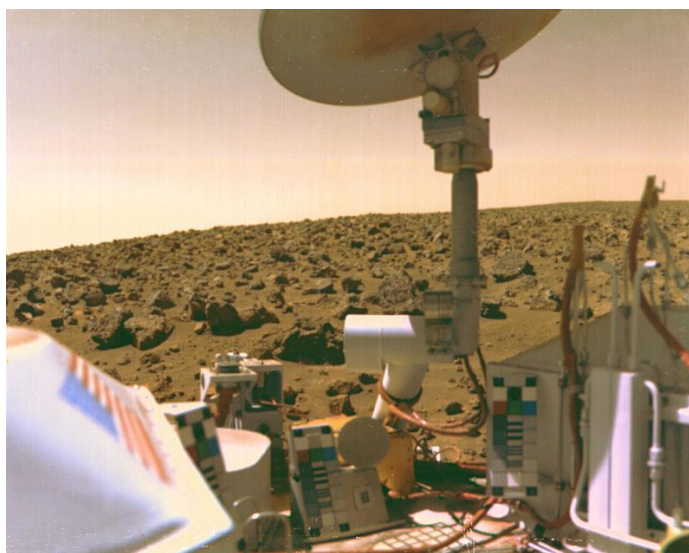
References: [1] Chaudhuri S. K. (2002) *Appl. Environ. Microbiol.*, 68, 4425–4430. [2] Hecht M. B. et al. (2009) *Science*, 325, 64–67. [3] Glavin D. P. et al. (2013) *JGR: Planets*, 118, 1955–1973. [4] Hubbard J. S. (1971) *Proc. Natl. Acad. Sci.*, 68, 574–578. [5] Stern J. C. et al. (2015) *PNAS*, 112, 4245–4250. [6] Ming, D. W. et al. (2006) *JGR*, 111, E02S12. [7] Coates J. D. et al. (1999) *Appl. Environ. Microbiol.*, 65, 5234–5241. [8] Kounaves S. P. et al. (2010) *JGR: Planets*. 115, E1.

Acknowledgements: K.B. acknowledges support from the NASA Postdoctoral Program. R.Q. acknowledges support from the NASA Astrobiology Institute. The authors thank the Dr. John Coats’ laboratory at the University of California, Berkeley, for the *A. suillum* cultures.

Search for upper limit on chlorobenzene in the original Viking GCMS data set

Melissa Guzman, Chris McKay
Science Topic: Astrobiology

The Gas Chromatograph Mass Spectrometer (GCMS) experiments onboard the twin Viking Landers (VL) were the first such analytical chemistry instruments on Mars. They conducted the most comprehensive search for organics in the Martian soil. The resulting data set played a decisive role in the continuing search for organics on Mars. Recently, the Sample Analysis at Mars (SAM) instrument on board the Curiosity rover has detected chlorobenzene above background levels using pyrolysis GCMS in the mudstone at Yellowknife Bay. Chlorobenzene is not present as a clearly defined peak in the Viking GCMS data or it would have been reported by the original Viking team. However, it was possible that data analysis focused on this compound and motivated by the knowledge of perchlorate in the Martian soil would indicate chlorobenzene is present in the Viking GCMS data at a statistically plausible level. Correlations between m/z 112 and m/z 114 were used to search for any coincident peaks close to the noise limit. The elution time of chlorobenzene from the Viking column is unknown but is estimated from a laboratory simulation using a Viking-analog GC column. No coincident peaks at m/z 112 and m/z 114 were identified, meaning there is no definitive detection of chlorobenzene by the Viking GCMS. Since the team saw no chlorobenzene in the Viking GCMS data set, a secondary aim was to set an upper limit for chlorobenzene based on the detection limit of Viking. This was completed by using toluene, which has known abundance levels reported by the original Viking team, as a reference compound. During the directed search for chlorobenzene, it was also seen that the mass scans from both VL-1 and VL-2 show mass peaks that are present in all scans. It was found that there is a plausible match between the persistent mass peaks in both VL-1 and VL-2 and contaminants identified in the sampling system in VL-1 and VL-2 by the Viking team.



The first Martian selfie by Viking.

Hypersaline environments as analogs for habitats on past Mars

Angela M. Detweiler^{1,2}, Christopher P. McKay¹, Jon C. Rask¹, Brad M. Bebout¹, R. Craig Everroad^{1,2}, Jackson Z. Lee^{1,2}, Jeffrey P. Chanton³, Marisa H. Mayer¹, Adrian A. L. Caraballo¹, Bennett Kapili¹, Meshgan Al-Awar⁴, and Asma Al-Farraj⁵, Cheryl A. Kelley⁶, Jose Q. García-Maldonado⁷

¹NASA Ames Research Center, Moffett Field CA 94035, USA

²Bay Area Environmental Research Institute, Petaluma, CA 94952, USA

³Department of Earth, Ocean and Atmospheric Science, Florida State University, Tallahassee, FL 32306, USA

⁴Research and Studies Center, Dubai Police Academy, Dubai, United Arab Emirates

⁵Geography Department, United Arab Emirates University, P.O. Box 17771, Al Ain, United Arab Emirates

⁶Department of Geological Sciences, University of Missouri, Columbia, MO 65211, USA

⁷Centro de Investigación y de Estudios Avanzados del Instituto Politécnico Nacional (CINVESTAV) Unidad Mérida, Merida, Mexico

Hypersaline environments have been reported from Mars and may be locations within which to search for evidence of past (and possibly extant) microbial activity. These salty environments are of interest to Astrobiology because of the capacity of salts to lower the vapor pressure and freezing point of liquid water, which are relevant properties to Mars today. Once salts reach their saturation point, they quickly precipitate and can preserve biomarkers over time. These salt precipitates, or evaporites, can provide protection from harmful radiation, while still allowing for the transmission of light used by photosynthetic organisms. We have conducted microbial ecological investigations across various types of hypersaline environments in California (USA), Baja California (Mexico), Atacama Desert (Chile) and most recently in the dunes of the Liwa Oasis (United Arab Emirates). We document the spatial distribution and identity of organisms based on 16S ribosomal RNA (rRNA) gene sequences as well as sequences of the *mcrA* (methyl coenzyme-M reductase) gene in some hypersaline mats, and we also report on methane measurements in these environments, as an example of a biosignature produced by methanogens here on Earth.

*Science Topic – Astrobiology

Title: Changes in the salt crust microbial community after exposure to martian conditions.

Authors Heather Smith Science Topic: Astrobiology,
Abstract:

We report on changes in the salt crust photosynthetic microbial community measured when exposed to martian conditions (UV, pressure, temp) in a Mars chamber. Halophile ecosystems are models for life in extreme environments including planetary surfaces: Our research was on the microbial preservation potential of salt to Mars, pressure, UV, and temperature. Figure A is a picture of the research site with the inset showing the microbial stratigraphy within the salt crust. Visual changes within the stratigraphic layering and phospholipid fatty acid (PLFA) analysis were used to determine changes in microbial community. The microbial community was reduced but not eliminated.

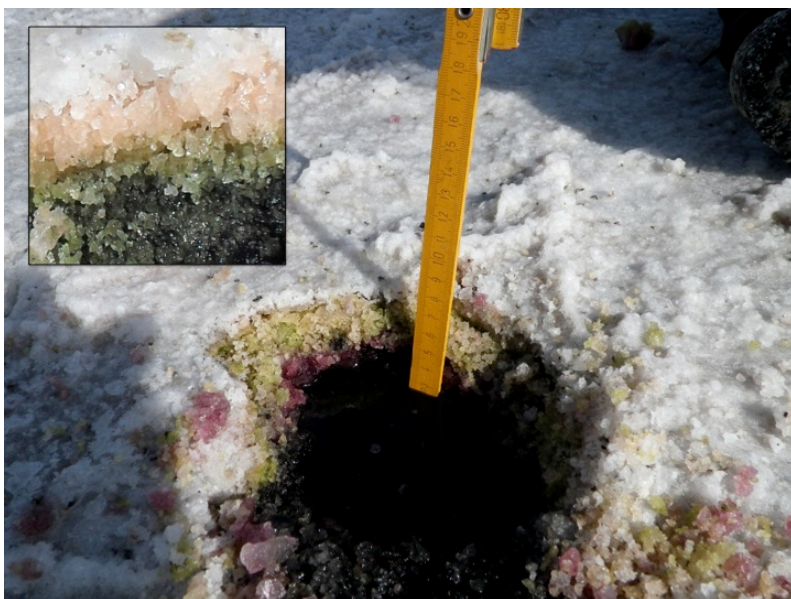


Figure 1 The microbial ecology of the salt crust - black, green, and pink stratified layers of photosynthetic organisms (shown above) vary with depth as a function of environmental conditions.



Figure 2. The salt crust in the Mars Simulation Chamber

BUILDING A BIOSIGNATURE ROCK SAMPLE LIBRARY AND DEVELOPING AUTOMATED CLASSIFIERS.

V.C. Gulick¹, P.M. Freeman^{1,2}, T. Johnsen^{1,3}, J. Angell^{1,4}, P. Morkner^{1,5}, and J. Bello⁶. ¹ARC-SST/SETI, ²UCSC, ³UC-Irvine, ⁴NYU, ⁵CalPoly-SLO, ⁶EIC Labs.

Introduction: Identifying minerals, organics and other potential biosignatures within individual rock samples is an important part of both terrestrial field and planetary surface exploration studies. To help with this effort, Raman spectrometers are being increasingly utilized as they provide a nondestructive method to acquire spectra relatively quickly with little or no sample preparation, making it ideal for use on future planetary missions. This method provides unique fingerprint spectra of the sample being examined. However, because the resulting spectra from rocks may contain a variety of minerals and biosignatures, in addition to sources of noise including background and mineral fluorescence, it can be difficult for a field scientist to immediately identify the individual spectral constituents. Consequently, rock samples are often collected and re-analyzed back in the lab under controlled conditions and compared with a library of known mineral and biosignature spectra.

Automatically Classifying Minerals: Our group has previously developed an automated mineral classifier to autonomously identify pure minerals from Raman spectra [1]. We utilized Principle Component Analysis (PCA) to reduce the dimensionality of the data prior to training with an Artificial Neural Network (ANN) implemented by the Multi Layer Perceptron (MLP) algorithm to automatically classify some of the major rock forming minerals, including quartz, olivine, potassium feldspar, plagioclase, mica, and pyroxene. Using Raman Spectra of mineral samples from our library and our 852 nm laser excitation instrument, our classifier performed with an overall accuracy of ~83%. Quartz and olivine returned an accuracy of 100%. Using the online RRUFF mineral database (<http://rruff.info>) of these same minerals, our classifier performed with an overall accuracy of ~80%, while quartz, olivine and pyroxene returned an accuracy of 100%.

Since then, we used a similar classifier on mineral spectra common to sedimentary rocks using the RRUFF database. We selected sulfates, carbonates, oxides, feldspars, quartz, and micas. Our classifier returned an overall accuracy of ~92% [4]. Having demonstrated the efficacy of our mineral identification system, we are now set to develop automated algorithm(s) that will enable individual minerals and biosignatures to be automatically identified and classified from rock spectra. Such automated algorithms can aid in a variety of applications and can contribute to rock identification systems when combined with image analysis algorithms [2,3] to classify rock samples.

Building the Spectral Library of Rock and Biosignature Samples: However the development of automated classifiers for multi-minerals, mineral mixtures and biosignature spectra requires establishing a library of biosignature samples as well as analyzed rock samples containing multiple minerals and biosignatures. Such a custom library is required since no publically available online sample library currently exists. To this end, we have been building such a sample library.

Currently our sample library encompasses over 1200 samples that have undergone careful hand sample analysis and macro imaging under uniform lighting conditions. We are in the process of acquiring Raman spectra of these samples with our in house dual excitation (532nm and 785nm) Raman instrument provided by EIC Laboratories. Approximately 700 of these samples are igneous rocks, with the remainder being of sedimentary and metamorphic origin. We also have a wide variety of common rock forming minerals that we have analyzed with our Raman instrument. More recently, as part of SETI Institute's NASA Astrobiology Institute (NAI) team, we have begun to collect a variety of sedimentary samples containing biosignatures, including travertine from California hot springs (Figure 1) containing beta-carotene and other biosignatures, gypsums and salts from the Atacama Desert, palmitic acid and gypsum and anhydrite containing palmitic acid, diatomite, and microbial mats.

References: [1] Ishikawa, S.T. and V.C. Gulick (2013) *Computers & Geosciences*, doi: 10.1016/j.cageo.2013.01.011; [2] Freeman et al., 2014, LPSC, 2739; [3] Valenzuela et al., 2015, LPSC, 3009; [4] Gulick et al. 2016, LPSC, 2825.

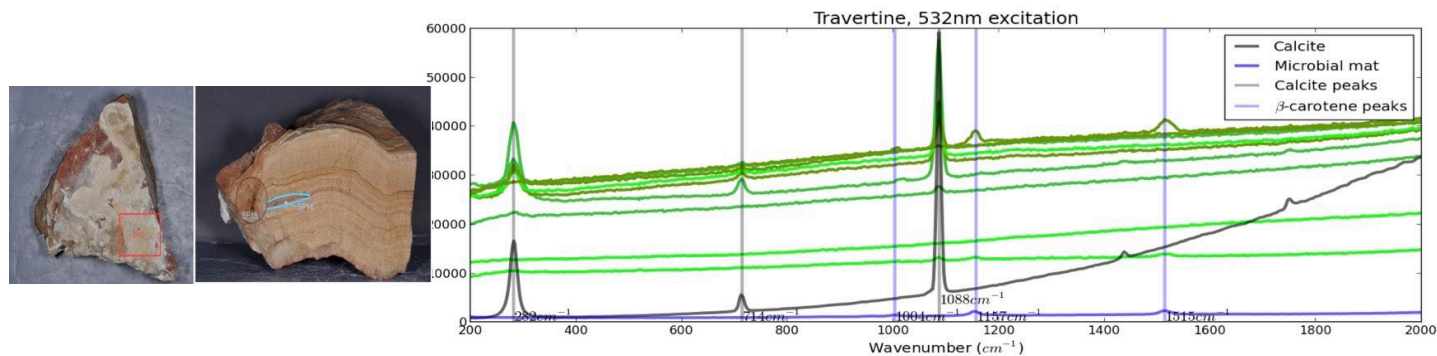


Figure 1: Travertine sample from Travertine Springs, CA. Image on left shows region where no biosignatures were identified. Image on right contained beta-carotene peaks in two protected regions circled. Plot shows several Raman spectra of the sample (green) compared with β -carotene peaks in a microbial mat (blue) and calcite (gray) spectra. Distinct calcite peaks (gray vertical lines) as well as distinct β -carotene peaks (blue vertical lines) in the sample demonstrate the ability to detect both minerals and biosignatures in the same spectra. (L. Bebout (NASA-ARC) provided microbial mat sample).

Elucidating the abiotic origins of citric acid cycle compounds detected in carbonaceous meteorites.

Andro C. Rios¹ and George. Cooper², ¹NASA Postdoctoral Program, Universities Space Research Association ² Exobiology Branch, NASA Ames Research Center, Andro.c.rios@nasa.gov.

Science Topic: Astrobiology

Pyruvic acid is a small organic molecule that is vital to all cellular metabolism. It has recently been detected in carbonaceous meteorites indicating that it can be formed from abiotic processes and might have been present before the origin of life (1). We have previously reported that pyruvic acid has the intrinsic ability to produce many of the intermediary metabolites associated with the citric acid cycle (1). These observations have led us and others previously to hypothesize that the natural chemistry of pyruvic acid may have played a role in the emergence of a proto-metabolism. In extant cells, chemical reactions associated with the citric acid cycle are carried out by the action of highly evolved enzymes, but it is assumed that in a prebiotic epoch, enzymes could not have been present to produce the citric acid cycle intermediates.

We have been investigating the abiotic chemistry of pyruvic acid under alkaline conditions using the analytical method of liquid chromatography-mass spectrometry and synthetic organic chemistry in order to elucidate reaction pathways taken by pyruvic acid that lead to the production of intermediary metabolites (i.e., oxaloacetic acid, malic acid, isocitric, citric acid, fumaric acid, etc.). We have found that pyruvate needs to proceed first via a series of aldol reactions before any of the citric acid cycle compounds are produced (Figure 1). It is of particular interest that the fragile compound, oxaloacetic acid is consistently the first observed intermediary metabolite originating in these pyruvate reaction mixtures. It also tends to maintain a steady state abundance even at temps that reach 85°C. In extant metabolism there is also a close biosynthetic relationship between pyruvate and oxaloacetate. The entire pyruvate structure can enter the citric acid cycle via a enzyme mediated carboxylation reaction that forms oxaloacetate. Understanding the abiotic molecular pathway for these reactions is the only way to determine if all of the citric acid cycle metabolites share a common core precursor or a set of related precursors that may have influenced their natural selection from prebiotic chemistry. **References:** [1] Cooper G. et al. (2011) *Proc. Natl. Acad. Sci. U.S.A.* 108, 14015–14020.

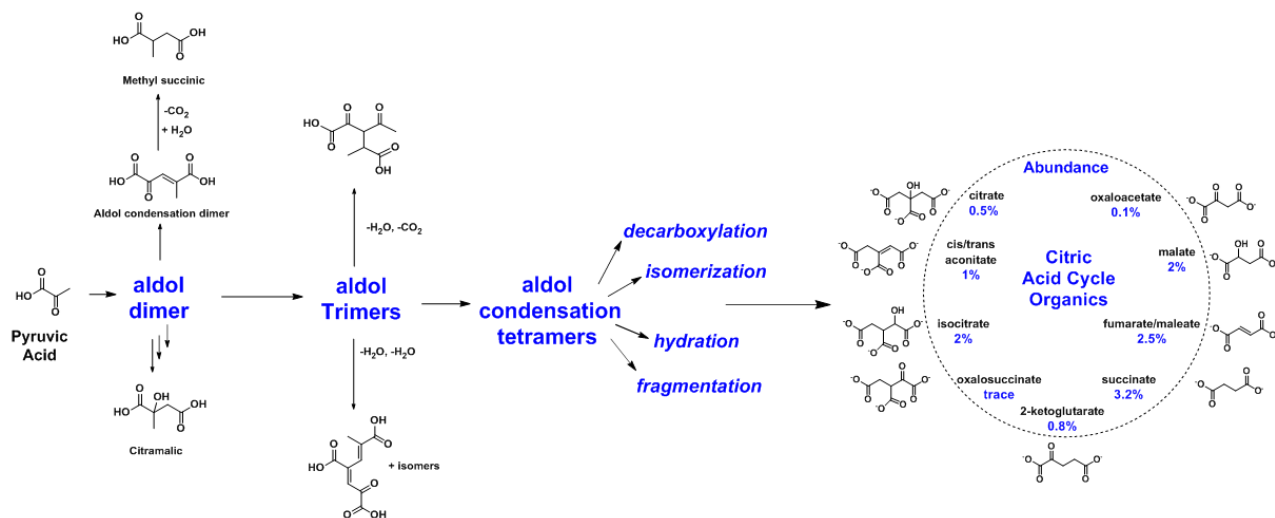


Figure 1. A general reaction pathway that explains the formation of metabolic and non-metabolic compounds that originate from pyruvic acid under alkaline aqueous conditions.

Rare and Common Sugar Derivatives in Carbonaceous Meteorites: Anomalous Enantiomer Excesses and Racemic Mixtures

George Cooper¹ and Andro C Rios^{1,2}, ¹Exobiology Branch, Space Science and Astrobiology Division, george.cooper@nasa.gov, ²NASA Postdoctoral Program, andro.c.rios@nasa.gov
Science Topic: Astrobiology

ABSTRACT

In extant life, biological polymers such as nucleic acids and proteins are constructed of only one - the “D” or “L” - of the two possible non-superimposable mirror images (enantiomers) of selected organic compounds. However, before the advent of life it is generally assumed that chemical reactions produced 50:50 (racemic) mixtures of enantiomers as evidenced by common abiotic laboratory syntheses. Carbonaceous meteorites contain clues to prebiotic chemistry because they preserve a record of some of the Solar System’s earliest (~ 4.6 Gyr) chemical and physical processes. In multiple carbonaceous meteorites we found that both rare and common sugar mono-acids (aldonic acids) composed of four carbons (4C) to 6C contain significant excesses of the D-enantiomer while other (comparable) sugar derivatives are racemic. While the proposed origins of such excesses are still tentative, the findings imply that meteoritic compounds and/or the processes that operated on meteoritic precursors may have played an ancient role in life’s biopolymer composition.

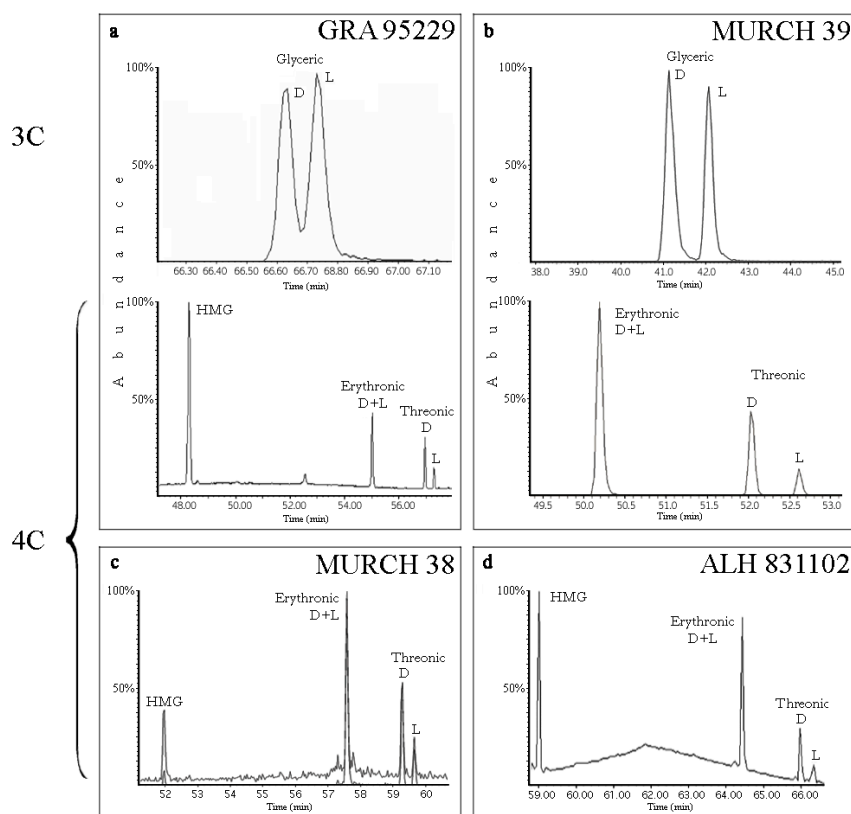


Figure 1. GC-MS analysis of three-carbon (3C) and 4C sugar acids and enantiomers from various meteorites. a, Glyceric acid - top panel, and 4C acids - bottom panel, from GRA 95229. b-d, Analyses from other indicated meteorites. In all analyzed interior samples glyceric acid is racemic but threonic acid has highly anomalous D enantiomer excesses. To date, one measurement of erythronic acid also shows a significant D excess (54%, not shown). The very rare, and branched acid, 2-hydroxymethyl glyceric acid (HMG) is present in all but one sample. It is a possible formose ($\text{CH}_2\text{O} + \text{H}_2\text{O}$) reaction product on the meteorite parent body.

Title: Upper Atmosphere Detection of Meteoritic Organics by a Mid-Infrared Small Satellite Spectrometer (MIRSSS)

Authors: D. P. Summers, A. Colaprete, A.J. Ricco, N. Bramall, K.A. Ennico, D. Landis, D.D. Squires

Science Topic: Astrobiology

Introduction:

The objective of this mission is to detect exogenous organics being delivered by meteors and interplanetary dust particles to the upper atmosphere and to quantify and characterize the delivered organics.

Organics could survive ablation upon atmospheric entry because they undergo too few collisions to be destroyed and the entrainment of meteoritic material will lower the oxidation level of the train. The detection of a C–H stretch emission in persistent meteor trains has been observed. Material is also being delivered as interplanetary dust particles and settling through the atmosphere. This material provides the bulk of the mass influx but little is known about the amounts of material being delivered, how it survives, or in what forms it may survive.

Mission:

This mission would put a mid-infrared telescope/spectrometer into low Earth orbit. Once there, this instrument would use solar occlusion of the upper atmosphere, along a viewing path that grazes the Earth's atmosphere in the 80 to 100 km altitude region, to obtain long-path-length IR absorption spectra. This will provide a sensitive way of detecting the presence of delivered organic material by the mid-IR absorbance of molecular bands. It would be designed to fit into a 6U small satellite footprint and would be capable of a sensitivity of 2.2% transmittance or better. It will have a spectral resolution of 6 cm⁻¹. We will capitalize on BioSentinel's development at Ames Research Center by utilizing the nearly identical SC bus, thus leveraging existing NASA investment. This bus will provide 4U and 5.3 kg of payload volume and mass, with 15 W average power to the payload. It includes a star-tracker-based 3-axis attitude control system expected to provide better than 0.1° pointing stability.

Impact:

The data from this mission will let us characterize the amounts of meteoritic organic material being delivered to the upper atmosphere and understand how much of it survives. The use of infrared characterization will provide some understanding of the nature of the organics and so will also help us understand the types of material being delivered. By a better understanding of the material that gets delivered, we can constrain and better consider the nature of the extraterrestrial source material. This mission will help us understand how such material contributed to prebiotic chemistry and the origins of life.

These results will help us better understand the origin of life on Earth and also the potential for life on Mars and Europa. It would inform us about the prebiotic chemistry on these bodies and possible presence of organics on others. It would help us understand the asteroids and comets that represent sources of extraterrestrial material.

Title: Wildlife photography in extreme environments at the microbial scale.

Authors: Ariel Waldman¹ and Chris McKay²

1. Founder, Spacehack.org, San Francisco, CA

2. Space Science Division, NASA Ames Research Center, Moffett Field CA, 94035

Topic: Astrobiology

Abstract:

Images are an important tool in science, both for technical work and for outreach. Microbial ecosystems in extreme environments pose a challenge in photo-documentation.

Here we present a series of context and detail images that illustrate some of the diversity and structure of life forms in extreme environments.

Our examples include cryptoendoliths from upper elevations of the Antarctic Dry Valleys, hypoliths from the Namib and Mojave Desert, algae specially adapted to life on fog as source of water, corals, and tardigrades – a tiny multicellular organism renown for its ability to survive extremes.

Abstract

Microbial Ecology and Space Life Science: Applications for Human Space Exploration

Skylar J. Laham, Oksana Coban, Angela M. Detweiler, Brad M. Bebout(mentor)

Astrobiology

Water reclamation techniques are essential for crew health and safety when considering missions beyond Earth's orbit. Microbial mats are some of the Earth's earliest known living ecosystems, and contribute to Earth's thick oxygen rich atmosphere. Microbial mat microorganisms survive conditions of desiccation, extreme temperature fluctuations, high elevation, high radiation, hypersalinity, and even simulated space flight, and so would seem ideal for surviving austere conditions as part of a robust bioregenerative life support system. Therefore, astrobiology-based investigations and understanding of microbial mat ecology and evolution would seem highly appropriate to inform future efforts to use these communities of organisms to support extended human exploration, and in situ resource utilization technologies.

Constructed microbial mats consist of artificial media such as hydrophilic open cellular foam inoculated with microorganisms from natural microbial environments, and/or isolated strains of cyanobacteria and bacteria. Microorganisms distribute themselves, or can be distributed artificially, throughout the media to recreate the three dimensional laminated ecosystems found in nature, with each lamination performing distinct biogeochemical transformations according to microbial community composition and redox conditions. Constructed microbial mats reclaim wastewater, and may produce and/or consume compounds and gases vital for astronautic exploration.

Constructed mats may provide robust and diverse filtration and atmospheric cycling properties similar to their natural microbial mat counterparts. However, as opposed to natural microbial mats, which contain thousands of microbial species, the use of constructed mats enable crew members to manage and monitor microbial ecosystems with a sifted set of species. Constructed microbial mats, like their natural counterparts, can operate at very high metabolic rates on a per volume basis, and so would benefit any ISS (or extended duration human exploration vehicle) water reclamation system, removing their present dependency of heavy and harmful wastewater treatment chemicals.

We present here the results of initial experiments with constructed microbial mats in simulated waste streams, as well as a prototype bioreactor developed from constructed microbial mat ecology and technology.

Isolation and characterization of perchlorate resistant halophiles from Big Soda Lake

Toshitaka Matsubara^{1,2}, Kosuke Fujishima³, and Lynn J Rothschild⁴

¹Advanced Studies Laboratories, University of California Santa Cruz – NASA Ames Research Center, Moffett Field, CA 94035-1000 USA; ²Department of Bioengineering, Graduate School of Bioscience and Bioengineering, Tokyo Institute of Technology, Yokohama 226-8503, Japan; ³University Affiliated Research Center (UARC), NASA Ames Research Center, Moffett Field, CA, USA; ⁴NASA Ames Research Center, Moffett Field, CA, USA.

Martian soil is known to contain a 0.4 to 0.6 wt % perchlorates (ClO_4^-) at the Phoenix landing site, a concentration toxic for most living organisms. Ground ice in the northern polar region and recently confirmed surface brine water will become a potential resource for human and other terrestrial organism to propagate on Mars. However remediation of highly saline and toxic water remains a challenge due to the limitation of resources and energy. Thus, bioengineering a fast growing perchlorate-resistant halophile would be ideal for the use of utilizing natural Martian resources without undue purification, as well as for converting toxic perchlorate to molecular oxygen and chlorite. In order to discover potential model organisms on Mars, we have isolated total four perchlorate-resistant fast-growing halophilic bacteria from Big Soda Lake in Nevada. Sequencing of the 16S ribosomal RNA sequences revealed that these halophiles belong to genus *Bacillus*, *Alkalibacillus* and *Halomonas*. Growth curves were obtained using a saline medium with different concentrations of 1:1 mixed magnesium perchlorate and calcium perchlorate salt to simulate the Martian eutectic brine water. All four species grew in high saline media in the presence of 0.5% and 1% (w/v) magnesium/calcium perchlorate and reached stationary phase within 24 hours. This is the first experiment utilizing multiple perchlorate salts, and these results revealed potential new model organisms adapted to the salt environment on Mars.

Biomining materials from e-waste

Jesica Urbina-Navarrete¹ and Lynn J. Rothschild²

¹University of California Santa Cruz ²NASA Ames Research Center

The overall objective of this work is to take the first steps toward an end-to-end integrated circuit (IC chip) recycling and reprinting facility on Earth or space, using a biological approach to reduce mass, toxic waste and high heat requirements. Using synthetic biology tools, we have developed a recycling method for e-waste (end-of-life electronics waste). Our innovation is to use a naturally-occurring silica-degrading enzyme to depolymerize the amorphous silica in metal- and glass- containing e-waste components such as IC chips in order to release the metals contained within. Once the metals are released from the silicate matrix, we propose novel use of engineered bacterial surfaces to selectively bind metals in solution with atomic precision. This allows for the separation of the metals from a solution at ambient temperature and under non-toxic conditions. The bio-mined elemental components will then be used to reprint a new IC chip, using novel plasma jet electronics printing. The plasma electronics printing technology can potentially use Martian atmospheric gas to print and alter the electronic and chemical properties of the printed materials. Additionally, the properties of the electric field and plasma can allow for printing in a micro gravity environment and on unconventional substrates – such as 3D objects. Ultimately, our vision is to have an integrated in-space/*in situ* manufacturing facility with printable electronics capability as a means of obtaining or repairing complex electronics without requiring an extensive manufacturing infrastructure. This technology can significantly lower energy and materials requirements for electronics production by using low temperature, biological techniques to generate the feedstock for printed electronics and/or by allowing for the editing of an existing IC chip with the same technology/methods. The biotechnology can also be used for ISRU to extract metals such as Cu, Fe, Al, and Ti from terrestrial, Martian and lunar basalts.

“POWERCELL” on EuCROPIS:**The interface between Mars resources and human exploration**

Lynn Rothschild, Ryan Kent, Griffin McCutcheon, Ivan Paulino Limo, Evie Pless

NASA Ames Research Center, Mail Stop 239-20, Moffett Field, CA 94035, USA

The barriers to forming human settlements on Mars are high but surmountable within our lifetime. While the Apollo astronauts carried their life support with them, our success in exploring and forming settlements on Mars depends on our ability to use local Martian resources to generate the materials and conditions humans need to survive, so-called in situ resource utilization (ISRU). On Earth, biology provides us with food, shelter, oxygen, and other materials. Off-planet, synthetic biology will enable numerous parallel productions: optimized food production, water treatment, air treatment, environmental monitoring, regolith biomining, waste management, cell based biomaterial production, biocementation, and in situ synthesis based on received DNA sequences. How will the organisms responsible for these synthetic production systems obtain organic carbon and fixed nitrogen in the hostile Martian environment? We envision a synthetic-biology enabled Martian colony and introduce here the critical intermediate component – a biological “power” source – needed to transform the in situ resources found on Mars into biological feedstocks to enable growth of production organisms. Here, we present our first “PowerCell”, a photosynthetic and nitrogen-fixing filamentous cyanobacterium engineered to provide a carbon-rich fuel source for a biological life support system on Mars. We provide a vision of how the PowerCell system will operate in a Martian colony based on ground experiments and preparations for testing in space as a NASA secondary payload aboard the upcoming DLR Eu:CROPIS satellite mission experiments.



Computing Anharmonic Vibrational Spectra for Polycyclic Aromatic Hydrocarbons: Naphthalene, Anthracene, and Tetracene

Timothy J. Lee^a, Cameron J. Mackie^b, Alessandra Candian^b, Xinchuan Huang^a, Alexander G. G. M. Tielens^b, Elena Maltseva^c, Annemieke Petrignani^b, Jos Oomens^d, and Wybren Jan Buma^c

^aSpace Science & Astrobiology Division, NASA Ames Research Center

^bLeiden Observatory, Leiden University

^cUniversity of Amsterdam

^dRadboud University

It is now widely accepted that polycyclic aromatic hydrocarbons (PAHs) are ubiquitous throughout the galaxy. The vibrational frequencies of PAH molecules in the infrared (IR) have been shown to be an excellent fingerprint for their existence and for assessing the physical conditions of the astrophysical environment in which they are observed. The Ames PAH database is now used routinely by astronomers to understand the specific PAH features, enabling them to determine the importance of ionized PAHs, nitrogen-containing PAHs (PANHs) etc. for a specific object. While the laboratory spectra and theoretical calculations that make up the PAH database have been enormously useful, it is becoming clear that future space telescopes will be high-resolution and thus there is a need for high-resolution gas-phase experiments and theoretical calculations that explicitly include anharmonic effects and rotational structure in a given vibrational band. In this presentation, recent studies focused on explicitly computing anharmonic spectroscopic constants and vibrational spectra for the linear PAH molecules, naphthalene, anthracene, and tetracene, will be shown. Some of the details include advances in manipulating normal coordinate quartic force fields which are used together with vibrational second-order perturbation theory to compute the anharmonic spectroscopic constants and vibrational spectra, the importance of resonances especially in the C-H stretching region, an improved method for distributing the IR intensity across the bands of a polyad resonance, and the importance of anharmonic IR intensities, especially in regions of the spectrum where no resonances occur. Where available, comparison to recent experiments will be shown as well.

PAH-Mineral Interactions. A Laboratory Approach to Astrophysical Catalysis

Gustavo A. Cruz-Diaz and Andrew Mattioda

Polycyclic Aromatic Hydrocarbon (PAH) molecules carry the infrared emission features (aka the PAH bands) which dominate the spectra of most galactic and extragalactic sources. Our study investigates the chemical evolution, chemical properties, physical properties, thermal stability, and photostability of samples produced from the UV irradiation of simulated mineral dust grains coated with aromatics and astrobiologically relevant ices, using infrared spectroscopy. We investigate the chemical evolution of aromatic organics (e.g., PAHs, PANHs, etc.) via anhydrous (no H₂O ice) and hydrous (H₂O ice) mechanisms. The anhydrous mechanisms will involve UV-induced catalytic reactions between organics and dense-cloud mineral grains, whereas the hydrous mechanism will incorporate H₂O-rich ice mixtures with the minerals and organics. These investigations will identify the chemical and physical interactions occurring between the organic species, the dust grains and water-rich ices.

These laboratory simulations also generate observable IR spectroscopic parameters for future astronomical observations with infrared telescopes such as SOFIA and JWST as well as provide empirical parameters for input into astronomical models of the early stages of planetary formation. These studies give us a deeper understanding of the potential catalytic pathways mineral surfaces provide and a deeper understanding of the role of ice-organic compositions in the chemical reaction pathways and how these processes fit into the formation of new planetary systems. As a second stage, we will examine the organic residue generated from the photolysis of simple organic molecules within water ice with respect to the organics found within our solar system. We will look for an answer to whether such residues enhance the sticking or binding of smaller particles, thus assisting the build-up of larger particles within a forming planetary system.

In order to achieve these goals we use the Harrick 'Praying Mantis' Diffuse Reflectance Accessory (DRIFTS), which allows FTIR measurements of dust samples under ambient conditions by measuring the light scattered by the dust sample. We have also incorporated a low -temperature reaction chamber permitting the DRIFTS measurements at low temperatures and high-vacuum. This set-up permits the analysis of the solid particles surfaces revealing the chemical species adsorbed as well as their chemical evolution via the introduction of reactant gases, UV irradiation, temperature change, etc.

Recent Progresses in Laboratory Astrophysics with Ames' COSmIC Facility: Interstellar and Planetary Applications.

(Science Topics: Astrophysics, Planetary Atmosphere & Climate)

Farid Salama¹, Cesar S. Contreras^{1,2}, Ella Sciamma-O'Brien^{1,2} and Salma Bejaoui^{1,3}

¹NASA ARC, Moffett Field, CA, ²Bay Area Environmental Research Institute, Petaluma, CA; ³NPP, Oak Ridge Associated Universities.

We present and discuss the characteristics and the capabilities of the laboratory facility, COSmIC, that was developed at NASA Ames to generate, process and analyze interstellar, circumstellar and planetary analogs in the laboratory [1]. COSmIC stands for "Cosmic Simulation Chamber" and is dedicated to the study of neutral and ionized molecules and nano particles under the low temperature and high vacuum conditions that are required to simulate space environments. COSmIC integrates a variety of state-of-the-art instruments that allow forming, processing and monitoring simulated space conditions for planetary, circumstellar and interstellar materials in the laboratory. COSmIC is composed of a Pulsed Discharge Nozzle (PDN) expansion that generates a plasma in free supersonic jet expansion coupled to two high-sensitivity, complementary in situ diagnostics: a Cavity Ring Down Spectroscopy (CRDS) and laser induced fluorescence (LIF) systems for photonic detection and a Reflectron Time-Of-Flight Mass Spectrometer (ReTOF-MS) for mass detection [2].

Recent laboratory results that were obtained using COSmIC will be presented, in particular the progress that has been achieved in the domain of the diffuse interstellar bands (DIBs) [3] and in monitoring, in the laboratory, the formation of dust grains and aerosols from their gas-phase molecular precursors in environments as varied as stellar/circumstellar outflows [4] and planetary atmospheres [5]. Plans for future, next generation, laboratory experiments on cosmic molecules and grains in the growing field of laboratory astrophysics will also be addressed as well as the implications of the current studies for astronomy.

References:

- [1] Salama F., In *Organic Matter in Space*, IAU Symposium 251, Kwok & Sandford Eds. Cambridge University Press, Vol. 4, S251, p. 357 (2008) and references therein.
- [2] Ricketts C., Contreras C., Walker, R., Salama F., *Int. J. Mass Spec*, 300, 26 (2011)
- [3] Salama F., Galazutdinov G., Krelowski J., Biennier L., Beletsky Y., In-Ok Song, *The Astrophys. J.*, 728, 154 (2011)
- [4] Cesar Contreras and Farid Salama, *The Astrophys. J. Suppl. Ser.*, 208, 6 (2013)
- [5] Sciamma-O'Brien E., Ricketts C., and Salama F. *Icarus*, 243, 325 (2014)

Laser Induced Emission Spectroscopy of Cold and Isolated Neutral PAHs and PANHs: Implications for the Red Rectangle Emission

S. Bejaoui^(a,b), **F. Salama**^(a) and **E. Sciamma-O'Brien**^(a,c)

(a) NASA Ames Research Center, Mail Stop 245-6, Moffett Field, California 94035-1000

(b) NPP, Oak Ridge Associated Universities, (c) BAER Institute, Petaluma, CA

salma.bejaoui@nasa.gov

Blue luminescence (BL) in the emission spectra of the red rectangle centered on the bright star HD 44179 was reported by Vijh et al [1]. These results are consistent with the broad band polarization measurements obtained earlier by Schmidt et al. [2]. Experimental and theoretical studies indicate that BL emission could be attributed the luminescence of Polycyclic Aromatic Hydrocarbons (PAHs) excited by ultraviolet light from the center of the star [3 and reference therein]. The relative abundance of N compared to C in the interstellar medium suggests that nitrogen substituted PAHs (PANHs) are likely abundant in the interstellar medium [4]. They exhibit similar spectral features as PAHs and could contribute to the unidentified spectral bands. Comparing the BL to laboratory spectra obtained in similar environment is crucial for the identification of interstellar PAHs.

Interstellar aromatics are expected to be present as free, cold, neutral molecules and/or charged species [5]. Matrix isolation spectroscopy (MIS) fulfills these conditions [6]. This technique consists of isolating molecule or ions in solid inert gas matrices and studying the spectral signature (band position and profile) of the trapped species. We present in this works the absorption and the Laser Induced Emission (LIE) spectra of several isolated and cold PAHs and PANHs isolated in Argon matrix at 10 K. We focus, here, on the emission spectra (fluorescence and/or phosphorescence) of these molecules and we discuss their potential contributions to the blue luminescence emission in the Red Rectangle nebula. A typical example of the results obtained with MIS technique is reported in Fig. 1.

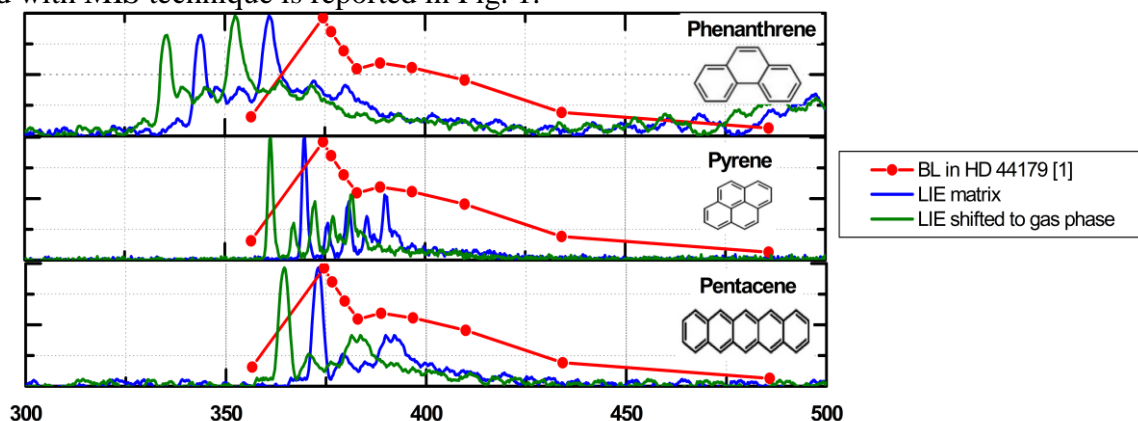


Fig.1. Laser induced emission of Phenanthrene ($C_{14}H_{10}$), Pyrene ($C_{20}H_{12}$) and Pentacene ($C_{22}H_{14}$) isolated in Argon matrices at 10 K and laser excited at 278.18 nm, 341 nm and 316 nm, respectively. The laboratory spectra are compared to spectra of HD 44179 [1]

- [1] Vijh, U.P., Witt, A.N. & Gordon, K.D, APJ, 606, L69 (2004)
- [2] Schmidt, G. D., Cohen, M. & Margon, B., ApJ, 239L.133S (1980)
- [3] Salama, F., Galazutdinov, G. A., Krelowski, J., Allamandola, L. J., & Musaev, F. A. ApJ, 526,(1999)
- [4] Spitzer, L., Physical Processes in the Interstellar Medium (New York Wiley-Interscience) (1978)
- [5] F. Salama, E. Bakes, L.J. Allamandola, A.G.G.M. Tielens, Astrophys. J. 458 (1996) 621
- [6] F. Salama, the ISO Revolution, EDP Sciences, Les Ulis, France (1999) 65

Title: Calibrating the Charge State of Polycyclic Aromatic Hydrocarbons Across Reflection Nebulae

Authors: Dr. Christiaan Boersma, Dr. Louis J. Allamandola, Dr. Jesse Bregman

Science Topic: Astrophysics

Polycyclic aromatic hydrocarbons (PAHs) are an important constituent of interstellar dust. Intermediate in size between molecules and particles, PAHs have characteristics of both. This unique property, coupled with their spectroscopic response to changing conditions and the ability to convert ultraviolet to infrared (IR) radiation, makes them powerful probes of astronomical objects at all stages of the stellar life cycle. PAH emission can dominate as much as 20% of the total IR luminosity in the many Galactic and extragalactic objects where they are seen and they are thought to hold up to 10-15% of all cosmic carbon. Due to their omnipresence and stability, PAHs play important roles in many astronomical environments and a defining role in the star- and planet formation process; and perhaps even in the origin of life itself.

A sample of ten *Spitzer*-IRS spectral maps on reflection nebulae have been analyzed using the data and tools made available through the NASA Ames PAH IR Spectroscopic Database (PAHdb; www.astrochemistry/pahdb/). The PAH emission at each pixel in these maps has been broken down, *quantitatively*, into contributing PAH charge state components (neutral and positively charged) using a novel database fitting approach. In this approach the physics of the PAH emission process is taken into account and uses target appropriate parameters, e.g., a stellar atmosphere model for the irradiating star, etc.

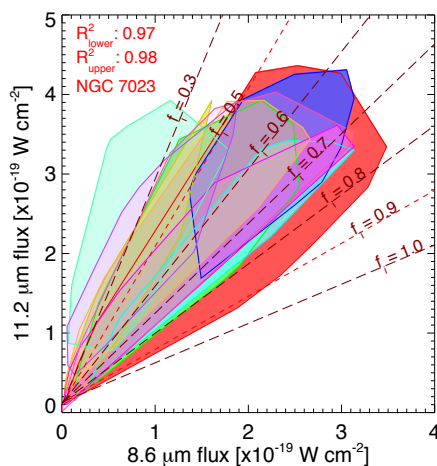


Fig. 1: The 11.2 vs. 8.6 μm PAH band strength plot calibrated for PAH ionization fraction (f_i). Each colored region shows the data range for a reflection nebula. The squared linear relation coefficients for the lower and upper limits for the bifurcated data on NGC 7023 are also given.

ionization and/or PAH edge structure, is largely driven by variations in PAH ionization.

The *quantitative* breakdown results have been used to calibrate the *qualitative* results derived using the traditional PAH band strength approach, which interprets particular PAH band strength ratios as *qualitative* proxies for the PAH charge state. This calibration allows one to directly tie observables such as PAH band strength ratios to physical conditions in the emitting regions, namely the strength of the radiation field, gas temperature and electron density. Further, a plot of the 8.6 vs. 11.2 μm PAH band strength for the northwest PDR in the reflection nebula NGC 7023 (Fig. 1) is shown to be a robust diagnostic template for the PAH ionization fraction in reflection nebulae.

Additionally, it is shown that variations in the strength of the astronomical 12.7 μm PAH band, which has been taken as either a tracer for PAH ionization and/or PAH edge structure, is largely driven by variations in PAH ionization.

Lastly, PAH spectroscopic templates have been constructed and verified as principal components. Spectra derived from the reflection nebulae NGC 7023 and NGC 2023 compare extremely well with each other and those derived for NGC 7023 are able to successfully reproduce the PAH emission observed in NGC 2023.

Title: Determining the Gas Mass of Protoplanetary Disks

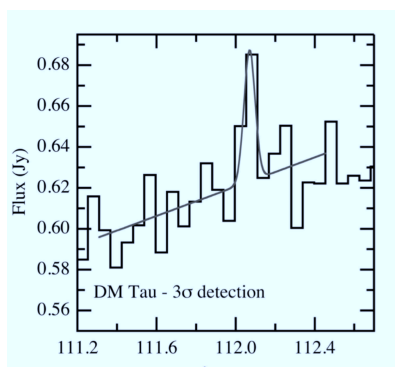
Authors: Uma Gorti (Ames/SETI)

Science Topic: Astrophysics

Abstract

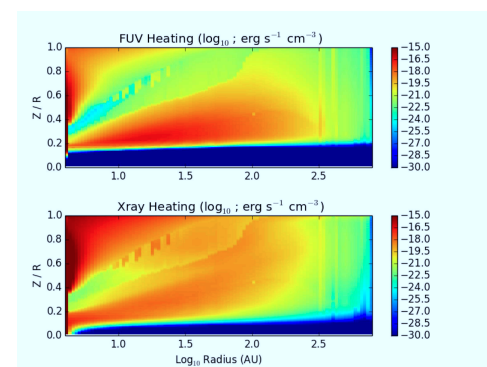
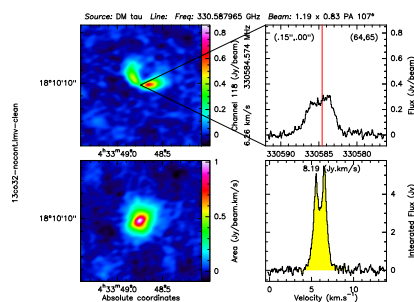
Protoplanetary disks provide the raw material from which planets form before the disks disperse. The advent of highly sensitive infrared and sub-millimeter facilities (*Spitzer*, *Herschel* Space Observatory, ALMA) has recently resulted in rapid advances in our understanding of disk physics, chemistry and evolution. Yet, fundamental properties such as the disk mass, or gas density, and the temperature structure—which govern nearly *all* physical and chemical processes in disks—still remain very poorly constrained. The primary gas component, H_2 , cannot be easily observed, but recent *Herschel* detections of emission from its main isotopologue, HD, have made it possible to determine the masses of disks for the first time. Converting the emission flux to a direct mass measure, however, involves *a priori* knowledge of the temperature structure of the disk.

Here, we present results from a targeted program to resolve some of these issues for the protoplanetary disk around DM Tau, one of three disks with detected HD emission. Following the methodology of a previous successful effort to determine the gas mass of the disk around TW Hya, we use thermochemical disk models to match various emission lines (e.g., [OI]63 μm , HD, [CI]609 μm , HCO^+ and CO isotope rotational lines) and determine the disk density and temperature structure. A Cycle 2 ALMA program was designed to empirically constrain the temperature structure and to calibrate the models by reproducing the observed spatial and velocity maps of the 1-0, 2-1 and 3-2 transitions of ^{12}CO , ^{13}CO and C^{18}O . The model disk comparisons provide insight into the importance of disk heating mechanisms, especially the role of Polycyclic Aromatic Hydrocarbons (PAHs) and FUV radiation. PAHs evolve along with dust, as grains grow to forming planetesimals. We further attempt to constrain gas heating mechanisms using the lack of PAH features in *Spitzer* IRS spectra which places an upper limit on their abundance. The DM Tau disk is inferred to have a higher abundance of PAHs than the older, TW Hya disk. All the above available information is used to infer the gas content of DM Tau, making it the second protoplanetary disk to have a gas mass determination.



(a) Herschel HD 1-0 detection (PI: E. Bergin)

(b) ALMA ^{13}CO observed emission (PI: U. Gorti)



(c) DM Tau Disk Model: Gas Heating due to FUV and X-rays

Testing Tidal Synchronization with Heartbeat Stars

Susan E. Thompson¹, Mara Zimmerman², Jim Fuller, Avi Shporer, Kelly Hambleton and Don Kurtz

¹susan.e.thompson@nasa.gov, SETI Institute, 189 Bernardo Ave., Mountain View

²ZIMMEMK12@juniata.edu, Juniata College

Topic: Astrophysics

Highly eccentric binary stars that undergo extreme, dynamic, tidal forces, were discovered in the *Kepler* data and are known as Heartbeat stars. As the two stars pass through periastron, these tidal forces are strong enough to significantly change the shape of the star. This, in addition to varying irradiation and gravity darkening causes periodic and sudden changes in the observed brightness of the system. Currently, more than 100 of these Heartbeat stars have been found in the *Kepler* data. In tidally interacting systems, rotation rates are known to synchronize with the orbital period. For eccentric binaries, Hut (1981) predicts that the rotation will pseudosynchronize instead, matching the weighted mean orbital angular velocity of the binary. Heartbeat stars give us the opportunity to test this theory. We measure the rotation rate of a dozen heartbeat stars by measuring the spot signature in the light curve. Then we measure the orbital parameters of the binary by modeling the shape of the periodic change in brightness that occurs at periastron. We find that not all heartbeat stars have reached pseudosynchronization, despite the predicted synchronization time scale being much shorter than the age of these stars. Radial velocity follow-up measurements are in progress that will help constrain the orbital and stellar properties of these systems.

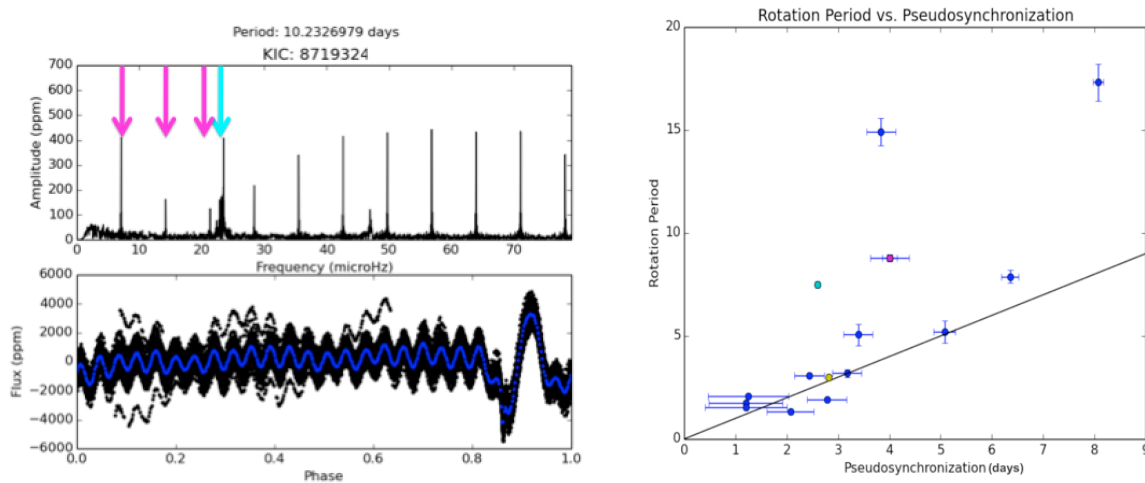
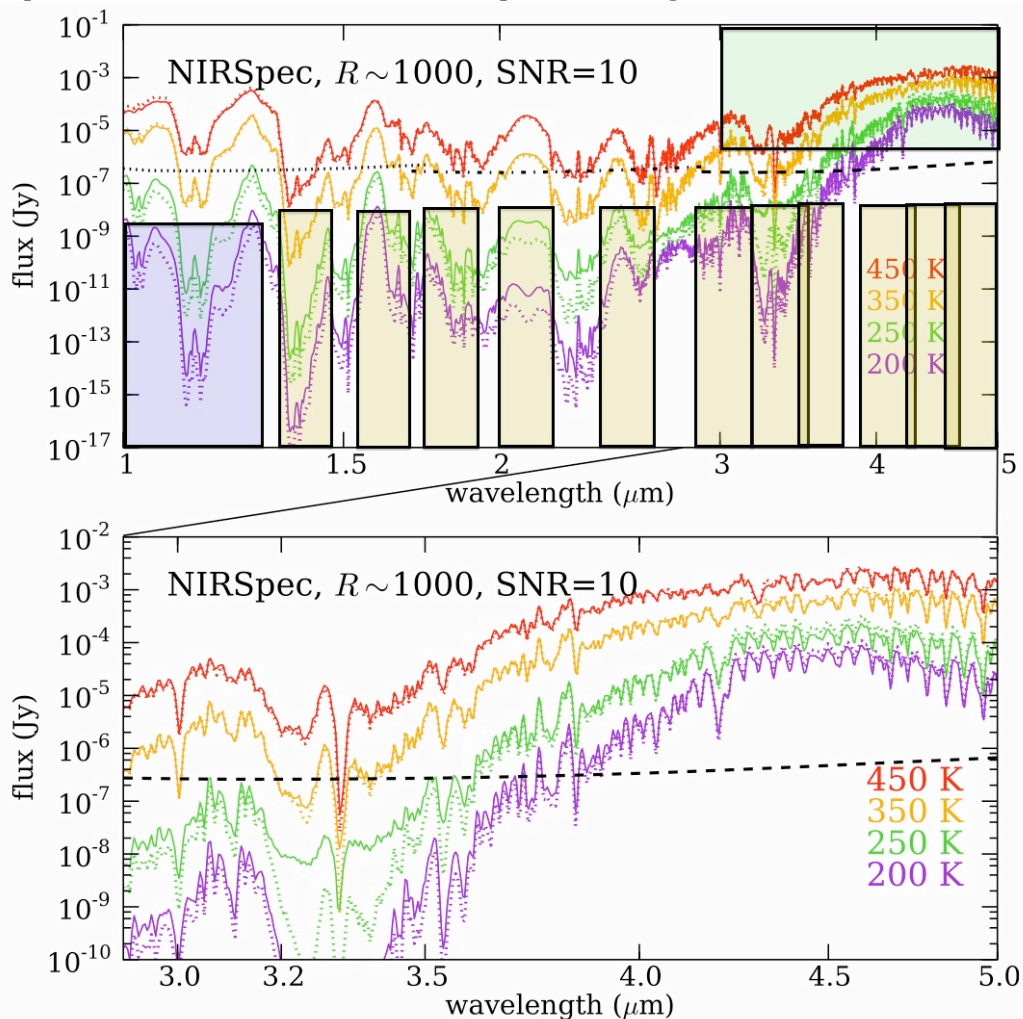


Figure 1: **Left:** The Fourier transform of a Heartbeat star with a blue arrow pointing to the peak caused by stellar rotation. The lower panel shows a folded light curve of the Heartbeat star. **Right:** The rotation period plotted against the pseudosynchronization period (calculated from the orbital period and eccentricity) for 15 Heartbeat stars. The one-to-one line is shown in black. For one system (pink square) the rotation period of both stars in the binary are seen and we were able to measure the rotation rate for both stars. The rotation rates of the two stars are close enough that they appear as one point on this figure.

OBSERVING Y-DWARFS WITH JWST

Tom Roellig (SSA), Tom Greene (SSA), Marcia Rieke (U. Arizona)
Astrophysics

Y-Dwarf objects are the coldest class of brown dwarf “failed-star” objects, objects whose mass is too low to initiate the nuclear fusion reactions that power the more normal main-sequence stars. Y-dwarfs are no larger than the planet Jupiter in size, and are roughly the same temperature as well. As a result they are very faint and are very poorly understood since they are barely detectable with the current astronomical instrumentation. The upcoming James Webb Space Telescope now in development for a launch in the Fall of 2018 will have vastly increased sensitivity in the near and mid-infrared compared to any current facilities and will be an ideal tool to obtain information about the composition and temperature-pressure structure in Y-dwarf atmospheres. The figure below shows the $10\text{-}\sigma$ sensitivity of the JWST instruments compared to modeled spectra of Y-dwarfs at various effective temperatures located at a distance of 5pc in an integration time of 10^5 seconds.



Title: How does the cosmic web influence galaxy evolution?

Authors: Mehmet Alpaslan & Pamela Marcum

Science topic: Astrophysics

Abstract: When viewed at large scales, the distribution of galaxies in the Universe is highly inhomogeneous. In fact, we observe a complex 'cosmic web' of galaxies that generate an intricate filamentary structure: vast linear formations of galaxies called filaments that surround empty regions called voids. Simulations and theory have established that filaments – the largest structures in the Universe - have formed in the billions of years after the Big Bang, and serve as conduits for transporting gas into galaxies, which they then turn into stars.

In this talk I will outline a recent observational detection of the complex interplay between the cosmic web and the stellar populations of spiral galaxies. I will begin by outlining some earlier work in detecting and characterising filamentary structure from galaxy survey data, before discussing my current work in tracking the star formation rates of spiral galaxies in filaments.

Title: An HI Survey of Extremely Isolated Early-type Galaxies

Authors: Pamela M. Marcum, Trisha L. Ashley, & Michael N. Fanelli

Science Topic: Extragalactic Astronomy

Abstract: We present preliminary results from an ongoing HI survey of extremely isolated early-type galaxies (IEGs) conducted using the NRAO Robert C. Byrd Green Bank Telescope (GBT). Each IEG is separated by at least 2.5 Mpc from nearest neighbors brighter than $M_V = -16.5$. Previous optical imaging/spectroscopy investigations of these galaxies by our research team found a higher percentage of the sample exhibiting recent or ongoing star formation, relative to their counterparts in higher density environments. Preliminary findings from our HI survey, the first comprehensive assessment of neutral gas content within and around such systems, indicate **at least 40% of the observed isolated early-type galaxies have detectable HI gas.**

Resolved dust emission analysis in IC1459 and NGC2768.

A. Amblard, P. Temi

Science Topic : Astrophysics

Elliptical galaxies are considered red and “dead” galaxies, due to their typical color and star formation rate (SFR). However, far-infrared(IR) MIPS Spitzer observations from Temi et al. 2007 revealed that some local elliptical galaxies possess an amount of dust beyond what can be lost by their star population. These observations suggest a potential feedback mechanism between the central AGN and the dusty gas, that transports buoyantly the dust several kpcs away from the core.

To better understand this feedback, we obtained PACS Herschel (70 and 160 μm) data for two galaxies, IC1459 and NGC2768, these data allow to map the cold dust at higher angular resolution (5.6” & 11.4”) . These two galaxies present a disturbed morphology at these far-infrared wavelengths that is very different from the smooth stellar light distribution expected from elliptical galaxies and observed in the optical and IR wavelengths for these galaxies.

In this work, we analyze the spectral energy distribution (SED) analysis of IC1459 and NGC2768, two local elliptical galaxies. We performed a pixel-by-pixel SED fitting of each of these objects, allowing us to characterize the spatial distribution of such parameters as the stellar mass, the SFR, the metallicity, young star fraction, etc. We compare these estimates to previous observations.

TELL US, IN LAYMAN'S
TERMS, WHAT YOUR
BREAKTHROUGH MEANS.

CERTAINLY.
 $K - \frac{4n^3}{7} \sqrt{P} \dots 4 \cdot \frac{\Sigma L}{5T}$



J. Harris



Title: Estimation of chromatic errors from broadband images for high contrast imaging

Authors: D. Sirbu and R. Belikov

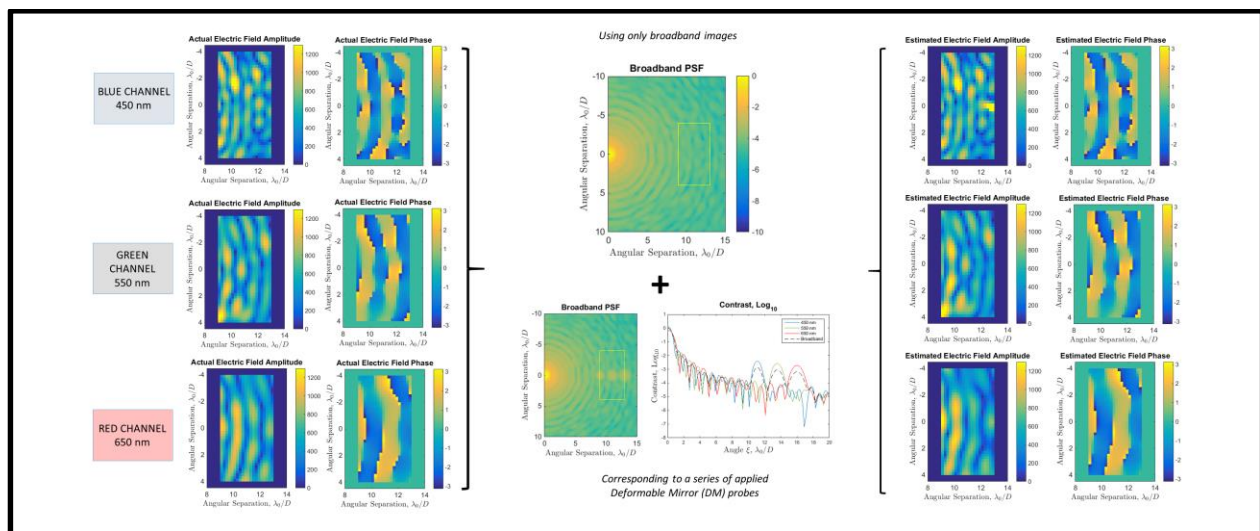
Science Topic: Exoplanet

Abstract:

Usage of an internal coronagraph with an adaptive optical system for wavefront correction for direct imaging of exoplanets is currently being considered for many mission concepts, including as an instrument addition to the WFIRST-AFTA mission to follow the James Web Space Telescope.

To date, most broadband lab demonstrations use narrowband filters to estimate the chromaticity of the wavefront error, but this reduces the photon flux per filter and requires a filter system. Previously, we have proposed a method to estimate the chromaticity of wavefront errors using only a broadband image (Single Filter Broadband Estimation – SFBE). This is achieved by using special DM probes that have sufficient spatially-localized chromatic diversity.

Here, we demonstrate through simulation the feasibility of direct estimation using broadband images wide bands of 20% (similar to the WFIRST-AFTA).



Focal plane phase and amplitude retrieval using direct broadband images using three different channels at 20% wavelength bands.

Why Alpha Centauri is a Particularly Good Target for Direct Imaging of Exoplanets

Ruslan Belikov, Eduardo Bendek, Sandrine Thomas, Jared Males
and the ACESat team

Science Topic: Exoplanet

ARC SSA Jamboree 2016.

Several mission concepts are being studied to directly image planets around nearby stars. It is commonly thought that directly imaging a potentially habitable exoplanet around a Sun-like star requires space telescopes with apertures of at least 1m. A notable exception to this is Alpha Centauri (A and B), which is an extreme outlier among FGKM stars in terms of apparent habitable zone size: the habitable zones are $\sim 3x$ wider in apparent size than around any other FGKM star and are thus in theory accessible to much smaller telescopes. Alpha Centauri is also an extreme outlier in terms of how bright its planets are. For example, an Earth-like planet would be several magnitudes brighter around Alpha Centauri than around any other Sun-like star. Alpha Centauri lies in the galactic plane but its high brightness and proper motion make confusion with background stars unlikely, and extinction by our own galaxy makes confusion with extragalactic sources unlikely. The high brightness also helps any planet stand out against exozodiacal light. Alpha Centauri B has a (probable) planet, which establishes that a planetary system has formed in the system despite the multiplicity of the system. Dynamical simulations show that the habitable zones around both Alpha Centauri A and B are stable, and RV measurements rule out any large planets in the system that may have disrupted the formation of habitable planets. Recently developed high contrast techniques enable the detection of planets in multi-star systems, enabling imaging planets around Alpha Centauri. In particular, a small $\sim 30\text{-}45\text{cm}$ visible light space telescope equipped with a modern high performance coronagraph or starshade is sufficient to directly image any potentially habitable planet that may exist in the system.

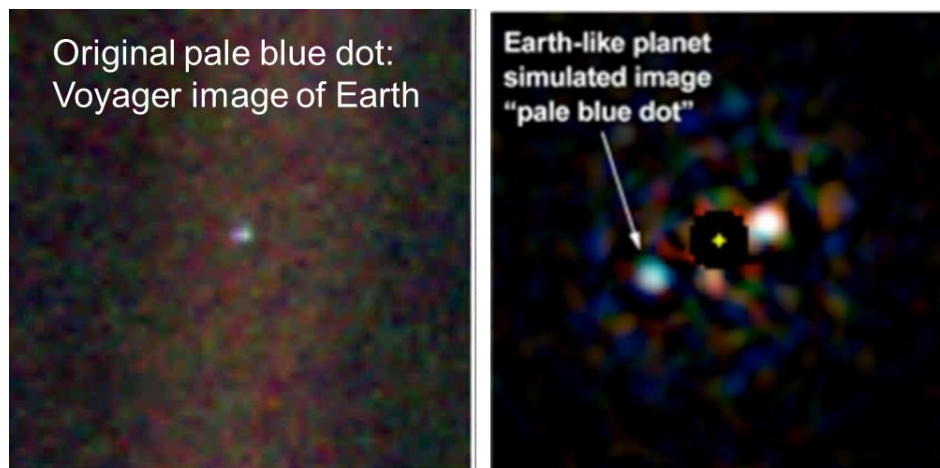
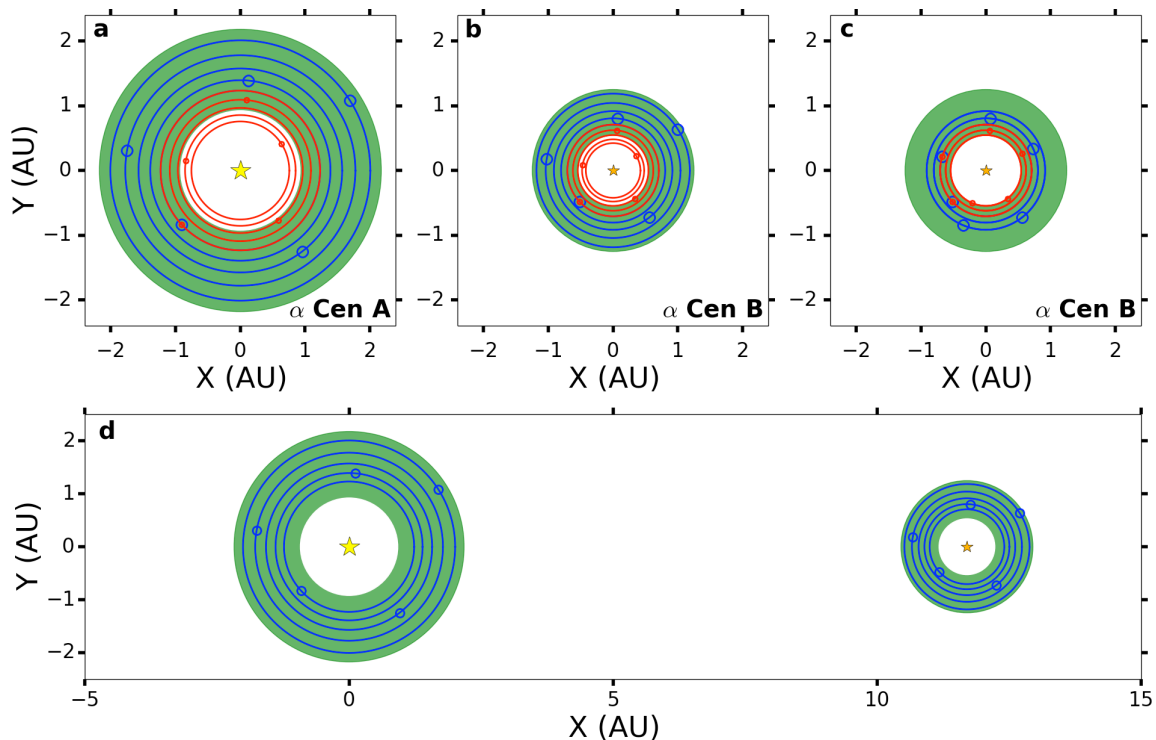


Figure 1. Left: Image of our Earth taken by the Voyager spacecraft from the edge of the Solar System. Right: A simulated image of a hypothetical Earthlike planet in the Alpha Centauri system as could be seen by a 45cm space telescope such as ACESat. (Also shown are a Venus-like and Mars-like planets).

Long-Term Stability of Planets in the Alpha Centauri System

Jack Lissauer & Billy Quarles

The alpha Centauri system is billions of years old, so planets are only expected to be found in regions where their orbits are long-lived. We evaluate the extent of the regions within the alpha Centauri AB star system where small planets are able to orbit for billion-year timescales, and we map the positions in the sky plane where planets on stable orbits about either stellar component may appear. We confirm the qualitative results of Wiegert & Holman (Astron. J. 113, 1445, 1997) regarding the approximate size of the regions of stable orbits of a single planet, which are larger for retrograde orbits relative to the binary than for prograde orbits. Additionally, we find that mean motion resonances with the binary orbit leave an imprint on the limits of orbital stability, and the effects of the Lidov-Kozai mechanism are also readily apparent. Overall, orbits of a single planet in the habitable zones near the plane of the binary are stable, whereas high-inclination orbits are short-lived. However, even well within regions where single planets are stable, multiple planet systems must be significantly more widely-spaced than they need to be around an isolated star in order to be long-lived.



Top 3 diagrams show to scale initial conditions for simulations with 3 or 5 planets, with the innermost or outermost receiving the same energy from the star it orbits as the Earth does from the Sun; optimistic habitable zones are shown in green. The bottom diagram shows planets around both stars with the stellar separation at closest approach.

The Frequency of Giant impacts on Earth-like worlds

Elisa V. Quintana, Thomas Barclay, William Borucki, Jason F. Rowe, Chris Henze, and John E. Chambers

The Earth's geological record has established that a large number of significant impacts onto Earth helped to shape its composition and habitability. Several Earth-sized planets have been discovered in the habitable zones of distant stars, but we dynamical models are needed in order to gain insight on the flux of giant impacts experienced by these types of planets during their formation.

We recently updated a popular N -body code to include a state-of-the-art collisions model that allows a wide range of outcomes, including fragmentation, for each collision. Giant impacts can deliver or strip away water and other volatiles that are necessary ingredients for carbon-based life. Our new model enables us to study where Earth-like planets can form, and also allows us to trace impact histories, the delivery and evolution of water content, and estimate bulk compositions of the final terrestrial planets (Figures 1 and 2).

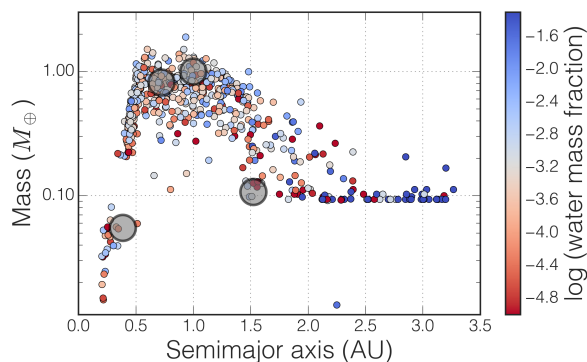


Figure 1. Distributions of final planets from 150 simulations of planet formation around the Sun with Jupiter and Saturn included. The four large circles indicate the location of Mercury, Venus, Earth and Mars. The planets are shaded according to their final water mass fraction, where blue planets are water-rich and red planets are dry. Bodies located in the asteroid region and beyond were originally given 5% water mass fraction.

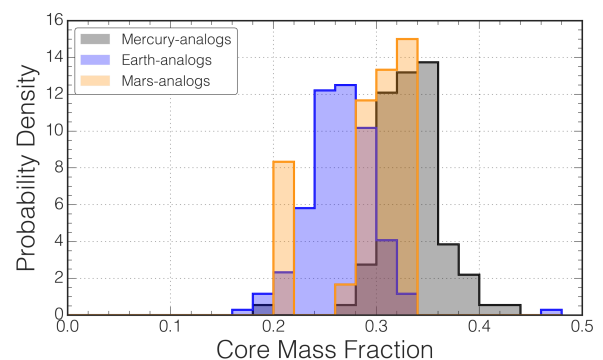


Figure 2. Distributions of final core mass fraction for analogs of Mercury, Earth and Mars from 150 simulations of planet formation around the Sun with Jupiter and Saturn included. All bodies began with a 30% core mass fraction.

Most of the observed Earth-sized planets reside in environments quite different than our Solar System. Observations suggest that the occurrence rates of Jupiter-analogs around Sun-like stars is about 6%. We have performed hundreds of simulations of late stage planet formation around the Sun, with and without giant planets, to statistically infer the effects of giant impacts onto Earth-analogs. Our preliminary results are showing that in systems with Jupiter the final giant impact onto an Earth-analog typically occurs within 100 Myr (Figure 3). In contrast, Earth-analogs that form in systems that lack giant companions can still experience final giant impacts beyond 1 Gyr. We will present results from both sets of simulations and discuss whether Jupiter-analogs help or impede habitability for Earth-like planets around Sun-like stars.

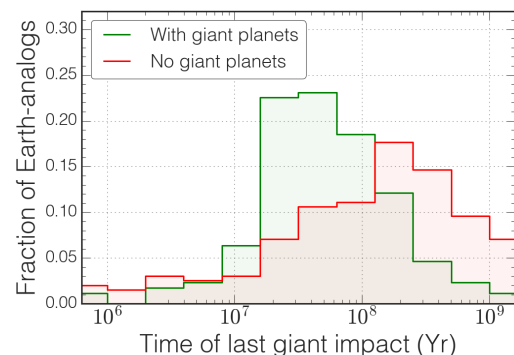


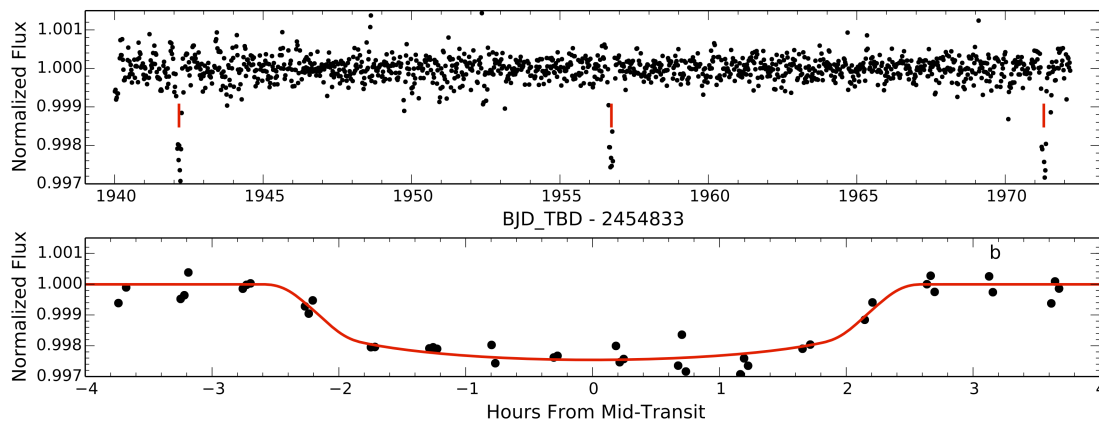
Figure 3. Final giant impact time onto Earth-analogs formed in systems with and without giant planets.

Small Stars with Small Planets from *K2*: The *K2* M Dwarf Program

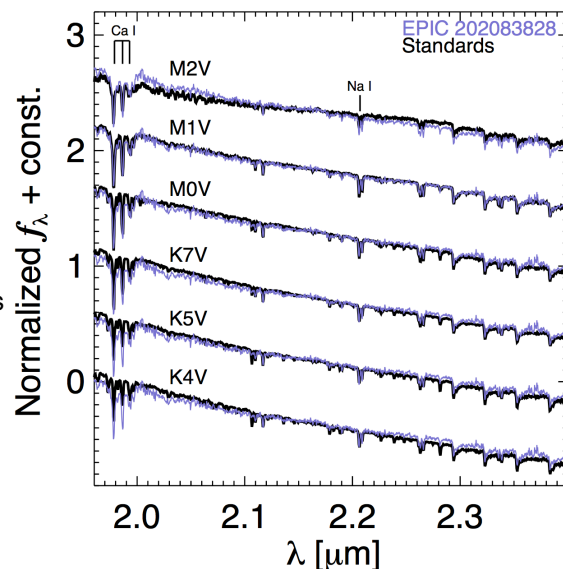
Joshua Schlieder, Ian Crossfield, Erik Petigura, Andrew Howard, Evan Sinukoff, Kimberly Aller, Chas Beichman, David Ciardi, Sebastien Lepine, Courtney Dressing, Arturo Omar Martinez, Tom Greene, Mike Werner

Topic: Exoplanets

The prime *Kepler* mission revealed that small planets ($<4 R_{\text{Earth}}$) are common, particularly around low-mass M dwarfs. *K2*, the repurposed *Kepler* mission, continues this exploration of small planets around small stars. For the past year we have proposed M dwarfs as *K2* targets, searched their photometry for candidate planets, and pursued follow-up to validate new planetary systems. Our program aims to identify new targets for transit spectroscopy with the HST and *JWST*; find RV targets to measure the mass/radius relationship and understand bulk planet compositions; and further our understanding of planet occurrence frequencies. I will present the methodology of the *K2* M Dwarf Program (*K2*-MDP), highlight published results, and provide a progress report of our continued follow-up and validation efforts.



Figures: **Top:** detrended, normalized light curve of K2-26 (EPIC 202083828), showing the transits of a newly validated M dwarf planet from the *K2*-MDP. The bottom plot shows the phase folded light curve with a best fit transit model. **Right:** K-band spectrum of K2-26 compared with late-type spectral standards. Features in the spectrum allow us to measure the star's temperature and metallicity and infer its mass and radius. These values combined with the *K2* light curve provide estimates of the planet parameters. The planet, K2-26b, is a sub-Neptune with a radius $\sim 2.7 R_{\text{Earth}}$ and an equilibrium temperature of ~ 430 K.



DAVE: Detection and Vetting of Exoplanets (in K2)

Fergal Mullally¹, Susan E. Thompson, Christopher J. Burke, Knicole Colon, Tom Barclay, Elisa Quintana & Geert Barensten

Subject Keywords: Astrophysics, Exoplanets

We present initial results from a new software pipeline to find transiting planets and eclipsing binaries in K2 data. K2 is the follow-up mission to Kepler using the same flight hardware, but observing different regions of the sky. The K2 project releases calibrated lightcurves for observed targets, but unlike Kepler does not undertake a planet search. This task is performed by various groups in the community.

We have created one such planet detection pipeline, which we name DAVE (for Detection and Vetting of Exoplanets). Unlike other available projects, DAVE not only finds transit signals, it automatically vets those signals and determines whether they are planets, eclipsing binaries, background events, or systematic noise sources masquerading as transits.

We show first results from our pipeline on K2's Campaign 6. We describe our target selection algorithm, and discuss some of the vetting techniques we use to distinguish between planets and other periodic signals in the data.

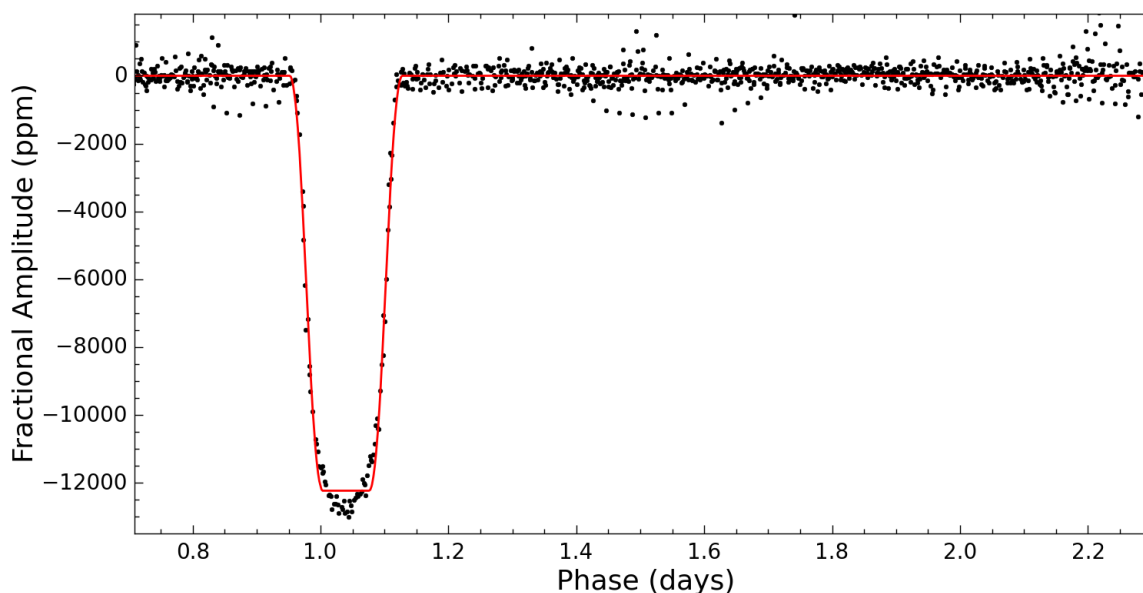


Figure 1: A previously known planet, Wasp-47b, found by DAVE in K2 data. The lightcurve is folded at the detected orbital period (4.16 days), and a portion around the transit is shown. We overlay the best fit trapezoid model of the transit as the red solid line. A trapezoid fit makes no effort to model the round shape of the bottom of the transit, which has limited use in determining whether the source of the signal is a planet transit or not.

¹fergal.mullally@nasa.gov

Jamboree 4 Abstract, J. Van Cleve et al.

Title: *That's How We Roll – The NASA K2 Mission Science Products and Their Performance Metrics*

Authors: Jeffrey E. Van Cleve^{1,2}, Steve B. Howell¹, Jeffrey C. Smith^{1,2}, Bruce D. Clarke^{1,2}, Susan E. Thompson^{1,2}, Stephen T. Bryson¹, Mikkel N. Lund^{3,4}, Rasmus Handberg⁴, William J. Chaplin^{3,4}

Science Topics: Exoplanets and Astrophysics

Abstract: NASA's exoplanet Discovery mission *Kepler* was reconstituted as the *K2* mission a year after the failure of the 2nd of *Kepler's* 4 reaction wheels in May 2013. The new spacecraft pointing method now gives typical roll motion of 1.0 pixels peak-to-peak over 6 hours at the edges of the field, two orders of magnitude greater than for *Kepler*. Despite these roll errors, the flight system and its modified science data processing pipeline restores much of the photometric precision of the primary mission while viewing a wide variety of targets, thus turning adversity into diversity. We define metrics for data compression and pixel budget available in each campaign; the photometric noise on exoplanet transit and stellar activity time scales; residual correlations in corrected long cadence light curves; and the protection of test sinusoidal signals from overfitting in the systematic error removal process. We find that data compression and noise both increase linearly with radial distance from the center of the field of view, with the data compression proportional to star count as well. At the center, where roll motion is nearly negligible, the limiting 6 hour photometric precision for a quiet 12th magnitude star can be as low as 30 ppm, only 25% higher than that of *Kepler*. This noise performance is achieved without sacrificing signal fidelity; test sinusoids injected into the data are attenuated by less than 10% for signals with periods up 15 days. At time scales relevant to asteroseismology, light curves derived from *K2* archive calibrated pixels have high-frequency noise amplitude within 40% of that achieved by *Kepler*. These improvements follow from the data analysis efforts of *Kepler* Science Operation Center and *Kepler* Science Office, and from the operational improvements developed by Ball Aerospace and LASP, during the first 1.5 yr of *K2*. The paper from which most of these results are drawn has been accepted by PASP <http://arxiv.org/abs/1512.06162>

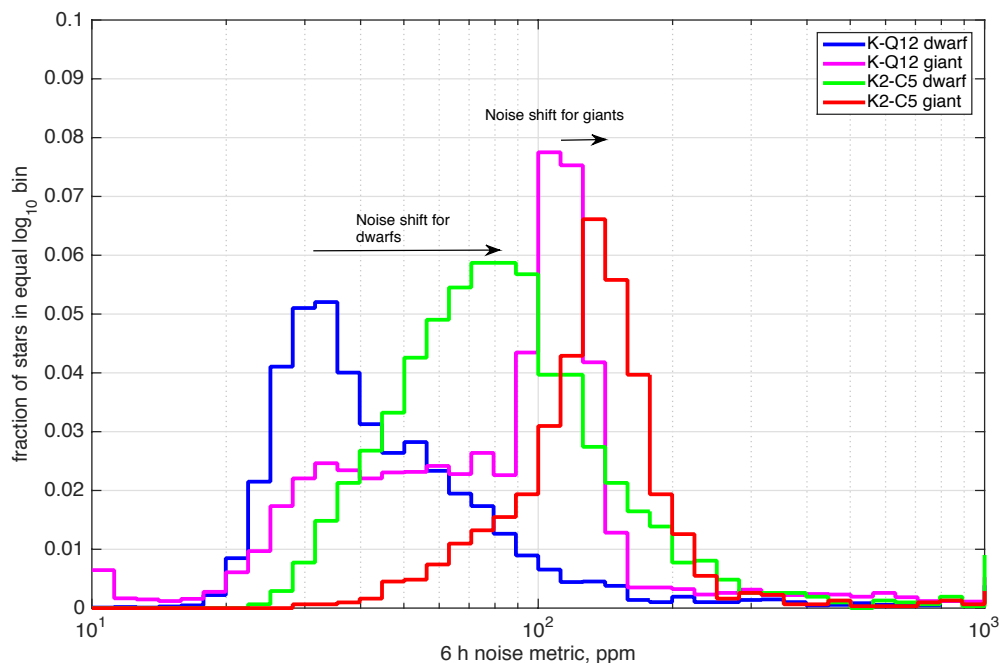


Figure 1: Histogram of transit time scale noise for *Kepler* Quarter 12 and *K2* Campaign 5 12th magnitude stars, identified as dwarf and giant stars from stellar surface gravity, $\log g$ (Huber et al., 2015). While the typical noise for dwarf stars has increased considerably, *K2* remains nearly astrophysically limited for most giant stars. For comparison, an Earth-Sun transit is an 84 ppm signal.

¹NASA Ames ²SETI Institute ³University of Birmingham ⁴Aarhus University

Photochemical hazes in exoplanetary atmospheres

Hiroshi Imanaka (NASA Ames Research Center/SETI Institute), Dale P. Cruikshank (NASA Ames Research Center), Christopher P. McKay (NASA Ames Research Center), Mark Marley (NASA Ames Research Center), Mark A. Smith (University of Houston)

Topic: Exoplanet

Recent transit observations of exoplanets have demonstrated the possibility of a wide prevalence of haze/cloud layers at high altitudes. Hydrocarbon photochemical haze could be the candidate for such haze particles on warm sub-Neptunes, but the lack of evidence for methane poses a puzzle for such hydrocarbon photochemical haze. The CH_4/CO ratios in planetary atmospheres vary substantially from their temperature and dynamics. An understanding of haze formation rates and plausible optical properties in a wide diversity of planetary atmospheres is required to interpret the current and future observations.

Here, we focus on how atmospheric compositions, specifically CH_4/CO ratios, affect the haze production rates and their optical properties. We have conducted a series of cold plasma experiments to constrain the haze mass production rates from gas mixtures of various CH_4/CO ratios diluted either in H_2 or N_2 atmosphere. The mass production rates in the $\text{N}_2\text{-CH}_4\text{-CO}$ system are much greater than those in the $\text{H}_2\text{-CH}_4\text{-CO}$ system. They are rather insensitive to the CH_4/CO ratios larger than at 0.3. Significant formation of solid material is observed both in $\text{H}_2\text{-CO}$ and $\text{N}_2\text{-CO}$ systems without CH_4 in the initial gas mixtures. The complex refractive indices were derived for haze samples from N_2/CH_4 , H_2/CH_4 , and H_2/CO gas mixtures. These are the model atmospheres for Titan, Saturn, and exoplanets, respectively. The imaginary part of the complex refractive indices in the UV-Vis region are distinct among these samples. Especially, very dark solid generated from a H_2/CO gas mixture can be a good candidate for aerosol material in warm exoplanets with very low albedos.

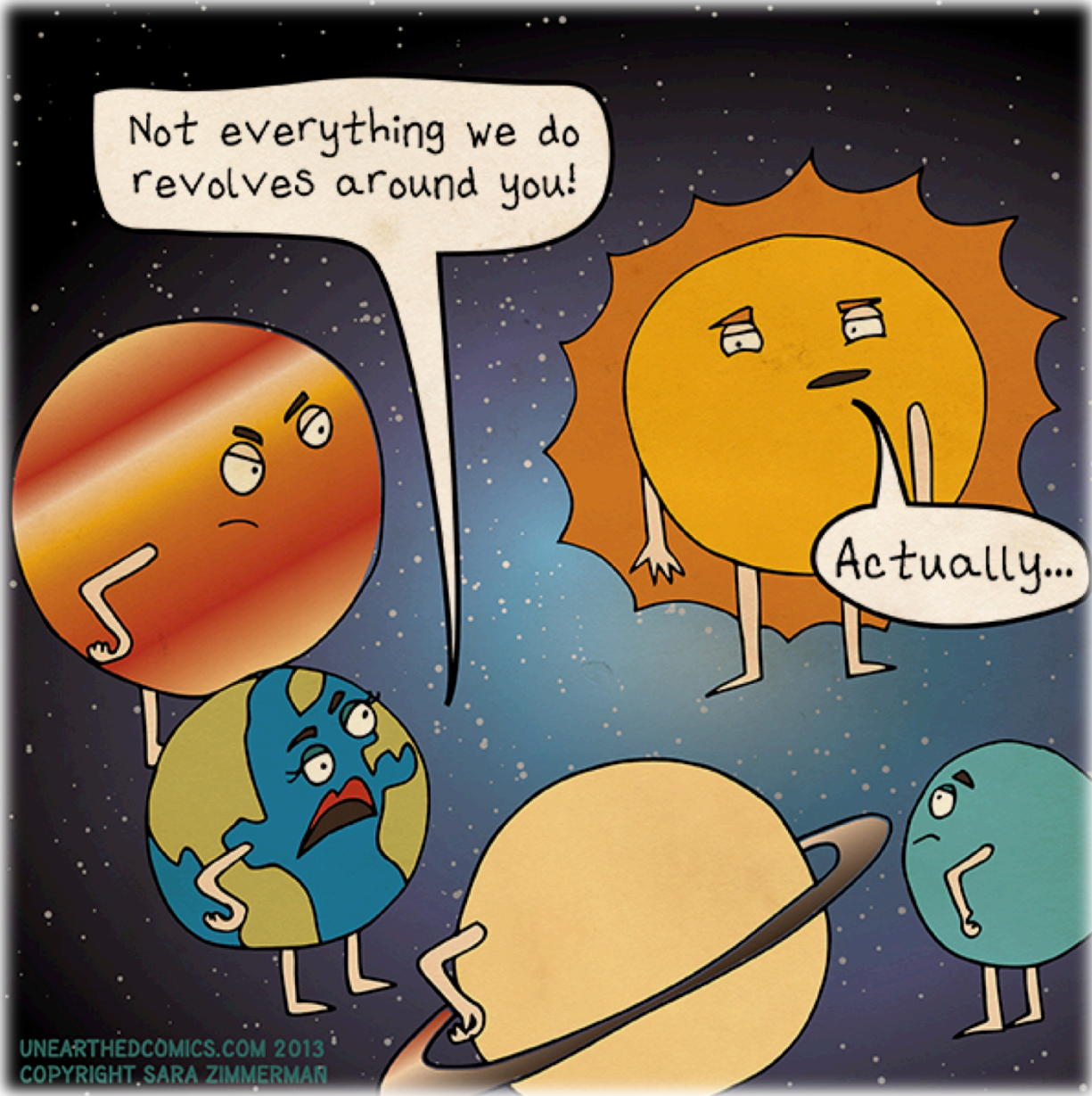
Titan-like exoplanets: Variations in geometric albedo and limb transit height with haze production rate**Jade Checlair (NASA/University of Toronto), Christopher P. McKay (NASA), and Hiroshi Imanaka (NASA/SETI)**

Topic: Exoplanet

Extensive studies characterizing Titan present an opportunity to study the atmospheric properties of Titan-like exoplanets. Using an existing model of Titan's atmospheric haze, we computed geometric albedo spectra and limb transit height spectra for five values of the haze production rate (zero haze to twice present) over a wide range of wavelengths (0.2-2 μm). In geometric albedo spectra, the slope in the UV-visible changes from blue to red when varying the haze production rate values from zero to twice the current Titan value. This spectral feature is the most effective way to characterize the haze. Methane absorption bands in the visible-NIR compete with the absorbing haze, being stronger for smaller haze production rates. Reflectivity is increased by a larger haze production rate in the IR range, affected by the haze and surface properties. The limb transit heights probe a region of the atmosphere where the haze and gas are optically thin and thus not effectively probed by the geometric albedo. The limb transit height decreases smoothly with increasing wavelength, from 376 km to 123 km at 0.2 and 2 μm , respectively. When decreasing the haze production rate, the methane absorption bands become stronger, and the limb transit height decreases with a steeper slope with increasing wavelength.

To match our transit heights with published results based on Cassini data we reduce the specific density of the haze material to 0.4 (from 1). In that case the limb transit height decreases from 433 to 195 km at 0.2 and 2 μm , respectively. Limb transit height values for all haze production rates increase when reducing the specific density of the haze material.

When adding methane condensation clouds in the lower atmosphere with a particle radius of 10 μm , geometric albedo spectra are greatly affected, with values being increased especially in the visible-IR range. Limb transit height spectra are insensitive to the presence of clouds and to changes in surface properties, as they do not probe altitudes less than 34 km. The slope of the geometric albedo in the UV-visible increases smoothly with increasing haze production rate, while the slope of the limb transit height spectra does not provide a way to characterize the haze. We conclude that geometric albedo spectra provide the most sensitive indicator of the nature and properties of the background Rayleigh gas, haze, methane absorption bands, troposphere, and the surface – and should be preferred over transit spectra.



UNEARTHEDCOMICS.COM 2013
COPYRIGHT SARA ZIMMERMAN

K2 Observations of a Variable Planet: Neptune as Model of Brown Dwarf Variability

Mark S. Marley, Amy A. Simon, Jason F. Rowe, Patrick Gaulme, Heidi B. Hammel, Sarah L. Casewell, Jonathan J. Fortney, John E. Gizis, Jack J. Lissauer, Raul Morales-Juberias, Glenn S. Orton, Michael H. Wong

Planetary Atmosphere & Climate

NASA has devoted thousands of hours to searches by HST and Spitzer for brown dwarf variability. These searches have found that a large fraction of all brown dwarfs are indeed variable, but there has been remarkably little solar system context with which such observations can be compared. In order to better understand the variability of a giant planet atmosphere on a variety of timescales we observed Neptune with the Kepler Space Telescope as a K2 science target. Observations yielded a 49-day light curve with 98% coverage at a 1-minute cadence. A significant signature in the light curve comes from discrete cloud features. We compare results extracted from the light curve data with contemporaneous disk-resolved imaging of Neptune from the Keck 10-meter telescope at 1.65 microns and Hubble Space Telescope visible imaging acquired 9 months later. This direct comparison validates the feature latitudes assigned to the K2 light curve periods based on Neptune's zonal wind profile, and confirms observed cloud feature variability. Although Neptune's clouds vary in location and intensity on short and long time scales, a single large discrete storm seen in Keck imaging dominates the K2 and Hubble light curves; smaller or fainter clouds likely contribute to short-term brightness variability. In particular we suggest that the balance between large, relatively stable, atmospheric features and smaller, more transient, clouds controls the character of substellar atmospheric variability. Atmospheres dominated by a few large spots may show inherently greater light curve stability than those which exhibit a greater number of smaller features.

In my talk I will show the remarkable movie of Neptune obtained by K2, place the observations in context with brown dwarf variability observation, and briefly describe other remarkable features of the data, including the detection of solar oscillation modes in reflected light.

Earth 2.7 billion years ago had half the air pressure of today

Sanjoy M. Som¹, Roger Buick², James W. Hagadorn³, Tim S. Blake⁴, John M. Perreault⁵, Jelte P. Harnmeijer⁶, and David C. Catling²

¹Blue Marble Space Institute of Science / NASA Ames Research Center, Moffett Field, CA

²University of Washington, Seattle, WA

³Denver Museum of Nature & Science, Denver CO

⁴University of Western Australia, Crawley, WA, Australia

⁵University of Alaska, Fairbanks, AK

⁶Edinburgh Centre for Carbon Innovation, Edinburgh, Scotland

We constrain air pressure on Earth 2.7 billion years ago to half modern levels using gas bubbles in lava flows. Air pressure is a fundamental descriptor of the Earth system due to its link to biogeochemical cycles and the Earth interior. Understanding the evolution of air pressure through time is key to understanding the evolution of our atmosphere through time. Because our planet has remained habitable over at least 3.8 billion years, temporal snapshots of Earth's atmosphere may add insight into atmospheric properties that sustain life. Such a database of "habitable atmosphere" will be invaluable when the chemical and physical properties of exoplanetary atmospheres are returned by the next generation of telescopes.

Previous studies have only placed maximum levels on this critical variable for the ancient Earth. Here, we calculate an absolute value for barometric pressure using gas bubble size distributions in lava flows that solidified 2.7 billion years ago at sea-level in the Pilbara Craton, Western Australia. Gas bubble dimensions are quantified using high-resolution X-ray computer tomography from core samples obtained from the top and bottom of the lava flows. The bubble modal size expressed at the top and at the bottom of a flow can be linked to atmospheric pressure using the ideal gas law. Such a technique has been verified as a paleoaltimeter using modern lava flows on Hawai'i.

Perhaps as significant as the "great oxidation event", this "great nitrogen draw-down" may suggest an interplay between redox states, tectonics, and the emergence of biological nitrogen fixation that was previously unrecognized.

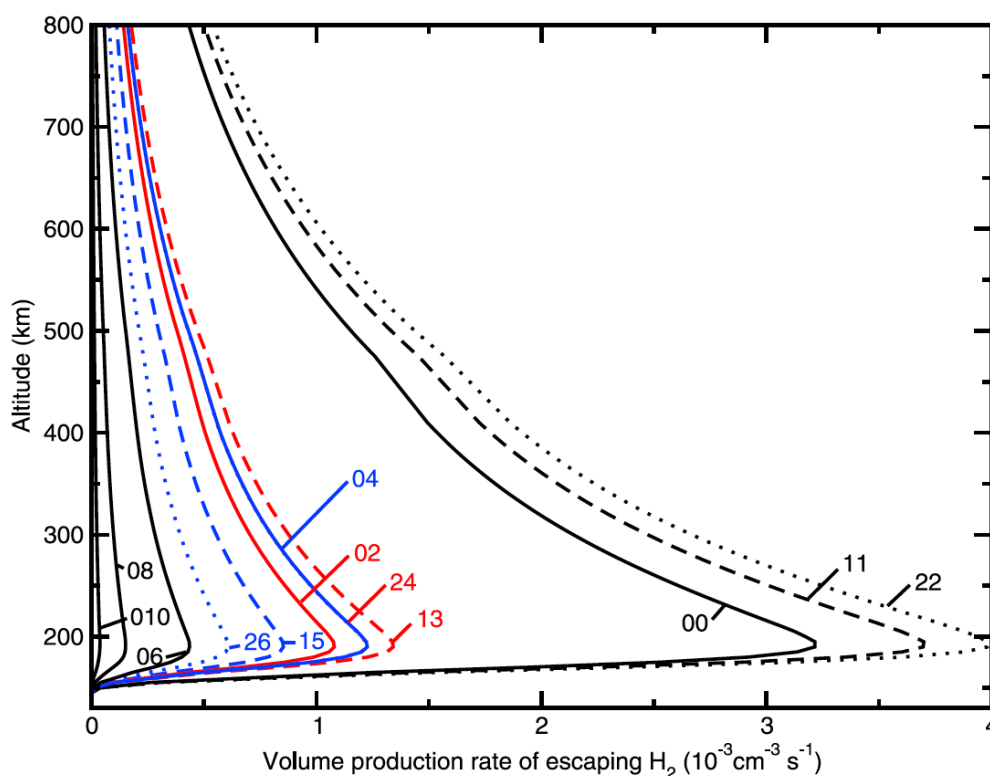
Topic: Planetary Atmospheres & Climate

Title: Non-thermal escape of molecules from planetary atmospheres

Author: Marko Gacesa

Science Topic: Planetary Atmosphere & Climate

Dissociative recombination of oxygen molecular ions and precipitation of solar wind ions are among the main production mechanisms of hot oxygen atoms in the upper atmosphere of Mars and other planets with similar atmospheric composition. The hot oxygen atoms perturb local thermodynamic equilibrium conditions by depositing their kinetic energy in collisions with thermal atmospheric gases, inducing chemical reactions, and forming rotationally and vibrationally excited products. A specific process of interest in upper atmospheres of Mars, Earth, and Venus is the reactive collision of hot O atom with a hydrogen molecule, leading to production of excited H_2 , HD, and OH molecules. Here, we present a detailed description of the process obtained from state-to-state reactive quantum scattering calculations and discuss implications on the escape of small molecules from Mars and other terrestrial planets, their local non-thermal environment, and atmospheric H/D ratios. Our results indicate that direct collisional escape of light molecules from terrestrial planets occurs and contributes to the total energy balance of their atmospheres (Fig. 1, below). These processes have not been accounted for in existing global circulation models. We also briefly discuss the variability of molecular non-thermal escape rates on Mars with respect to solar cycle, seasons, and varying solar radiation, as well as possibility of escape of larger molecules (*e.g.* CH_4 , NH_3), potentially of interest for evolution of Titan and small exoplanets with CO_2 - H_2 - N_2 atmospheres.



What Have We Learned from the LADEE Mission?

R. C. Elphic, M. Horanyi, A. Colaprete, M. Benna, P. R. Mahaffy, G. T. Delory, S. K. Noble, J. S. Halekas, D. M. Hurley, T. J. Stubbs, M. Sarantos, S. Kempf, A. Poppe, J. Szalay, Z. Sternovsky, A. M. Cooke, D. H. Wooden, D. Glenar

Introduction: NASA's Lunar Atmosphere and Dust Environment Explorer, LADEE, concluded a fully successful investigation of the Moon's tenuous gas and dust atmosphere on April 18, 2014. LADEE hosted three science instruments to address atmospheric and dust objectives. The three science instruments were an ultraviolet-visible spectrometer (UVS), a neutral mass spectrometer (NMS), and a lunar dust experiment (LDEX). A mission overview and science instrument descriptions are available [1,2,3,4]. LADEE entered a low-altitude, retrograde lunar orbit optimized for observations at the sunrise terminator, where surface temperatures rise abruptly. LADEE carried out observations over a wide range of local times and altitudes. Here we describe some of the initial results.

Lunar Exospheric Dust: LDEX measurements have revealed the presence of a tenuous but persistent "cloud" of small dust grains, from <0.3 to >0.7 μm in radius [5]. The number density of these grains maximizes over the morning side of the Moon, the hemisphere on the "upstream" side of the Moon's motion about the sun. The cloud, with observed densities ranging between $0.4 - 4 \times 10^{-3} \text{ m}^{-3}$, is made up of ballistic ejecta from micrometeoroidal impacts on the lunar surface. The cloud density increases as the Earth-Moon system passes through known meteoroid streams, such as the Geminids, which are derived from cometary debris trails. LDEX data show no evidence for an electrostatically-lofted dust component [6].

Lunar Exospheric Structure and Composition: LADEE's NMS instrument immediately detected helium (^4He) in the lunar atmosphere during high altitude commissioning. At lower altitudes it also measured neon (^{20}Ne) and argon (^{40}Ar). NMS measurements revealed systematic variations in density and scale height for these three noble gas species [7]. The diurnal variation of helium, neon and argon are largely controlled by surface. Helium density closely tracks the input of He^{++} from the solar wind; loss is by way of thermal escape. ^{20}Ne is a minor solar wind constituent, but it has a long lifetime at the Moon and builds up to significant densities in the lunar atmosphere. ^4He , ^{20}Ne and ^{40}Ar are the three most abundant species in the lunar exosphere. ^{40}Ar density maximizes over the western maria, in particular the KREEP-rich Mare Imbrium and Oceanus Procellarum areas, part of the PKT. There is also an overall, many-lunation variation in argon density, perhaps reflecting changes in the rate

of release out of the subsurface, either the interior diffusive source or impacts.

NMS also ran an ion-only mode, which revealed the presence of multiple species that are ionized by solar EUV and accelerated by the solar wind electric field, as measured in the lunar neighborhood by ARTEMIS [8]. These species include H_2^+ , He^+ , $^{20}\text{Ne}^+$, Na^+ , K^+ and $^{40}\text{Ar}^+$, as might be expected, but also seen are $^{12}\text{C}^+$, $^{14}\text{N}^+$ and mass 28, which could be Si^+ , N_2^+ or most likely CO^+ . While masses 17 and 18 (OH and H_2O) were also observed in ion mode, their flux did not correlate with the solar wind electric field – these are considered probable outgassing artifacts, from the local spacecraft "coma".

Remote Sensing of Na and K: LADEE's UVS made measurements of the sodium and potassium exospheres. The sodium exosphere exhibits a systematic variation with lunar phase, peaking near Full Moon, but with temporal structure in the density that suggests solar wind sputtering (absent in the geomagnetic tail) is an important source term. Meanwhile, mobile Na atoms that are not lost to photoionization can be trapped on the cold nightside, and recycled into the atmosphere after sunrise. As the Moon leaves the geomagnetic tail, sputtering resumes and the abundance rises with newly-released Na atoms. There is a long-term trend to the sodium, with an overall decline similar to ^{40}Ar . Its cause is not yet known, but may relate to micrometeoroid impact vaporization.

The potassium exosphere is similar to that of sodium but there is less evidence for magnetotail-related drops in density. There are indications of regional enhancements related to surface composition, with higher values of K over the PKT.

References: [1] Elphic, R. C. et al., (2014) *Space Sci. Rev.* doi: 10.1007/s11214-014-0113-z; [2] Colaprete, A. et al., (2014) *Space Sci. Rev.*, doi: 10.1007/s11214-014-0112-0; [3] Horanyi, M. et al. (2014) *Space Sci. Rev.* doi: 10.1007/s11214-014-0118-7; [4] Mahaffy, P. R. et al., (2014) *Space Sci. Rev.* doi:10.1007/s11214-014-0043-9, [5] Horanyi, M. et al. (2015) *Nature*, doi:10.1038/nature14479; [6] Szalay, J. and M. Horanyi (2015) *Geophys. Res. Lett.* doi: 10.1002/2015GL064324; [7] Benna, M. et al. (2015) *Geophys. Res. Lett.*, doi: 10.1002/2015GL064120; [8] Halekas, J. et al. (2015) *Geophys. Res. Lett.* doi: 10.1002/2015GL064746; [9] Colaprete, A. et al. (2015) *Science*, doi: 10.1126/science.aad2380.

Title: **Rainfall estimates to sustain an unfrozen lake in Gale Crater Mars 3.5 Gy ago**

Authors: Robert Haberle, Alexandre Kling, Christopher McKay, Thomas Bristow, Kevin Zahnle

Topic: Planetary Atmosphere & Climate

NASA's *Curiosity Rover* has been exploring the bottom of Gale Crater Mars since August 2012. Among its many findings are presence of sedimentary deposits and deltas that suggest for a period of perhaps 500 My after the crater formed (~3.6 Gy ago) a series of unfrozen lakes formed at the bottom of the crater that lasted for tens of thousands to millions of years. The implication is that the climate at the time was intermittently warm enough to sustain an active hydrological cycle with rainfall and runoff. The resulting rivers and tributaries then carried sediments from the crater rim and nearby terrains into the bottom of the crater thus providing an explanation for the mudstones seen, for example, at Yellowknife Bay (YB). This process is also believed to have laid the foundation of Mt. Sharp, the 5 km high mound that emerges from the center of the crater.

We examine the climatic implications of this hypothesis and find that to sustain an unfrozen lake at 273K against evaporative losses for tens of thousand of years or longer earthlike rainfall rates are required (~20-80 cm/year, depending on wind and surface pressure). Warmer lakes would require even higher rates. Such rates cannot be sustained without the presence of large bodies of open water (oceans or seas) which in turn requires global and annual mean temperatures at or above freezing – something that only one state-of-the art climate model has achieved and only then if the atmosphere had at least 1.3 bars of CO₂ and 20% of it was H₂. Yet the lack of siderite in the YB deposits suggests much less CO₂ was present in the atmosphere at the time the lakes existed. So either the climate models have yet to identify a powerful - and sustainable - greenhouse gas, or the lakes formed in a colder environment than thought.

We explore the possibility that early Mars may have been *cold* and wet instead of *warm* and wet. Ice-covered lakes that never completely freeze are much easier to reconcile with climate models and can still produce sedimentary deposits and deltas. The main requirement is that glaciers are nearby and a heat source is available. The perennially ice-covered lakes in the McMurdo dry valleys of Antarctica provide one analog to the model we are proposing. There, mean annual temperatures are well below freezing (~250K). Meltwater is provided by nearby glaciers when seasonal temperatures rise above freezing but for only a few weeks out of the year. The meltwater flows across the surface in small streams that feed the lakes. Heat balance is maintained by ablation losses at the ice surface and latent heat gains during freezing at the ice bottom. However, this model does require surface pressures above ~ 100 mb to prevent boil off, and climate conditions that can produce daily-averaged temperatures above freezing seasonally. Another example, however, which does not require either of these, is the glacially-dammed Lake Untersee in East Antarctica where solar heating of the ice provides the heat source even when temperatures are below freezing. Though we do not yet fully understand the heat balance of this lake, it does provide an example of a long-lived ice-covered lake in very cold conditions, a situation very analogous to what was mostly likely the case for early Mars.

SALTS AS WATER ICE CLOUD NUCLEI ON MARSD. L. Santiago-Materese^{1,2}, L. Iraci¹, P.Y. Chuang², R. Urata^{1,3}, M.A. Kahre¹¹ NASA Ames Research Center, Moffett Field, CA, 94035, USA² Earth and Planetary Sciences, University of California at Santa Cruz, Santa Cruz, CA 95064, USA³ Bay Area Research Environmental Research Institute (BAERI), Moffett Field, CA 94035, USA**Science Topic:** *Planetary Atmosphere & Climate*

In recent years, observations of the Martian surface have indicated the presence of chlorine-bearing minerals, including perchlorates, on the surface of Mars. These salt-bearing minerals would potentially be source material for dust lofted from the surface into the Martian atmosphere, thus providing potential nucleation sites for water ice clouds. Considering that salts play an important role in cloud formation on Earth, it is important to have a better understanding of how salt may affect nucleation processes under Mars-like conditions. We perform laboratory experiments to examine water ice nucleation onto salt substrates. We use a vacuum chamber that simulates the temperatures and pressures observed of the Martian atmosphere. Using infrared spectroscopy we measure the onset of nucleation and calculate the temperature-dependent critical saturation ratio (S_{crit}) for water ice nucleation onto salts, specifically sodium chloride and sodium perchlorate. Values of S_{crit} are useful for understanding the realistic conditions under which water ice clouds may form on Mars, and for calculating the contact parameters used in cloud microphysical models. Preliminary results of S_{crit} values for water ice nucleation on sodium perchlorate show a negative temperature dependence, as did other substrates from previous experiments. This negative temperature dependence could have implications on the water cycle on Mars, as seen in recent simulations with the NASA Ames Mars General Circulation Model.

Constraining early martian P_{CO_2} from in situ mineralogical analysis at Gale crater

Thomas Bristow, Robert Haberle, David Blake, Kevin Zahnle, David Des Marais

Topic: Planetary Atmosphere & Climate

CO_2 is an essential early martian atmospheric component in climate models that successfully reconcile a faint young sun with planet-wide evidence of liquid water in the Noachian and Early Hesperian. Early martian CO_2 levels have been estimated using observable global inventory of martian carbonate minerals, with particular focus on clay mineral-bearing terrains that were demonstrably subject to low temperature aqueous alteration. However, the possibility of hidden carbonate deposits and formation of clay minerals in subsurface settings uninfluenced by the atmosphere introduce uncertainties to these estimates. Here we use mineral and contextual sedimentary environmental data measured by the Mars Science Laboratory Rover *Curiosity*, to estimate atmospheric P_{CO_2} levels that coincide with a long-lived lake system in Gale crater at ~ 3.5 Ga. A reaction-transport model of olivine-bearing lacustrine mudstones is used to simulate the mineralogy observed within the Sheepbed member at Yellowknife Bay. Model calculations that couple mineral equilibria with carbonate precipitation kinetics and rates of sedimentation establish a maximum atmospheric P_{CO_2} of ~ 0.5 bar. However, this upper limit is obtained using endmember values of model parameters. With more realistic values, P_{CO_2} levels are estimated to be in the 10's mbar range. At such low P_{CO_2} levels, climate models are unable to warm early Mars anywhere near the freezing point of water. Thus, either the observed planet-wide fluvial and lacustrine features formed in a cold environment by a mechanism yet to be determined, or the climate models still lack an essential component that would serve to elevate surface temperatures on early Mars.

Production and Analyses of Titan Laboratory Aerosols Analogs at Low Temperature with the NASA Ames Titan Haze Simulation (THS) experiment

(Science Topic: Planetary Atmosphere & Climate)

Ella Sciamma-O'Brien^{*1,2}, Kathleen Upton³, Jack L. Beauchamp³, Farid Salama¹

¹NASA ARC, Moffett Field, CA, ²Bay Area Environmental Research Institute, Petaluma, CA, ³Noyes Laboratory of Chemical Physics and the Beckman Institute - Caltech, Pasadena, CA.

In Titan's atmosphere, a complex chemistry occurs at low temperature between N₂ and CH₄ that leads to the production of heavy organic molecules and subsequently solid aerosols. Because the reactive carbon and nitrogen species present in Titan's aerosols could meet the functionality requirements for precursors to prebiotics, the study of Titan's aerosol has become a topic of extensive research in the fields of astrobiology and astrochemistry.

In the study presented here, we used the Titan Haze Simulation (THS) experiment, an experimental setup developed at the NASA Ames Cosmic simulation (COSmIC) facility to study Titan's atmospheric chemistry at low temperature, and produce aerosols representative of the early stages of Titan's aerosol formation. In the COSmIC/THS, the chemistry is simulated by plasma in the stream of a supersonic expansion. With this unique design, the gas is jet-cooled to Titan-like temperature (~150K) *before* inducing the chemistry by plasma^[1], and remains at low temperature in the plasma discharge (~200K). Different N₂-CH₄-based gas mixtures can be injected in the plasma, with or without the addition of heavier precursors present as trace elements on Titan, in order to monitor the evolution of the chemical growth. Both the gas phase and solid phase products resulting from the plasma-induced chemistry can be monitored and analyzed using a combination of complementary *in situ* and *ex situ* diagnostics.

Following a recent mass spectrometry study^[2] of the gas phase that demonstrated that the THS is a unique tool to probe the first and intermediate steps of Titan's atmospheric chemistry at low temperature, we have performed a complementary study of the solid phase with the same gas mixtures as for the gas phase analysis. The findings are consistent with the chemical growth evolution observed in the gas phase when adding heavier precursors to the initial gas mixture. Grains and aggregates form in the gas phase and can be jet deposited onto various substrates for *ex situ* analysis. Scanning Electron Microscopy (SEM) images show that more complex mixtures produce larger aggregates, from 100-300 nm grains in N₂-CH₄ to 5 μm aggregates in N₂-CH₄-C₂H₂-C₆H₆ mixtures. In addition, different growth mechanisms seem to occur depending on the gas mixture: the mixtures containing acetylene (C₂H₂) appear to produce more spherical grains, and the aggregates produced in mixtures containing benzene (C₆H₆) appear to be submitted to additional growth after grain aggregation. A Direct Analysis in Real Time (DART) mass spectrometry analysis coupled with Collision Induced Dissociation (CID) has detected the presence of aminoacetonitrile, a precursor of glycine, in the THS aerosols. X-ray Absorption Near Edge Structure (XANES) measurements also show the presence of imine and nitrile functional groups, showing evidence of nitrogen chemistry. Infrared and μIR spectra of samples deposited on KBr and Si substrates show a more predominant presence of aromatic functional groups for more complex gas mixtures, and allow to determine the samples' thickness. These complementary studies show the unique potential of COSmIC/THS to better understand Titan's chemistry and the origin of aerosol formation.

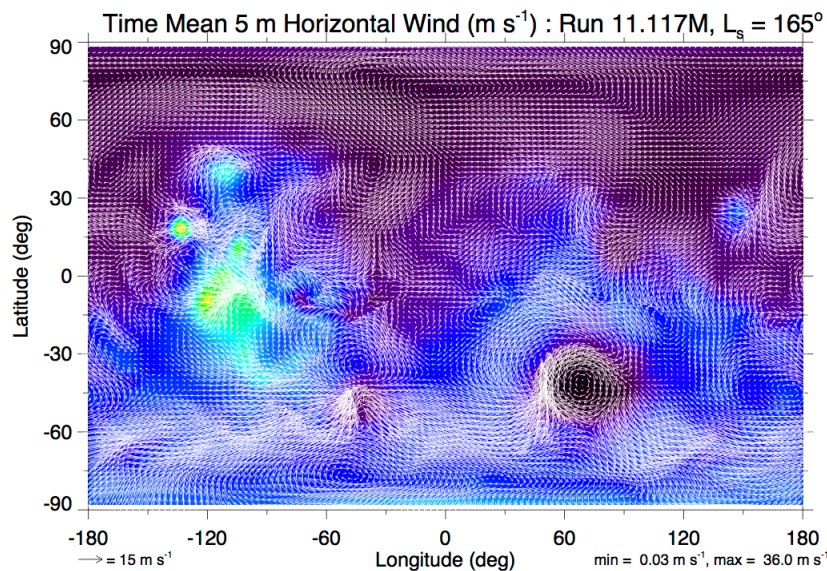
References: ^[1]Biennier et al., 2006, *Chem. Phys.* 326, 445. ^[2]Sciamma-O'Brien et al., 2014, *Icarus* 243, 325.

Acknowledgments: This research is supported by the NASA SMD PATM Program. K. T. Upton acknowledges the support of the NASA JFPF Program. The SEM images were obtained at the UCSC MACS Facility at Ames (NASA grant NNX09AQ44A to UCSC). The authors acknowledge the outstanding technical support of R. Walker and E. Quigley.

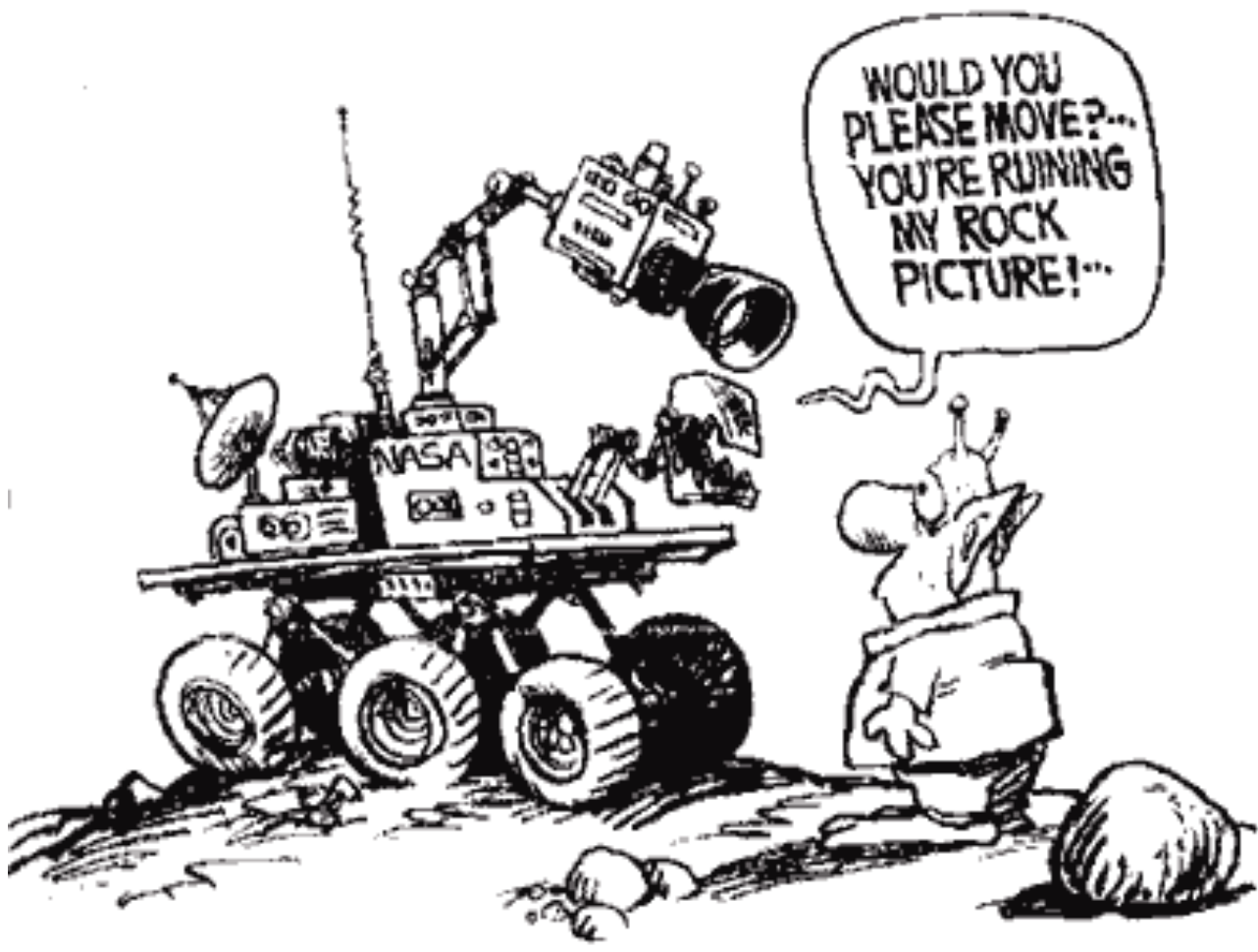
TITLE: Large-Scale Weather Disturbances in Mars' Southern Extratropics
 AUTHORS: J.L. Hollingsworth, M.A. Kahre, Planetary Systems Branch (Code SST)
 DATE: Sun Feb 7 13:56:46 PST 2016
 SCIENCE TOPIC: Planetary Atmospheres & Climate

ABSTRACT

Mars' middle and high latitudes present within its atmosphere substantive mean thermal gradients between the tropics and poles (i.e., atmospheric baroclinicity). Observations from both the Mars Global Surveyor (MGS) and Mars Reconnaissance Orbiter (MRO) indicate this strong baroclinicity supports intense, large-scale eastward traveling weather systems (i.e., transient synoptic-period waves). These extratropical weather disturbances are *fundamental components* of the global circulation. Such wave-like disturbances transport heat and momentum, and generalized scalar/tracer quantities (e.g., atmospheric dust, water-vapor and ice clouds) within the atmosphere. The character of large-scale, traveling extratropical synoptic-period disturbances in Mars' southern hemisphere during late winter through early spring is investigated using a moderately high-resolution Mars global climate model (Mars GCM). This Mars GCM utilizes interactively lifted and radiatively active dust based on a threshold value of the surface stress. This model exhibits a reasonable "dust cycle" (i.e., globally averaged, a dustier atmosphere during southern spring and summer occurs). Compared to their northern-hemisphere counterparts, southern synoptic-period weather disturbances and accompanying frontal waves have smaller meridional and zonal scales, and are far less intense. Influences of the zonally asymmetric (i.e., east-west varying) topography on southern large-scale weather are examined. The simulations and analyses indicate Mars' transient barotropic/baroclinic eddies are highly influenced by the great impact basins of the southern hemisphere (e.g., Argyre and Hellas). The occurrence of a southern storm zone in late winter and early spring is anchored to the western hemisphere via orographic influences from the Tharsis highlands, and juxtaposition of the Argyre and Hellas impact basins. Localized transient-wave activity diagnostics (e.g., the 3D Plumb flux) are constructed, illuminating dynamical attributes amongst the simulations.



--



Oxygen released during analysis of Mars surface materials: A comparison of Viking and Curiosity mission results. Kathryn F. Bywaters (SST/NPP), Chris P. McKay (SST) and Richard C. Quinn (SST/SETI Institute)

Introduction: The Viking mission results were the first to indicate that the martian surface material contains a number of different reactive oxidizing species that likely impact the preservation potential of biomarkers [1]. Following Viking, results from the Phoenix mission revealed that the samples from the northern polar region contained ~0.5% (by wt.) perchlorate [2]. Although perchlorate salts can behave as strong oxidants at elevated temperatures, their stability precludes them from directly explaining the results of the Viking Gas Exchange (GEx) and Labeled Release (LR) experiments. However, perchlorate radiolysis products, specifically hypochlorite (ClO^-), and trapped oxygen species may provide an explanation for the LR and GEx results [3]. Recently, samples collected by the Mars Science Laboratory (MSL) and analyzed using the Sample Analysis at Mars (SAM) instrument suite produced oxygen, hydrochloric acid, chloromethane, dichloromethane, and other chlorinated hydrocarbons that have been attributed to the thermal decomposition of perchlorate and reactions of perchlorate with organics [4].

Experimental/Results: Ionizing radiation in the form of galactic cosmic rays (GCR) and solar energetic particles (SEP) is only slightly attenuated before reaching the martian surface and the penetration depth of the more energetic GCR radiation, exceeds the Viking and MSL sampling depths. The thermal decomposition and effects of humidification on irradiated versus non-irradiated perchlorates have been investigated in the context the MSL SAM and Viking results. Magnesium and calcium perchlorate samples were irradiated using a ^{60}Co source under both simulated Mars (CO_2) and inert (He) atmospheres. After irradiation, the thermal evolved gas analysis of irradiated- and control-samples was performed using a laboratory Pyroprobe-Quadropole Mass Spectrometer (QMS) using SAM-like analysis conditions (He carrier at 1.0 atm-cc/min and 30 mbar pressure). Figure 1 shows an example of laboratory measured O_2 release from irradiated and non-irradiated calcium perchlorate compared to the MSL SAM Rocknest (Sol 93) data obtained from the NASA Planetary Data System.

Discussion: Calcium perchlorate is good candidate for the higher temperature peak seen in the SAM Rocknest data and peak broadening can be attributed to sample matrix effects [5]. Compared to the control sample, the irradiated perchlorate decomposes at a

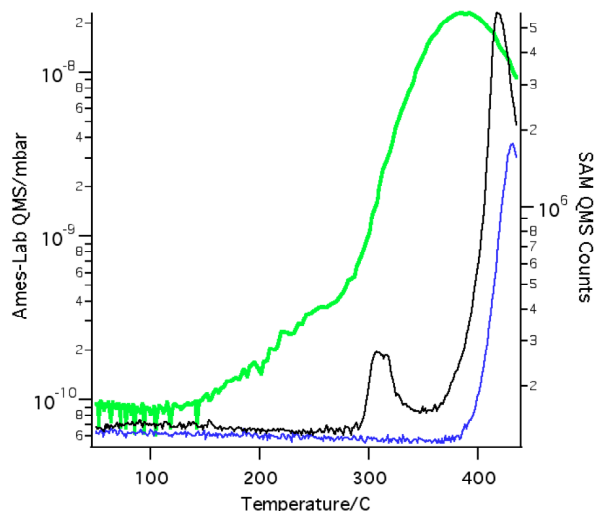


Fig. 1. Thermal analysis of $\text{Ca}(\text{ClO}_4)_2$ and irradiated $\text{Ca}(\text{ClO}_4)_2$ compared to SAM PDS data from the sol 93 analysis of the Rocknest sample. The irradiated perchlorate (black) data shows an additional low temperature O_2 peak, compared to the non-irradiated perchlorate sample (blue). Two distinct O_2 (overlapping) peaks below 500°C are present in the SAM data (green).

slightly lower temperature, and an additional $\sim 300^\circ\text{C}$ O_2 peak is observed. In the both laboratory EGA data (irradiated samples) and the SAM Rocknest data the evolution of two distinct O_2 peaks below 500°C can be seen. We attribute the lower temperature O_2 evolution to the release of trapped oxygen upon fusion/melting of perchlorate. Humidification also releases O_2 from irradiated perchlorate upon deliquescence. Quantitative results from laboratory experiments will be compared the MSL SAM and Viking data sets. These results have important implications for possible distributions of reactive oxidants, the history of water exposure, and the preservation of biomarkers in martian surface materials.

References: [1] Klein, H. P. et al. (1976) *Science* 194, 99–105. [2] Hecht, M. H. et al. (2009) *Science* 325, 64–67. [3] Quinn, R. C. et al. (2013) *Astrobiology* 13, 515–520. [4] Ming, D. W. et al. (2014) *Science* 343, 1245267. [5] Glavin, D. P. et al. (2013) *JGR: Planets* 118, 1955–1973.

Acknowledgements: The authors acknowledge support from the NASA Exobiology Program and the NASA Astrobiology Institute (R.Q.). K.B. acknowledges support from the NASA Postdoctoral Program.

The Lost River of Mars: Losing and Gaining Paleostreams in the Navua Valles, NE Hellas

Henrik I. Hargitai¹, Virginia C. Gulick², Natalie H. Glines²

¹ARC SST/NPP, ²ARC SST/SETI Institute

Science topic: Planetary Surfaces and Interiors, Astrobiology

The Navua Valles are valley and channel systems on the inner northeastern rim of Hellas Basin on Mars. Similar to the Lost Rivers on the Snake River plains of Idaho, these drainages traverse over volcanic terrains, repeatedly disappearing (infiltrating) into and then re-emerging onto the surface further down slope and forming a defined channel system. We have delineated and analyzed several drainage systems in this region, using CTX, HiRISE, MOLA, HRSC and CRISM data. The main drainage system, Navua A (Fig. 1) consists of several disconnected channel segments formed on Hesperian aged volcanic (lava flows and ash) units likely emplaced by the formation of Hadriaca Patera. We assume underground connection between the segments as there is a repeated pattern over the course of the system, starting with a deeply incised valley followed by a wide, flat-floored channel that terminates in an unconfined depositional reach, much like channels formed in volcanic terrains on Earth. The Navua A system originates in a 180×120 km non-volcanic region where the valleys first appear on the slopes of mountains – Noachian ridges and crater rims. Below this region, there are no tributaries connected to mountains. The Navua source valleys are commonly knobby, which we interpret as glacial features that formed after the channels dried out, in discontinuous permafrost conditions. Water was available only locally and at very rare occasions during the formation of valley networks in the Late Noachian to Early Hesperian, when these channels probably also started to form. However, interior channels are common, which suggests that subsequent periods of at least episodic stream flow continued in these systems. A Navua B confluence site reveals at least four separate erosional events that deepened the channels. In addition to the obvious signs of erosion, there was also deposition in these channels. We identified several channel sections containing fluvial bedforms, including cross-bar channels, streamlined islands and terminal deposits. We interpret the low, streamlined elevations to be depositional bars or alluvial plain remnants developed in at least 5-10 m water level in the last flood events. HiRISE color images suggest that the surface properties of these islands are different from their surroundings suggesting a depositional origin. Some valley sections are terraced, which may be due to drops in local base level or changing stream power as flow eroded into the underlying layers of ash and lava flows.

The channels terminate in lobate flows at different levels on the floor of Hellas Basin, and debouche into relatively small basins bordered by wrinkle ridges. The observed setting implies a paleoclimate episodically rich in liquid surface water that could potentially provide habitable environments periodically from the Late Noachian to the Late Amazonian.

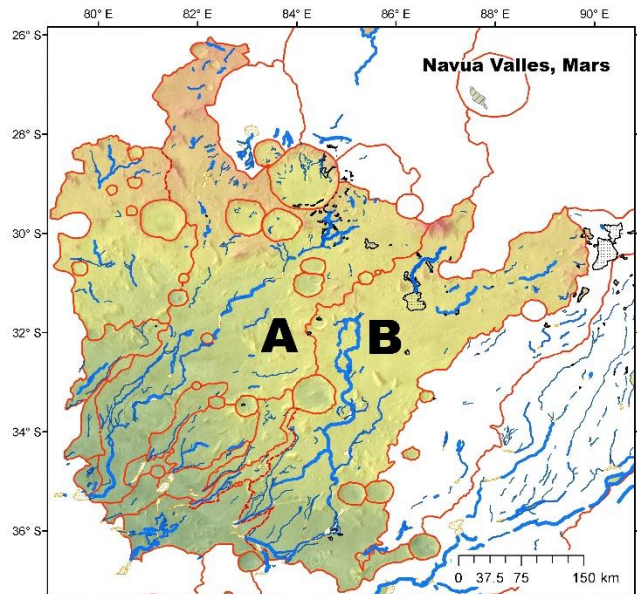


Figure 1 Navua Valles drainage basins (red lines) and channel segments (blue lines) over MOLA DTM. The small areas outlined in black in the source regions represent knobby terrain. Letters A and B shows the two main drainage basins, Navua A and Navua B. The drainage system on the right is on the flanks of Hadriacus Mons and is not part of the Navua Valles.

GEOMORPHOLOGICAL MAPPING OF THE ENCOUNTER HEMISPHERE ON PLUTO. O. L. White¹, S. A. Stern², H. A. Weaver³, C. B. Olkin², K. Ennico^{1,3}, L. A. Young², J. M. Moore¹, A. F. Cheng², and the New Horizons Geology, Geophysics and Imaging Theme Team. ¹NASA Ames Research Center, Moffett Field, CA, 94035-1000 (oliver.l.white@nasa.gov), ²Southwest Research Institute, 1050 Walnut Street, Suite 300, Boulder, CO, 80302, ³The Johns Hopkins University Applied Physics Laboratory, 11100 Johns Hopkins Road, Laurel, MD, 20723.

Science topic: Planetary Surfaces and Interiors

The New Horizons spacecraft has returned high quality images covering the encounter hemisphere of Pluto, which reveal it to have a highly diverse range of terrains, implying a complex geological history. This presentation will feature geomorphological mapping of the encounter hemisphere, which underlies interpretation of Pluto's terrains and their spatial and chronological relation to each other. Several terrains seem to be encountered only in a particular location (as far as we can tell), and are not obviously replicated in other parts of Pluto, indicating that unique sets of landscape modification conditions may occur on Pluto. All feature names used here are informal.

Sputnik Planum, with an area of $\sim 870,000 \text{ km}^2$, is notable for its smooth appearance and apparent total lack of impact craters at $\sim 320 \text{ m/pixel}$ resolution, and consists of N_2 ice with smaller concentrations of CH_4 and CO ice. The Planum displays a variety of textures across its expanse, including smooth and pitted plains in the south; bright cellular terrain in the center (the cells are bounded by troughs with medial ridges); and, in the north, darker cellular terrain which displays lobate patterns indicative of glacial flow into the rugged, hilly, cratered terrain north of Sputnik Planum. The cells likely form as a result of solid-state convection occurring within the N_2 ice. 200 individual cells have been mapped, with a mean diameter of 33.4 km. The network of troughs defining the edges of the cells becomes less interconnected in central Sputnik Planum, perhaps indicating thicker N_2 ice at this location. Ranges of chaotically-oriented mountains stretch all the way along the western margin of Sputnik Planum; these may represent fragments of Pluto's H_2O ice crust that have been transported and reoriented by the N_2 ice.

Bright, rugged, pitted uplands to the east of Sputnik Planum may have been resurfaced by deposition of N_2 ice that sublimated from Sputnik Planum, and which is reintroduced back into the Planum via glacial flow from the uplands. The pitted uplands eventually transition to the 'bladed terrain' of Tartarus Dorsa, which consists of several broad ($\sim 100 \text{ km}$ -wide), $\sim \text{NE-SW}$ -aligned swells that are covered in $\sim \text{N-S}$ -aligned blade-like ridges. Individual ridges are typically several hundred meters high, and are spaced 5 to 10 km crest to crest. Both the pitted uplands and bladed terrain may be remnants of a formerly continuous deposit degraded either by sublimation (forming features analogous to those of degraded terrestrial snow or ice fields - penitentes and sun-cups - but much larger), or through undermining and collapse, possibly through melting at depth.

To the north of the pitted uplands and the bladed terrain is 'eroded mantle terrain', i.e. material is draping underlying topography. The density of craters here is low except for a few degraded examples that are $>50 \text{ km}$ across. The mantle appears smooth with convex rounded edges. This terrain is also characterized by erosion via steep-sided pitting that reaches 3-4 km deep and tens of km across. The larger pits display elongate and irregularly-shaped planforms and may indicate that material is being sapped from the subsurface at these locations.

To the northwest of Sputnik Planum, smooth, flat and bright cratered plains are encountered. In some locations, these plains show a fretted appearance, whereby they are separated into polygons by a network of darker troughs reaching 3 to 4 km wide. This morphology may indicate tectonic disruption of the crust.

Terrain to the west of Sputnik Planum appears more heavily tectonized than that to the east, featuring numerous extensional fractures in various stages of degradation. This terrain includes Cthulhu Regio, which covers a swath from $\sim 15^\circ \text{N}$ to $\sim 20^\circ \text{S}$, and stretches westward almost half way around the planet to 20°E . Cthulhu Regio appears not to be a distinct physiographic province, but instead a region of dark mantling thin enough to preserve underlying topography, superimposed upon various geological terrains including plains, dendritic valleys, craters, and faults. Northeastern Cthulhu Regio, bounding Sputnik Planum, appears to be amongst the oldest terrains on Pluto, with a high spatial density of impact craters that appear relatively unmodified. To the north of Cthulhu Regio (at $\sim 30^\circ \text{N}$) there exists a region of mottled plains that is bounded by an arcuate scarp along part of its southern and western borders. These plains appear to have been exhumed through degradation of an overlying layer (perhaps through sublimation), and scarp retreat may be occurring at the edges of the plains.

To the south of Sputnik Planum is a $\sim 150 \text{ km}$ -diameter edifice (Wright Mons) that shows a rough, undulating surface with very few impact craters at $\sim 230 \text{ m/pixel}$ resolution. It features a very wide and deep summit depression. The bulk morphology of Wright Mons has caused it to tentatively be interpreted as a cryovolcanic edifice.

The Geophysical Significance of Sesquinary Ejecta: Phobos and Luna Case Studies

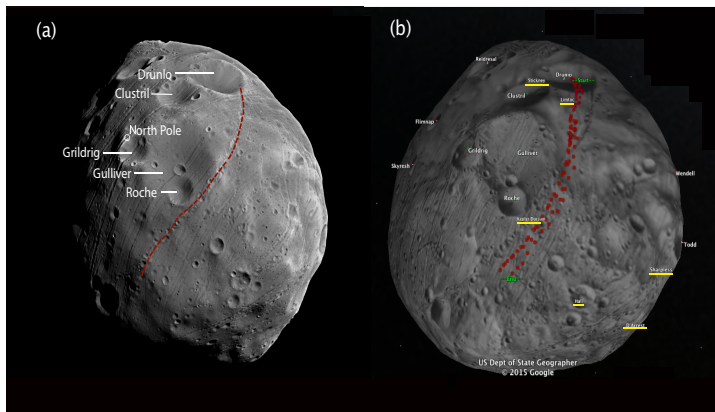
Michael Nayak^{1,2}

Department of Earth & Planetary Sciences, UC Santa Cruz; Code SST, NASA Ames Research Center

Planetary Surfaces and Interiors

Phobos:

The Martian satellite Phobos is crisscrossed by linear grooves and crater chains whose origin is unexplained. Tidal origins were originally suspected, as Phobos spirals down toward Mars^[1], but could not explain anomalous grooves crosscutting tidally predicted stress fields^[2] and the relatively young appearance of several grooves. I will show the strong correspondence between these anomalous features and reaccretion patterns of sesquinary^[3] ejecta created from impacts on Phobos. Escaping ejecta persistently imprints Phobos with linear, low-velocity crater chains (catenae) that match the geometry and morphology of prominent features that do not fit the tidal model. I will show that these cannot be any older than Phobos' current orbit inside the Roche limit of Mars.



These findings reconcile a forty-year old geophysical puzzle and reestablish the importance of ongoing tidal evolution on Phobos. Furthermore, I use the distinctive surface reimpact patterns to show that sesquinary craters may be traced back to their source (**Figure**). This creates a new planetary geophysical-dynamical relationship and a novel way to probe planetary

surface characteristics. For example, I will show that catena-producing craters likely formed in the gravity regime (that is, in deep regolith), providing a constraint on the ejecta velocity field and knowledge of the material properties in the source crater region.

Moon:

A number of magnetic anomalies are present along the northern edge of the lunar South Pole-Aitken (SPA) basin. I use two different methods to invert for source body characteristics and find a diverse set of magnetization directions around SPA, larger than found by previous magnetic surveys^[4,5]. I combine these results with other physical arguments to conclude that the source bodies were likely magnetized in a dynamo field, but the large paleopole diversity presents an enigma, implying either large amounts of true polar wander or non-axially centered dynamo fields. I suggest that iron-rich SPA ejecta may have become sesquinary ejecta and re-impacted on 10^4 - 10^6 year timescales to capture rapid adjustments to the Moon's orientation caused by the SPA impact. If true, these reimpacts may have contributed to pre-Nectarian magnetic anomaly formation across the Moon. **I am interested in research collaboration to advance this theory by using dynamical simulations of ejecta evolution post-SPA impact.**

References: [1] Soter and Harris, 1977, *Nature*; [2] Asphaug et al., 2015, *EPSC*; [3] Zahnle et al., 2008, *Icarus*; [4] Arkani-Hamed and Boutin, 2014, *Icarus*; [5] Takahashi et al., 2014, *Nature Geoscience*.

Title

The H-G Relation and its effect on Diameter and albedo (p_v) and taxonomy: A case study of Near-Earth Asteroid (NEA) 3691 Bede

Authors

Diane H. Wooden (NASA Ames), Susan M. Lederer (NASA JSC), Emmanuel Jehin (Institut d'Astrophysique de l'Université de Liège), Jessie Dotson (NASA Ames)

Abstract

Characterization of NEAs provides important inputs into models for atmospheric entry, risk assessment and mitigation. The apparent brightness, thermal emission and surface composition are observed to change with the solar phase angle. The questions we are addressing are: what are the systematic changes in Diameter due to assumptions in thermal modeling with NEATM and due to changes in viewing geometry through the phase angle parameter. Diameter is key to kinetic energy released in atmospheric entry. Diameters derived from Hmag depend on albedo p_v and the albedo p_v can be linked to surface composition or taxonomy through statistical studies of the NEO population. Thermal-Diameters are more reliable than Hmag-Diameters because the modeled thermal flux has a weaker dependence on the albedo than the Hmag-Diameter relation. The albedo (p_v) is fitted as a free parameter in thermal modeling. Since p_v is a free parameter, thermal Diameters can disagree with Hmag diameters. The problem is in the (often hidden) assumption in thermal modeling that $G=0.15$ where G is the slope parameter from the H-G Relation that describes the phase curve (absolute magnitude versus phase angle).

We present our investigation into the characterization of NEA 3691 Bede, through analyses of mid-IR photometry taken at UKIRT in 2015 Mar-Apr. We show that there are a family of solutions for (H, G, p_v) that all fit the thermal fluxes and derive the same thermal-diameter. To arrive a one solution out of this family of solutions, the slope parameter, G , must be chosen primarily from our knowledge of main belt asteroids of similar surface composition. The existence of a family of solutions for (H, G, and p_v) is rarely discussed in the literature and has implications for deriving the Hmag-Diameter when thermal fluxes have not been measured, which is the case for the majority NEAs. This effort contributes to the Asteroid Threat Assessment Project at Ames.

METEORITE FRACTURES AND SCALING FOR ATMOSPHERIC ENTRY. K. L. Bryson^{1,2} and D. R. Ostrowski^{1,2}, ¹ NASA Ames Research Center, Moffett Field, CA, 94035, kathryn.bryson@nasa.gov, ² Bay Area Environmental Research Institute, 625 2nd St. Ste 209 Petaluma, CA 94952.

Science Topics: Planetary Surfaces and Interiors

Introduction: We are attempting to understand the behavior of asteroids entering the atmosphere and quantify the impact hazard. Among the uncertainties required for this task are the composition and physical properties of the incoming objects [1] and their fracture mechanics [2,3]. Strength of meteorites play an important role in determining the outcome of impact events in which a meteorite is the impactor [3]. Our ultimate objective is to determine a scaling factor for fracture parameters in meteorites.

Experimental: Meteorites in the Natural History Museums of Vienna and London were examined using different strategies. In Vienna we looked at a few samples from all classes, while in London we looked at all of their H and L chondrites. The fracture patterns in selected fragments were imaged. The density and length of the observed fractures were measured (Fig. 1A), and similarly in selected thin sections (Fig. 1B).

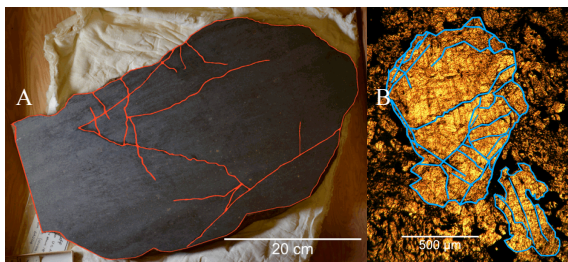


Figure 1. A. Fractures (red tracings) in this slab of Bluff (a) are insensitive to meteorite texture and have no point of origin. B. Fractures (blue tracings) in thin section of Bluff (a). Fracture density and length are used to determine the Weibull coefficient.

Results: In this study of over a thousand meteorite fragments (mostly hand-sized, some 40 or 50 cm across), we identified six kinds of fracturing behavior. (1) Chondrites usually showed random fractures with no particular sensitivity to meteorite texture. Approx. 80% of these indicated no point of origin, while 20% show an origin. (2) Approx. 10% of the chondrites, have a distinct and strong network of fractures making an orthogonal or triple intersection structure. (3) Fine irons with large crystal boundaries fragmented along the crystal boundaries. (4) Coarse irons fractured along kamacite grain boundaries, while other (5) fine irons fragmented randomly. Finally, (6) CM chondrites showed that water-rich meteorites fracture around clasts.

Discussion: We assume that fracturing follows the Weibull distribution [5], where fractures are assumed to be randomly distributed through the target and the likelihood of encountering a fracture increases with dis-

tance. The images collected of the six fracture behaviors provide a two-dimensional view of the fractures. A relationship exists between the distributions of measured trace length and actual fracture size [6], where the slope of a log-log plot of trace length vs fracture density is proportional to α , the shape parameter. The value for α is unclear [7] and a large range in α has been determined from light curve data [3]. α can be used to scale strengths. Figure 2 plots the fracture lengths and densities measured of both the slab and thin section of Bluff (a). A power law is fit to the data, and 0.166 was determined for the value of α based off these samples.

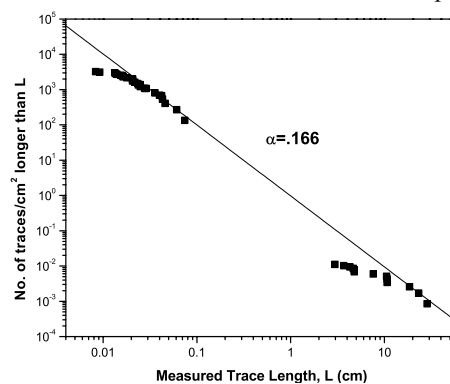


Figure 2. Distribution of flaw trace length for Bluff (a) determined from figures Figures 1 and 2. The line is based on equation 2 with a slope providing a value of 0.166 for α .

Conclusions: Based on the meteorites examined in our study, six fracture patterns have been observed. The majority of the meteorites displayed no particular sensitivity to meteorite texture. A value of α of 0.166 has been determined for a chondrite with a fracture pattern that shows no sensitivity to meteorite texture and have no point of origin. This study will continue to examine additional meteorites with similar fracture patterns along with the other 5 patterns to see if there is a correlation between fracture pattern and α . This may be able to explain the variations in α determined from fireball data [1,3]. Values of α will be used in the models created by the Asteroid Threat Assessment Project to attempt to determine the behavior of asteroids entering the atmosphere and quantify their impact hazard.

References: [1] Sears D.W.G. et al. (2016) *Proceedings of the AIAA SciTech*, AIAA-2016-0997 [2] Baldwin B. and Sheaffer Y. (1971) *JGR*. 76, 4653-4668. [3] Popova O. et al. (2011) *Meteorit. Planet. Sci.* 46, 1525-1550. [4] [5] Weibull W. (1939) *Proceedings of the Royal Swedish Institute for Engineering Research*. No. 153. [6] Piggot A.R. (1997) *JGR*, 102, 18,121-18,125. [7] Asphaug E. et al. (2002) *Asteroids III*. 463-484.

PHYSICAL PROPERTIES OF ORDINARY CHONDRITES. D. R. Ostrowski^{1,2} and K. L. Bryson^{1,2}, ¹ NASA Ames Research Center, Moffett Field, CA, 94035, daniel.r.ostrowski@nasa.gov, ² Bay Area Environmental Research Institute, 625 2nd St. Ste 209 Petaluma, CA 94952.

Science Topic: Planetary Surfaces and Interiors

Introduction: Measurements of the physical properties of meteorites are essential to help determine the physical characteristics of the parent asteroids. The study of the physical properties can also provide information that is useful to the understanding of meteoroid behavior in the atmosphere and help determine methods to deflect potentially hazardous asteroids. A large variety of material enters the atmosphere as seen by the over 45 classes of meteorites [1]. Only stony and iron meteorites play a greater relevance to planetary defense because of their quantity and/or likelihood of making it to the ground. Our initial focus is on ordinary chondrites because they make up most of the meteorites, over 70% [2].

Procedure: The physical properties of ordinary chondrites have been studied by non-destructive methods. Each meteorite is weighed and 3D scanned to obtain volume and density. Meteorites are then cut into two 1.5 cm cubes for other test. Grain density and porosity are then determined by a gas pycnometer using nitrogen gas displacement. The acoustic velocity is measured using an Olympus 45-MG meter. Thermal properties currently studied are emissivity, thermal conductivity, and heat capacity. For the thermal measurements the range studied is from 20 up to a maximum of atmospheric entry temperatures. Emissivity data is based on averaged measurements over the wavelength range of 8 to 14 μm .

Physical Properties Data: *Density and Porosity.* The understanding of the physical history of meteorites, and possible the asteroid parent body, is primarily done by measuring density and porosity. Density and porosity are key determinants in meteor behavior in the atmosphere and deflection [3].

Acoustic Velocity. This parameter provides an insight into the wave propagation through a meteorite, its internal structure, and porosity. Tamdakht has a much lower longitudinal velocity than the normal range. One possibility for this is that it has a higher porosity than the average H chondrite. The velocity is consistent across all three axes in both samples (Table 1). The one exception to this is the slightly slower velocity in the x-

axis for cube #2, which has been attributed to a fracture on the axis face.

Emissivity. The calculated emissivity range for ordinary chondrites is 0.984 to 0.991 at 20 °C [7]. The two samples of Tamdakht have emissivity values of 0.993 ± 0.003 (cube #1) and 0.9911 ± 0.0001 (cube #2) at 20 °C. Tamdakht is on the high end of the emissivity range for H chondrites. It can be observed in Figure 1 that the emissivity of Tamdakht decreases by roughly 0.06 when heated to 45 °C. The emissivity of the heated samples stays consistent at this lower value up to near 200 °C within error.

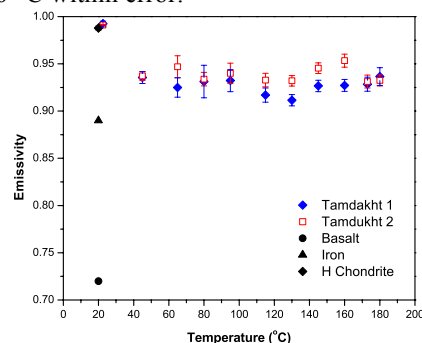


Figure 1: Emissivity measurements for Tamdakht from 20-180°C.

Conclusions: The properties of density, porosity and emissivity (at 20 °C), Tamdakht match to a typical ordinary chondrite. For heated emissivity, below 200 °C, stays constant at a slight decrease from room temperature. The oddity of Tamdakht is the longitudinal wave velocity. The higher than average porosity is the most likely cause of some of the depressed acoustic velocity.

References: [1] Sears D.W.G. et al. (2016) *Proceedings of the AIAA SciTech*, AIAA-2016-0997 [2] Grady M. M. (2000) *Catalogue Meteorites*, 5th ed., Cambridge University Press. [3] McCausland P. J. A. et al. (2011) *Meteoritics & Planet. Sci.*, 46, 1097-1109. [4] Consolmagno G. J. et al. (2008) *Chemie der Erde*, 68, 1-29. [5] Flynn G. J. (2004) *Earth, Moon, and Planets*, 95, 361-374. [6] Yomogida K. and Matui T. (1983) *JGR*, 88, 9513-9533. [7] Baldrige A. M. et al. (2009) *Remote Sensing of Environment*, 113, 711-715.

Table 1: Densities, porosity, and acoustic velocity for H chondrite averages and both pieces of Tamdakht. *Is the range for H chondrites covering all direction.

Meteorite	Bulk Density (g/cm ³)	Grain Density (g/cm ³)	Porosity (%)	Longitudinal Velocity		
				X-axis (mm/ μs)	Y-axis (mm/ μs)	Z-axis (mm/ μs)
H Chondrites ^[4,5,6]	3.42 \pm 0.18	3.72 \pm 0.12	7.0	2.66 to 6.99*		
Tamdakht cube 1	3.422 \pm 0.010	3.873 \pm 0.001	11.63 \pm 0.58	1.17 \pm 0.03	1.13 \pm 0.01	1.13 \pm 0.02
Tamdakht cube 2	3.386 \pm 0.010	3.865 \pm 0.001	12.41 \pm 1.53	1.01 \pm 0.02	1.15 \pm 0.02	1.14 \pm 0.03

MAGNETITE LABORATORY REFLECTANCE SPECTRA MODELED USING HAPKE THEORY AND EXISTING OPTICAL CONSTANTS. T. L. Roush¹, D. T. Blewett², and J. T. S. Cahill², ¹NASA Ames Research Center (ted.l.roush@nasa.gov), ²Johns Hopkins University Applied Physics Laboratory.

Topic: Planetary Surfaces

Introduction: Magnetite is an accessory mineral found in some meteorites, on the lunar surface, and in terrestrial environments. The reflectance of magnetite powders is relatively low [1], and this property makes it an analog for other dark Fe- or Ti-bearing components, particularly ilmenite on the lunar surface. The real and imaginary indices of refraction (optical constants) for magnetite are available in the literature [2-3], and on-line [4]. Here we use these values to calculate the reflectance of particulates and compare these model spectra to reflectance measurements of magnetite available on-line [5].

Methods: The three available sets of magnetite optical constants were used in calculations of the bidirectional reflectance for comparison to the laboratory measurements of a 45-90 μm grain size fraction of magnetite (RELAB spectrum C2CS25) over the ~ 0.2 - $2.6 \mu\text{m}$ region. Hapke theory was used for the calculations and two different representations of the particle phase function were used: isotropic (Hapke's b and c are both set to 0) and non-isotropic (using an estimate from the results of [6] with $b = -0.25$ and $c = 0.175$). The results are shown in Fig. 1.

Summary: None of the available optical constants of magnetite closely reproduce the measured spectra regardless of the representation of the particle phase function (Figs. 1a, 1b). The calculated reflectances for the sieve minimum and maximum grain sizes are essentially the same (Fig. 1a, 1b). The calculated reflectances are significantly lower and the slopes shallower than the measured values (Fig. 1a, 1b). The non-isotropic phase function produces a lower reflectance than the isotropic phase function (Fig. 1c).

We will discuss the potential causes of the discrepancies between calculated and measured reflectances.

References: [1] Adams, J.B. 1974 in *Infrared and Raman Spectroscopy of Lunar and Terrestrial Minerals*, C. Karr Ed., Academic Press, New York, 109-116. [2] Querry, M.R., 1985, Optical Constants, CRDC-CR-85034, US Army Armament, Munitions, and Chemical Command, Aberdeen Proving Ground, MD. [3] Huffman, D.R. and J.L. Stapp 1973, in *Interstellar Dust and Related Topics*, J.M. Greenberg and H.C. Van de Hulst, Eds., IAU Symposium 52, 297-301. [4] Triaud, A., www.astro.uni-jena.de/Laboratory/OCDB/mgfeoxides.html [5] www.planetary.brown.edu/relabdocs/

relab_disclaimer.htm. [6] Mustard, J.F. and C.M. Pieters 1989 JGR, 94, 13,619-13,634.

Acknowledgements: We are grateful to funding from NASA's PDART program in support of this work.

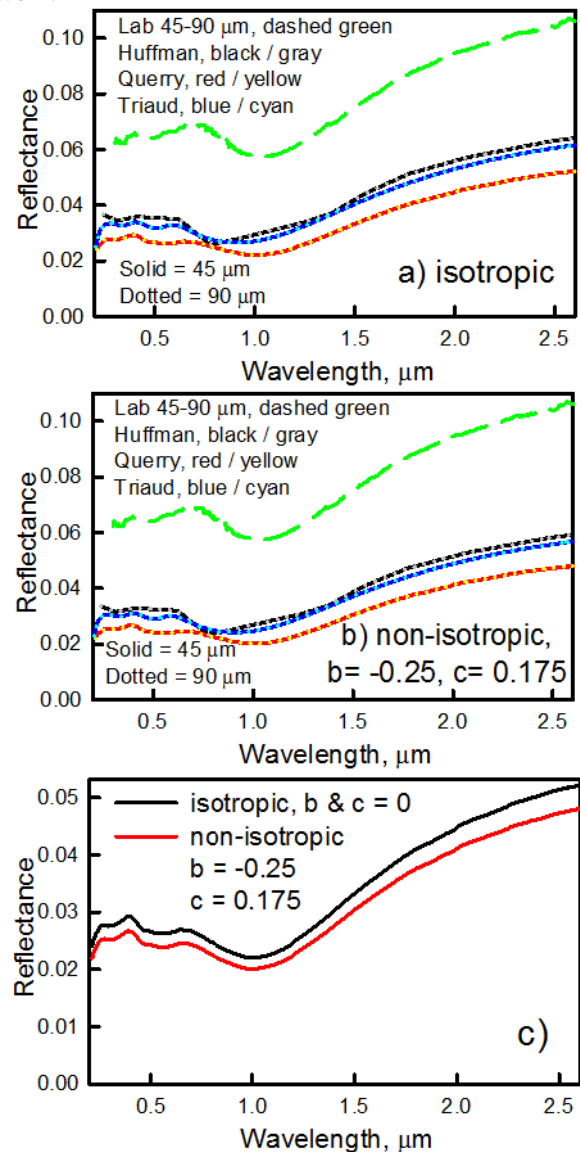


Figure 1. Laboratory reflectance of a 45-90 μm magnetite sample (RELAB, C2CS25), compared to calculations of the reflectance using Hapke theory assuming particle phase functions of a) isotropic b) non-isotropic, using scattering parameters from [6] and c) direct comparison of 45 μm grain size calculations for isotropic and non-isotropic phase functions.

A NEW METHOD – POTENTIALLY SUITABLE FOR SPACECRAFT INSTRUMENTATION – FOR DATING RECENT VOLCANISM ON PLANETARY SURFACES. D.W.G. Sears^{1,2} and S.S. Hughes³.

¹Division of Astrobiology and Space Science, NASA Ames Research Center, Moffett Field, CA, U.S.A., ²Bay Area Environmental Research Institute, NASA Ames Research Center, Moffett Field, CA, U.S.A., ³Geosciences Department, Idaho State University, Pocatello, ID, U.S.A. Email: derek.sears@NASA.gov.

Introduction: Craters of the Moon National Monument and Preserve in Idaho (COTM) is a site of plains volcanism which has often been considered a planetary analog [1-3]. It is one of the study areas for the SSERVI team named FINESSE (Field Investigations to Enable Solar System Science and Exploration; J. L. Heldmann, PI [4]). While investigating volcanism at COTM and surroundings we have been exploring a method of dating the volcanism using the thermoluminescence properties of the lavas.

Thermoluminescence-based instruments have been proposed for robotic spaceflight application as a means of obtaining dates for recent fluvial and aeolian processes [5,6]. The technique is relatively simple and the instrument has low weight, low power, and low data rate transmission needs. Previous groups are proposing to use the technique in the way it is used for Quaternary dating on Earth. That is, they use the natural TL signal to measure the radiation dose absorbed, determine the radiation dose for the environment, and divide the first quantity by the second to determine the time interval since the start of the build-up of the signal [7]. This would typically be the time since emplacement of the sample in the present location. Ages of up to 10^5 years are measurable above which the TL signal saturates and no longer changes with time. The technique is in widespread use terrestrially using optical stimulation, rather than heat, to release the signal.

While the apparatus is the same, we are proposing an entirely different approach based not on the accumulated natural TL signal, but the level of TL that can be induced in a sample by a standard radiation dose. We will call this “induced TL dating”. The approach derives from several decades of meteorite studies, both chondrites [8] and basaltic meteorites [9] where changes in induced TL are used to monitor time-dependent changes caused by metamorphism. The idea was briefly described in ref. [10]

There is some precedence for the approach explored here. In the late nineteen-seventies Rod May [11,12] showed that the induced TL of Hawaiian basalts increased with age. We decided to perform similar measurements to those of May as part of our studies at COTM [13]. With help from members of the FINESSE team, we collected basalt samples from 23 volcanoes of known age (Table 1) and measured their induced TL. We report the initial results here.

Table 1. COTM basalt samples, ages, and induced TL

Location	Age (ka)	Ind TL
Antelope Butte	470±25	626±127
Basalt of Portneuf Valley	430±70	4520±302
Big Cinder Butte NW	6.02±0.16	140±36
Blue Dragon flow	2.076±0.045	90±17
Carey Flow	12.01±0.15	116±57
Carey Kipuka flow	6.6±0.06	177±56
Cedar Butte	400±19	1620±35
Grassy	7.36±0.06	140±52
Grassy flow	7.36±0.06	375±206
Hell's Half Acre	5.2±0.15	31±7
Little Park flow	6.5±0.06	250±50
Mosby Butte	265±30	286±105
North Robbers	11.6±0.3	132±11
Packsaddle Butte	340±15	573±101
Pratt Butte	263±20	346±50
Quaking Aspen Butte	64±20	87±12
Serviceberry Butte	120±12	350±43
Split Top Butte	113±10	1106±61
Spud Butte	57±30	306±106
Sunset	12.01±0.15	245±64
The Blow Out	116±15	1233±321
Wagon Butte	120±25	1066±153

Methods: The basalt samples and their ages from the literature (radiocarbon and K-Ar methods) are listed in Table 1. The basalt samples were crushed and sieved and 4 mg aliquots placed in copper pans in a modified Daybreak Nuclear and Medical Co. TL rig. Crushing was gentle and performed in red light to avoid spurious effects. After draining the naturally present TL by a brief heating to ~500°C, samples were placed in a ⁹⁰Sr beta source and irradiated for 3 minutes. This gave an absorbed dose of 12.7 krad. Their induced TL was then measured. This was repeated three times to determine precision.

Results: The “glow curves” obtained (plots of TL against heating temperature) for the COTM basalts were very similar to the curves May obtained for his Hawaii samples. The induced TL values obtained

range over a factor of 100, as indicated in Table 1 in counts per second. One sigma uncertainties in the TL data are about 20% compared with about 10% for the ages, but there is considerable variation on this and uncertainties are smaller for larger TL values.

Discussion: The similarity of the glow curves for basalts from Idaho and Hawaii suggests that similar mineralogy and processes operate at both sites. This is reassuring and suggests that the technique, if successful, can be applied to any volcanic site.

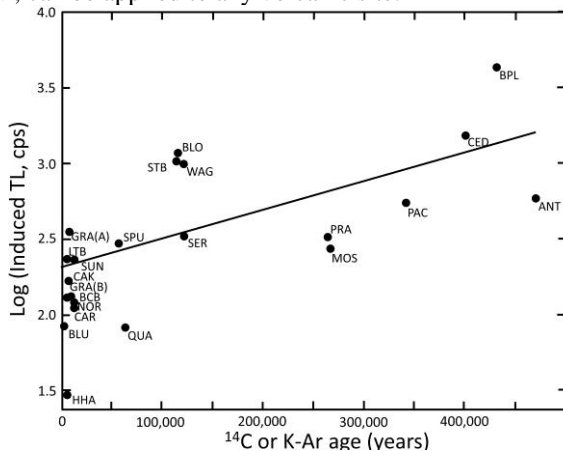


Figure 1. A plot of the log of the induced TL against the radiocarbon or K-Ar age for basalts from 23 volcanoes in the COTM region. The correlation has an R^2 value of 0.5, $n = 23$.

The induced TL values are compared with the radiocarbon and K-Ar dates in Fig. 1. A correlation is observed, similar to the correlation May reported for Hawaiian volcanics. While there is much to be resolved, such as the cause of the scatter in Fig. 1 and the large uncertainties on the TL data, there is the promise of a new, non-isotopic dating method being available for dating volcanic activity. Since there is no indication that the build-up in induced TL is saturating, and that pure feldspars have induced TL values 10^4 - 10^5 times higher than those of the present basalts, the technique could have a range of 10s or 100s of millions of years.

The main weakness of the radiocarbon method is that burned wood needs to be available for the flow being dated while the main weakness of the K-Ar method is the long half-life of ^{40}Ar and loss of Ar, although this is mitigated somewhat by the ^{40}Ar - ^{39}Ar version of K-Ar dating. The main weakness of the TL method, while still in its early days, is that the mechanism needs to be identified and quantified so that the method can be put on an absolute basis and its applicability to various locations addressed. This is aside from needing to reduce the scatter and experimental uncertainty.

May suggested that the cause of the correlation between induced TL and age was that TL traps (electron storage locations) were being created by radiation damage. This was an idea he adopted from meteorite literature of the time. However, this mechanism has been disproved, at least for meteorites [14]. Instead, work with chondrite meteorites and basaltic meteorites indicates that induced TL levels are governed by mineralogical and phase changes in the mineral producing the signal, namely feldspar.

In the case of chondrites, the induced TL increases in strength by a factor of 10^5 in ordinary chondrites with increasing metamorphism experienced by the meteorite. The mechanism seems clear. The mineral responsible for the TL signal in ordinary chondrites is feldspar. Primary unmetamorphosed ordinary chondrites do not contain crystalline feldspar but instead the feldspathic elements are in glass. With metamorphism, the glass crystallizes and the TL signal increases. Thus induced TL is acutely sensitive to metamorphism, e.g., devitrification.

Induced TL also increases with metamorphism in eucrites (basaltic meteorites), by about a factor of 100, but the mechanism is quite different. In this case, it is the diffusion of Fe out of the feldspar during metamorphism that causes the increased TL signal.

Either or both these mechanisms could be operative in the basalts which are rapidly formed nonequilibrium assemblages that will tend towards equilibrium with time.

Conclusions: While much work remains to be done induced TL measurement has the potential to be a new and very different means of dating volcanic rocks. Furthermore, it is a technique that should be readily adaptable for use on robotic spacecraft that land and can provide samples to the instrument.

Acknowledgements: We appreciate funding by NASA's SSERVI and the help of the FINESSE team members in collecting the samples.

References: [1] Greeley *et al.* 1977. In "Volcanism of the Eastern River Plain, Idaho", 171. [2] Kuntz *et al.* 1982. In "Cenozoic Geology of Idaho", 423. [3] Hughes *et al.* 1999. In "Guidebook to the Geology of Eastern Idaho", 143. [4] Heldmann *et al.* 2013. AGU Fall Mtg, abs #P54B-01. [5] McKeever *et al.* 2003. *Radiat. Meas.* 37, 527-534. [6] Jain *et al.* 2006. *Radiat. Meas.* Vol. 41, 755-761. [7] Bailiff *et al.* 2009. Proc. 12th Inter. Conf. Luminescence and Electron Spin Resonance Dating. [8] Sears *et al.* 1980. *Nature*, 287: 791-795. [9] Batchelor and Sears 1991. *Geochim. Cosmochim. Acta* 55, 3831-3844. [10] Sears 2015. *Ancient TL* 33, 15-19. [11] May 1977. *J. Geophys. Res.* 82: 3023-3029. [12] May 1979. *Geol. Surv. Prof. Paper* 1093. [13] Sears and Hughes 2015. AGU fall mtg. [14] Sears 1980. *Icarus* 44, 190-206.

A Sample Delivery System for Planetary Surface Missions

D. Willson¹, C.R. Stoker², L. G. Lemke², A. Duncan³

¹KISS Institute for Practical Robotics/NASA Ames, Bld 245, NASA Ames M.S. 245-3, Moffett Field CA, david.willson@nasa.gov. ²NASA Ames Reserch Center Bld 245, NASA Ames M.S. 245-3, Moffett Field CA

Topic: Planetary Surfaces

Introduction: Capturing and transferring samples of Mars soil or drill cuttings to instruments is a deceptively difficult problem. The 2008 Phoenix mission planned to dig into icy soils and deliver them to instruments for analysis using it’s robot arm scoop (Icy Sample acquisition device (ISAD)) (Fig 1) [1]. Sample transfer was unexpectedly difficult as samples were sticky. It clogged filters on instrument inlets, and stuck to the scoop even when it was tipped over. Sample delivery was fouled by wind blowing sample away, and dumped sample covered the deck by the end of the mission due to poor delivery control.

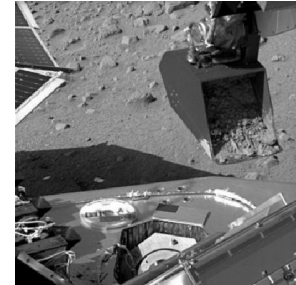


Fig (1): The ISAD Scoop Mars Phoenix mission

A complex system for sample handling (CHIMRA) was developed for the MSL rover robot arm [2] that used vibrator devices and robot arm manipulation to deliver definable quantities of 150 micron size dry sample. However this system would not work with sticky icy samples.

A simpler system for both dry and icy samples is needed and we have been developing a Sample Delivery System (SDS) similar to the Phoenix mission ISAD scoop that can excavate and deliver into instruments definable quantities of filtered icy sticky sample.

Concept Development: A prototype scoop [3] incorporating a rotating wire brush (Fig 3) positioned over a grate located in a simple scoop was developed and tested in Mars conditions (Fig 2). The grate slot size was set to the proposed Icebreaker instrument maximum particle size requirement of 1mm. The brush pushed particles through the grate, dispensing sample at a constant rate. The prototype avoided vibrator devices as they rely on gravity and do not actively push material through screens. However it was found that icy soil cohesiveness could still stick and bridge over the wire brush preventing material flow.

CIF Funded SDS: The latest SDS prototype developed with CIF funding has a plunger device that can push bridged sample onto the brush, as well as an excavator bucket and hopper geometry incorporated into the scoop. This scoop is intended to excavate, filter and dispense icy samples for Planetary surface missions.

References: [1] Chu P., Wilson J., Davis K., Shiraishi L., Burke K. (2008) Proceedings of the 39th Aerospace Mechanisms Symposium, NASA Marshall Space Flight Center. [2] Sunshine D. (2010) Proceedings of the 40th Aerospace Mechanisms Symposium, NASA Kennedy Space Center. [3] Willson D., Lemke L.G., Stoker C.R, Dave A., McKay C.P. (2014) 46th Lunar and Planetary Science Conference, 2503.pdf.

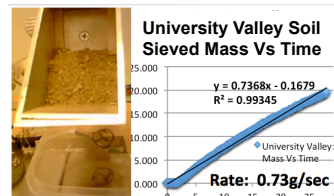


Fig (2)

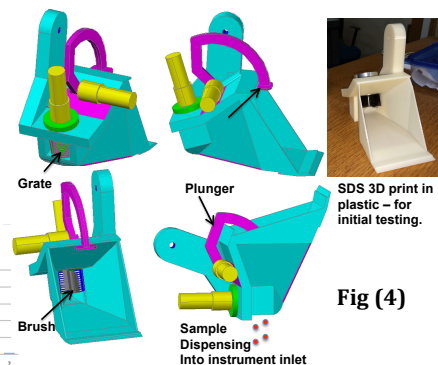
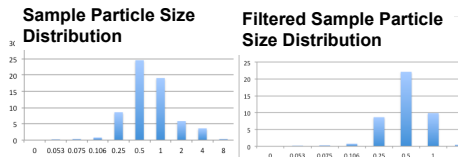


Fig (4)

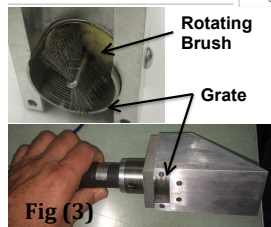


Fig (3)

Fig (2), Top Left: Prototype SDS results with dry Antarctic soil, dispensing rate, particle size distribution before and after filtering after filtering.
Fig (3) Bottom Left: Scoop showing rotating wire brush positioned over grate. **Fig (4) Top Right:** Current SDS being developed showing brush, grate, plunger and dispensing sample. Scoop rotates 70 degrees for dispensing into instruments.

Sample Delivery Challenges For An Auger-Based Mission: Contamination Paths, Mixing, And Dilution Of Results

A. Davé¹, D. Bergman¹, K. Zacny², H. Smith¹, B. Glass¹, B. Yaggi², and A. Davila¹

¹NASA Ames Research Center, M/S 269-3, Moffett Field, CA 94035, PH (650) 604-4855; email: arwen.i.dave@nasa.gov, ²Honeybee Robotics, 398 W Washington Blvd, Suite 200, Pasadena, CA 91103

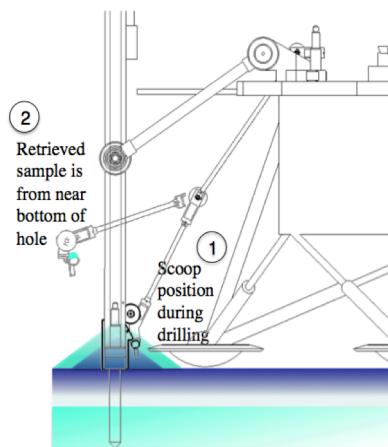


Figure 1: Vertical mixing between samples can be minimized by coordinating scoop movement with drill telemetry.

Concerns for a landed Mars mission's science return risk due to mixing or dilution of sample are addressed by measuring and characterizing these effects during fieldwork. Once understood, these effects can be minimized during the landed mission procedure. Mixing that can occur with particulates from other areas of the spacecraft is of special interest to Planetary Protection efforts. Mixing between samples from different locations and within a 10cm "bite" is of interest to instrument developers for the Icebreaker mission. The poster includes data from lab and field tests to characterize contamination paths, mixing, and dilution of results. Sample layers of different soil types or different colors have been tested with various delivery methods [Fig. 1]. The intent is to give mission planners procedural tools for addressing challenges to sample delivery of drill cuttings.

The Mars Icebreaker mission is a Mars mission concept with the goal of landing at the Mars Northern Polar Caps (the same location as the 2008 Mars Phoenix lander), drilling to at least 1 m depth in the icy permafrost and analyzing captured cuttings for extinct and extant life [1, 2].

The mission will use the 1-meter Icebreaker auger to excavate sample and deliver it to a sampling scoop that transfers the cuttings to the science instruments. Samples of interest include the interface between dry soils and ice-cemented soils (aka the ice table), and discrete deeper soil horizons. Mixing between samples of three different carbon distributions is examined [Fig. 2]. This maximizes the amount of material collected from the layers of interest. Mixing between samples as an artifact of scoop design is also characterized. Instrument designers would benefit from knowing the dilution rates of samples produced by the sampling path. We report characterizations from tests in the Honeybee Robotics lab and in the Rio Tinto field site.

REFERENCES: [1] McKay et al (2013), *Astrobiology*, 13(4): 334-353, [2] Bonitz et al. (2008), *JGR*, 113, E00A01.

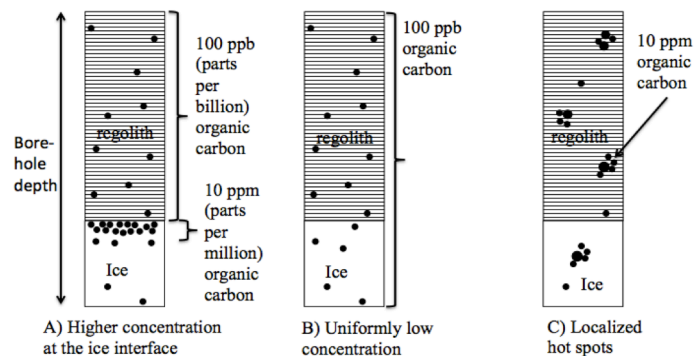


Figure 2: Three scenarios for organic carbon distribution in subsurface near ice table

OVERVIEW OF NASA FINESSE (FIELD INVESTIGATIONS TO ENABLE SOLAR SYSTEM SCIENCE AND EXPLORATION) SCIENCE AND EXPLORATION PROJECT. J. L. Heldmann¹, D.S.S. Lim¹, S. Hughes², S. Kobs Nawotniak², B. Garry³, D. Sears¹, C. Neish⁴, G.R. Osinski⁴, K. Hodges⁵, M. Downs⁶, J. Busto⁶, B. Cohen⁷, B. Caldwell⁸, A.J.P. Jones^{3,9}, S. Johnson¹⁰, L. Kobayashi¹, A. Colaprete¹, and the FINESSE Team. ¹ NASA Ames Research Center, Moffett Field, CA, ² Idaho State University, ³ NASA Goddard Space Flight Center, ⁴ University of Western Ontario, ⁵ Arizona State University, ⁶ NASA Kennedy Space Center, ⁷ NASA Marshall Space Flight Center, ⁸ Purdue University and NASA Indiana Space Grant, ⁹ Planetary Science Institute ¹⁰ NASA Idaho Space Grant Consortium.

Introduction: NASA's FINESSE (Field Investigations to Enable Solar System Science and Exploration) project was selected as a research team by NASA's Solar System Exploration Research Virtual Institute (SSERVI). SSERVI is a joint Institute supported by NASA's Science Mission Directorate (SMD) and Human Exploration and Operations Mission Directorate (HEOMD). As such, FINESSE is focused on a science and exploration field-based research program to generate strategic knowledge in preparation for human and robotic exploration of other planetary bodies including our Moon, Mars' moons Phobos and Deimos, and near-Earth asteroids. FINESSE embodies the philosophy that "science enables exploration and exploration enables science".

FINESSE Science: The FINESSE science program aims to further understand the effects of volcanism and impacts as dominant planetary processes on the Moon, near-Earth asteroids (NEAs), and Phobos & Deimos. Planetary volcanism research focuses on the formation of volcanoes, evolution of magma chambers and the formation of multiple lava flow types, as well as the evolution and entrapment of volatile chemicals. Impact cratering research focuses on impact rock modification, cratering mechanics, and understanding the chronologic record of other planetary bodies.

FINESSE Exploration: The FINESSE exploration program assesses which exploration concepts of operations (ConOps) and capabilities enhance and enable scientific return. Exploration research is focused on robotic ConOps, science ConOps and mission capabilities, communications, and hardware capabilities.

Fieldwork: To achieve the science and exploration research goals, FINESSE conducts multiple terrestrial field campaigns to study features as analogs relevant to our Moon, Phobos, Deimos, and asteroids. These campaigns have thus far centered on Craters of the Moon National Monument and Preserve in Idaho for volcanics, and West Clearwater Impact Structure in Canada for impact studies.

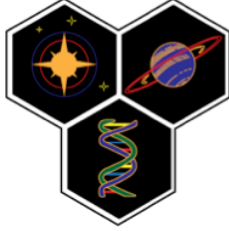
Craters of the Moon National Monument and Preserve (COTM). COTM, in the surrounding east Snake River Plane (ESRP), is a relatively young (~2-15 ka) dominantly basaltic volcanic system that hosts a variety

of well-exposed undisturbed analogs to volcanic formations on the Moon and other planetary bodies. Nearly every type of lunar volcanic feature is represented at COTM and immediate surroundings, and thus COTM is an ideal analog for conducting FINESSE field science for comparative planetology studies. FINESSE research at COTM is focused on understanding the geologic history and setting of multiple volcanic features, using multispectral data to constrain the mineralogy of various lava flows, measuring surface roughness with implications for lava formation and evolution, and understanding the formation of phreatic craters and ballistic ejecta fields.

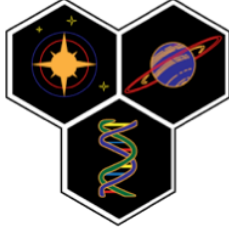
West Clearwater Impact Structure (WCIS). Located in northern Quebec, Canada, WCIS is composed of a large ~25 km diameter lake with a discontinuous ring of islands towards its interior. WCIS appears to possess one of the best records of impact melt rocks and breccias among terrestrial impact structures on Earth. FINESSE research at WCIS is focused on constraining the impact age through geochronology, assessing shock metamorphism and complex crater collapse, studying impact-induced geothermal activity, and characterizing unique impact features such as lineaments and melt veins.

Education and Communication (E&C): FINESSE conducts a robust E&C program. The flagship activity is Spaceward Bound, conducted with the NASA Idaho Space Grant Consortium, where we bring teachers to conduct fieldwork with the FINESSE team. Teachers take their field experience back to their classrooms to share the knowledge and excitement of planetary research with their students. FINESSE also supports additional E&C activities, including (but not limited to) other NASA Space Grant activity, International Observe the Moon Night, a NASA Museum Alliance seminar series, MIT K+12 video documentary series, NASA Open Houses, and KIGAM (Korea Institute for Geoscience and Mineral Resources) Creative Geo EduCamp for Students and Teachers.

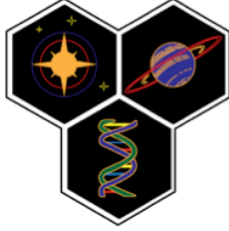
Acknowledgements: FINESSE appreciates the support of NASA / SSERVI, the National Park Service, and the NASA Idaho & Indiana Space Grant Consortiums.



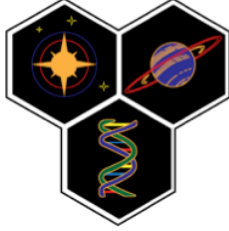
2016 NASA Ames Space Science & Astrobiology Jamboree
Notes



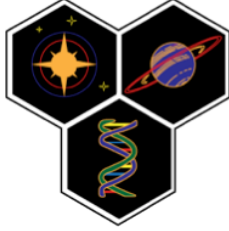
2016 NASA Ames Space Science & Astrobiology Jamboree
Notes



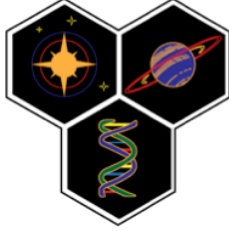
2016 NASA Ames Space Science & Astrobiology Jamboree
Notes



2016 NASA Ames Space Science & Astrobiology Jamboree
Notes



2016 NASA Ames Space Science & Astrobiology Jamboree
Notes



2016 NASA Ames Space Science & Astrobiology Jamboree
Notes